Primary Intestinal Epithelial Cell Response to *Helicobacter Hepaticus* in an *Ex Vivo* Setting



Sarah Abdullah Al-Rawaf

Oriel College, University of Oxford

A thesis submitted for degree of Master of Science (by Research) in Pathology,

Hilary Term 2016

Abstract

Primary Intestinal Epithelial Cell Response to *Helicobacter Hepaticus* in an *Ex Vivo* Setting

Sarah Abdullah Al-Rawaf, Oriel College, University of Oxford

A thesis submitted for degree of Master of Science (by Research) in Pathology, Hilary Term 2016

Epithelial cells lining the intestinal mucosa play a critical role in mucosal immune homeostasis. The inability to culture primary intestinal epithelial cells (IEC) *in vitro*, limited their use in *ex vivo* IEC functional studies. Recently, a method for developing primary intestinal crypt-like 3D structures termed organoids was described. The aim of this project was to establish 2D primary IEC monolayers that could be used to dissect the innate immune response of primary IEC *ex vivo* to bacterial pathogen *Helicobacter hepaticus* (*Hh)* as well as PRR ligands (PAMPs). Using the 3D organoid culture system to grow primary IEC *ex vivo* we managed to develop polarized 2D-monolayers that express appropriately distributed epithelial markers. Following infection with *Hh* we found that the bacteria exhibited good attachment to primary IEC monolayers and were internalized into IEC. Furthermore, a rapid MAPK and Nf-kB activation as well as cxcl2 chemokine expression and secretion was seen following *Hh* infection. However, primary IEC monolayers were largely unresponsive to common microbial PAMPs with the exception of TLR4 ligand *E.coli* LPS, which elicited a modest response. Therefore, this study implicates that isolated *ex vivo* IEC retain their immune function and can be used as a model to mimic natural *Hh* infection of primary IEC, in the absence of any effects from other immune and mucosal cells.

Acknowledgements

Immeasurable appreciation and thankfulness are extended to the following people for their help and support:

To my supervisor Dr.Kevin Maloy, who warmly welcomed me in his lab and allowed me to expand my knowledge and expertise and provided me with a wealth of information.

To Johanna Pott, for her guidance and constant supervision throughout my degree. Her scholarly advice has helped me to a very great extent. Your dedication and hard work has inspired me to do my best.

I would like to extend my sincerest thanks and appreciation to members of the Maloy lab: Andrea, Belen, Alison, Theo, Sandra, Sandrine, Paola, Luara, Sofia, Ollie, Nauren, George, Gökçen, Lucy, and Tamara. Thank you all for the support, insightful comments and constant encouragement. A special thanks is extended to Aga, who spent countless hours in the lab answering and explaining all the silly questions I had, and for supporting me in writing and completing this thesis.

I owe a deep sense of gratitude to my parents for allowing me to realize my own potential, to my brother Saad and sisters Hadeel, Tarfa, and Layla for their moral support.

Lastly, I would like to thank Ghaliya Al-Ajaji for being an awesome friend. I am very thankful to all my friends who stood by me, and to everyone who made my time in Oxford great.

Abbreviations

AMPs	Anti-microbial peptides
APC	Adenomatous polyposis coli
APRIL	A proliferation-inducing ligand)
BAFF	B cell Activating Factor
BMDM	Bone marrow-derived macrophages
BMP	Bone morphogenetic protein
CARD	Caspase recruitment domain
CBC	Crypt base columnar
CD	Crohn's disease
CDT	Cytolethal distending toxin
CF	Cystic fibrosis
CFTR	Cystic fibrosis transmembrane conductance regulator
CKI	Casein kinase I
CRC	Colorectal cancer
DAMP	Danger-associated molecular pattern
DAP	Diaminopimelic acid
DC	Dendritic cell
DSS	Dextran sodium sulfate
EGF	Epidermal growth factor
ESC	Embryonic stem cell
FCS	Fetal calf serum
GALT	Gut Associated Lymphoid Tissue
GF	Germ-free
GSK3	Glycogen synthase kinase 3
Hcp	Hemolysin co-regulated protein
Hh	*Helicobacter Hepaticus*
HHGI1	*Helicobacter hepaticus* Genomic Island 1
IBD	Inflammatory bowel disease
IEC	Intestinal epithelial cell
IEL	Intraepithelial lymphocyte
ILC	Innate lymphoid cell
ILF	Intestinal lymphoid follicle

iPS	Induced pluripotent stem
ISC	Intestinal stem cell
LAMP-1	Lysosomal-associated membrane protein 1
LP	Lamina propria
LPS	Lipopolysaccharide
LRP	Lipoprotein receptor–related protein
LRR	Leucine-rich repeat
mAb	Monoclonal antibody
Mal	MyD88 adaptor-like
MAMP	Microbial Associated Molecular Pattern
MAPK	Mitogen-activated protein kinases
MDP	Muramyl dipeptide
MyD88	Myeloid differentiating factor-88
NICD	Notch intracellular domain
NLRs	Nod-like receptors
NOD	Nucleotide binding and oligomerization domain (NOD)
PRR	Pattern recognition receptor
RIG-I	Retinoic acid-inducible gene-I
RLR	RIG like receptor
sIgA	Secretory immunoglobulin A
SPF	Specific pathogen-free
T6SS	Type 6 secretion system
TA	Transient amplifying
TCF/LEF	T cell factor/lymphocyte enhancer factor
TER	Transepithelial electrical resistance
TFF3	Trefoil factor 3
TGF	Transforming growth factor
TLR	Toll-like receptor
TRAM	TRIF related adaptor molecule
TSLP	Thymic Stromal Lymphopoietin
UC	Ulcerative colitis
VgrG	Valine glycine-repeat
WGA	Wheat germ agglutinin
ZO1	Zonula Occludens1

Table of Contents

CHAPTER 1 – GENERAL INTRODUCTION 5

1.1 Mucosal immunity 5

1.1.1 The mucosal barrier 5

1.1.2 The intestinal epithelial cell layer 6

1.1.3 The intestinal microbiota 12

1.1.4 Mucosal homeostasis and inflammation 13

1.2 Pattern recognition receptors (PRR) 15

1.2.1 Toll like receptors (TLRs) 16

1.2.2 Nod like receptors (NLRs) 18

1.3 Helicobacter Hepaticus (*Hh*) 20

1.3.1 Overview 20

1.3.2 *Hh* induced colitis 22

1.3.3 *Hh* innate immune signaling 24

1.3.4 *Hh* infection of IEC *ex vivo* 26

1.4 Growing primary IEC *ex vivo* 27

1.4.1 Intestinal stem cells (ISC) and the stem cell niche 27

1.4.2 *In vitro* IEC lines 31

1.4.3 Developing primary IEC organoid cultures 32

1.4.4 Adapting the 3D primary IEC organoid system into a 2D monolayer 35

1.4.5 Applications of IEC organoids 36

1.5 Project aims 38

CHAPTER 2 – MATERIAL AND METHODS 39

2.1 Conditioned medium 39

2.1.1 Production of Rspo1-Fc or Noggin-Fc conditioned medium 39

2.1.2 Spotblot analysis for detection of Fc-coupled proteins 39

2.1.3 Wnt-3A conditioned medium 40

2.1.4 β-catenin stabilization assay 40

2.2 Organoid culture 41

2.2.1 Mice 41

2.2.2 Crypt isolation and cell culture 42

2.2.3 Passaging of organoids 43

2.3 2D-Monolayers 43

2.3.1 Developing 2D-monolayers 43

2.3.2 Monolayer treatments and infection 44

2.3.3 Assays of innate immune activation through PRRs 45

2.4 Immunostaining 45

2.4.1 *Hh* internalization immunostaining 46

2.4.2 Antibodies and stains 47

2.5 *Helicobacter hepaticus* 48

2.5.1 Culture 48

2.6 Chemokine detection in cell supernatant using ELISA 48

2.7 Analysis of mRNA expression by qPCR 49

2.7.1 RNA extraction from cell isolates 49

2.7.2 Quantitative PCR (qPCR) 49

2.8 Western blot 50

2.8.1 Sample preparation 50

2.8.2 Western blot 50

2.9 Statistical analysis 51

CHAPTER 3 – CULTURING PRIMARY IEC IN AN *EX VIVO* SYSTEM 52

3.1 Introduction 52

3.2 Results 54

3.2.1 Growing primary IEC *ex vivo* 54

3.2.2 Adapting 3D organoid culture system to form 2D-monolayers 61

3.2.3 Characterization and optimization of the 2D monolayers 63

3.2.3.1 Optimizing the 2D monolayer system 67

3.2.3.2 Monolayers contain differentiated epithelial cells 70

3.3 Discussion 72

CHAPTER 4 – *HELICOBACTER HEPATICUS (HH)* INFECTION OF PRIMARY IEC 75

4.1 Introduction 75

4.2 Results 78

4.2.1 *Hh* surface adhesion and internalization into WT primary IEC 78

4.2.2 Response of WT IEC to *Hh* and chemokine secretion 83

4.2.3 Innate immune receptor expression by primary IEC 88

4.2.4 PRR receptors involved in *Hh* recognition 92

4.3 Discussion 94

CHAPTER 5: GENERAL DISCUSSION 98

REFERENCES 108

List of Figures

Figure 1.1 Schematic representation of intestinal epithelial crypt. 11

Figure 1.2 Interaction of ISC and their niche. 30

Figure 1.3 Schematic of crypt organoid. 34

Figure 3.1 Stably transfected HEK293T produce R-spondin, and Noggin. 58

Figure 3.2 L Wnt-3A cells express Wnt3A. 59

Figure 3.3 Time course of colonic organoid growth. 60

Figure 3.4 Adapting 3D organoid culture system to form 2D monolayers. 62

Figure 3.5 Primary IEC monolayers stain for Phalloidin and WGA. 65

Figure 3.6 Monolayer polarization expressing apical and basolateral markers. 66

Figure 3.7 Seeding 3 wells (24-well plate) of 3D organoids achieve near-confluent 2D IEC monolayers. 68

Figure 3.8 Primary IEC maintain their proliferative capacity post-seeding when treated with 50% conditioned media. 69

Figure 3.9 IEC monolayers contain differentiated goblet cells. 71

Figure 4.1 *Hh* exhibits adherence to primary IEC *ex vivo*. 80

Figure 4.2 *Hh is* internalized into cultured primary IEC following 4h of infection. 82

Figure 4.3 *H. hepaticus* stimulates both MAPK and Nf-κB intracellular signaling cascades in primary IEC. 85

Figure 4.4 Cxcl2 secretion is induced following *Hh* infection of primary IEC. 86

Figure 4.5 Cxcl2 production following *Hh* infection of IEC basolaterally (3D organoids). 87

Figure 4.6 Primary IEC monolayers respond to LPS, but not to other PRR agonists. 90

Figure 4.7 Responses of primary IEC organoids to basolateral stimulation with PAMPs. 91

Figure 4.8 Primary IEC responses to *Hh* and LPS are MyD88-dependent. 93

Chapter 1 – General Introduction

1.1 Mucosal immunity

1.1.1 The mucosal barrier

The mammalian gastrointestinal tract harbors trillions of commensal bacteria, which usually coexist peacefully with the host, without eliciting harmful inflammation. Although these large, dynamic microbial communities normally exist in a mutually beneficial relationship with the host, their close association with the intestinal epithelium and the large number makes them a possible threat [4]. Therefore, a tight and strong mucosal barrier exists at the microbiota – epithelial interface, which contains several components. The biochemical and physical mucosal barrier consists of a mucus layer, a single epithelial cell layer, and the lamina propria immune system. The mucus layer which covers the apical epithelial surface is divided into two distinct parts, a highly glycosylated mucin-rich inner layer, and a loose, less dense outer layer [5]. The inner layer is usually densely packed making it impermeable to bacteria and thus separates the epithelium from the luminal microbiota. The outer layer on the other hand, lies between the inner layer and the luminal bacterial community, and harbors many bacteria [5,6].

Mucus does not only provide physical protection, as biochemical compounds such as the anti-microbial peptides (AMPs), which are secreted by intestinal epithelial cells (IEC), and plasma cell-derived secretory immunoglobulin A (sIgA) accumulate in this viscous gel like mucus sheet, limiting bacterial colonization and thus reinforcing this barrier [6] The importance of this layer has been illustrated in $MUC2^{-/-}$ mice, where spontaneous colitis develops when MUC2 mucin (the main structural component of the mucus layer) is absent [5-7].

A single columnar IEC layer separates the intestinal lumen microbes and dietary antigens from the underlying immune cells residing in the lamina propria (LP)[6]. This layer, which forms the largest mucosal surface area in the human body, is constantly self-renewing and rapidly replacing its dying differentiated epithelial cells [8], making them a difficult target for infectious agents. In addition, these cells have apical surface extensions termed microvilli that help in preventing microbial attachment to the epithelial cell, as well as tight junction proteins expressed on the lateral wall to block paracellular microbial invasion into the lamina propria [9,10].

In addition to these physio-chemical barriers that reinforce mucosal defense, IEC have been recently recognized as a central player in mucosal immunity [9]. IEC have the ability to sample luminal microbes, and express pattern recognition receptors (PRR) that recognize conserved Microbial Associated Molecular Patterns (MAMPs), which can help in the discrimination between commensal and pathogenic microbes [11,12]. Furthermore, they have the ability to influence innate and adaptive immune cells in the LP, thus influencing the mucosal immune response to microbiota [9,13].

1.1.2 The intestinal epithelial cell layer

IEC Physiology

A single IEC layer covering the intestinal lumen forms the largest surface of the human body. This rapidly self-renewing epithelial layer is composed of differentiated epithelial cells, stem cells and their daughter transit amplifying (TA) cells [8]. The small intestinal epithelium is arranged into crypts and villi [8,14], whereas colonic epithelium has no villi and therefore the epithelial crypt surface appears smooth [15].

At the base of the intestinal crypts, rapidly self-renewing Lgr-5^+ intestinal stem cells (ISC) divide to form the TA cells, which in turn give rise to the four IEC lineages [8] (Fig 1.1). Enterocytes are the most common lineage, accounting for 80% of the IEC population [8]. These highly polarized simple columnar epithelial cells absorb nutrients and water via their luminal brush border [8]. Another common IEC population are the mucus-secreting goblet cells, their frequency increases distally from the small intestine to the crypts of the descending colon [8,16]. These cells produce mucus which forms a physical as well as a chemical barrier between the IEC and the lumen, and also aids movement and effective expulsion of gut contents [8]. Around 1% of the IEC population are hormone-secreting enteroendocrine cells, scattered throughout the IEC layer [17]. These three IEC lineages arise from the TA cells at the crypt base but are pushed away from the crypt base by the actively proliferating stem cells, thus they end up occupying the upper part of the crypts and the villi (Fig.1.1). Eventually these cells are shed into the intestinal lumen as they lose their extracellular anchorage leading to apoptosis [8], a phenomenon termed "anoikis" [18]. Under homeostatic conditions, a constant balance between the rate of cell production in the crypt base and apoptosis at the villus tip is maintained [8,15].

In the small intestine, a fourth IEC type, termed Paneth cells, reside in the crypt base, intercalated amongst the Lgr-5^+ ISC (Fig.1.1) [19]. In the large intestine, Paneth cells are only seen in the proximal colon and are absent distally [14], therefore enterocytes, enteroendocrine cells, and goblet cells are the main IEC types found in the colonic epithelium. Paneth cells play a major role in intestinal innate immunity through the secretion of AMPs, such as (cathelicidins and defensins) [8]. However, Paneth cells are not the only IEC known to secrete AMPs, as enterocytes have been also found to produce some AMPs, such as the C-type lectin regenerating islet-derived protein IIIγ (REGIIIγ),

β-defensins and cathelicidins, which are expressed in small intestine and colon [20,21].

In addition to their immune function, Paneth cells also provide support for the Lgr-5$^+$ ISC through the secretion of vital growth signals [19]. The importance of these signals for ISC has been illustrated *in vivo* by the genetic removal of Paneth cells, which resulted in the concomitant loss of Lgr-5$^+$ ISC [19]. In the small intestine, extracellular signals provided by Paneth cells include epidermal growth factor (EGF), Transforming growth factor-α (TGF-α) and Wnt3, as well as the Notch ligand Dll4 [3,19]. These signals maintain Lgr-5$^+$ ISC stemness and promote their survival. On the other hand, in the distal colon, where Paneth cells are absent, CD24$^+$ cells residing between Lgr-5$^+$ ISC provide these extracellular growth factors [3,8,19].

Intestinal epithelial cell immune function

As noted above, IEC have been recognized as an important player in mucosal immunity [20]. The mucosal barrier does not completely isolate the underlying sub-epithelial immune system from the microbiota, luminal antigens are being constantly delivered to lamina propria immune cells through specialized IEC, a process which is crucial for the development and maturation of the mucosal immune system [20,22]. Specialized microfold (M) cells, found in the epithelial layer covering the intestinal lymphoid tissue, constantly sample luminal antigens through non-specific transcytosis and specific transporting receptors, and deliver the antigens to lamina propria immune cells [22-24].

In addition, goblet cells have been also recently described to be another specialized IEC capable of microbial sampling and antigen delivery to underlying immune cells [25]. Other non-epithelial immune cells are also able to sample luminal content, for example a

subpopulation of intestinal dendritic cells (DCs) have dendrites that express tight junction proteins, which allow them to attach to lateral epithelial wall and extend through the paracellular epithelial space to reach the intestinal cavity microbiota [26,27].

Microbial sensing through innate immune PRRs is another way for IEC to communicate with the microbiota. Stimulation of IEC PRRs via conserved MAMPs shape the nature of mucosal immune responses towards intestinal antigens [9].

Microbiota – IEC interactions

At steady state, microbial sensing by IEC can drive anti-inflammatory or immunoregulatory signals that influence innate and adaptive immune responses in the lamina propria [9]. IEC promote a tolerogenic mucosal environment in response to commensals through the secretion of soluble factors such as TSLP (Thymic Stromal Lymphopoietin), TGF-β (Transforming Growth Factor-β), APRIL (a proliferation-inducing ligand), BAFF (B cell Activating Factor), interleukin (IL)-25 [20,28-30]. IEC may indirectly influence adaptive lymphocytes through interacting with local antigen-presenting mononuclear phagocytes, namely macrophages and DCs [20]. Thus, IEC-derived TSLP and TGF-β signals promote tolerogenic development of LP macrophages and DCs [28,31,32]. LP DC then migrate to draining lymphoid tissues and promote tolerogenic regulatory T (T reg) cell development and IL-10 production [33,34]. In addition, Tissue-residing LP macrophages enhance survival and expansion of primed T reg cells in the lamina propria [35]. In addition to T cell priming, DCs also promote maturation of naïve B cells into mature IgA secreting plasma cells, through class switching recombination [36]. In the mucosa, this process can be facilitated by DCs following their conditioning via TSLP, or by IEC secretion of APRIL and BAFF that directly regulate B cell maturation and class switching [29,30].

Furthermore, IEC have the ability to directly communicate with other adaptive immune cells, such as the intraepithelial lymphocytes (IEL) that are found embedded within the epithelium in close proximity to IECs through CD103 which interacts with IEC E-cadherin [37,38].

In addition to the microbial sensing role in regulating the barrier immune response, these bacteria-derived signals are critical for epithelial cell integrity and repair following injury [39]. For example, commensal derived signals promote IEC secretion of trefoil factor 3 (TFF3) that enforces the mucus integrity and play a role in IEC migration as well as resistance to apoptosis [40]. In addition, these signals drive IEC expression of epidermal growth factor receptor ligands and cytoprotective heat-shock proteins [39,41].

Furthermore, microbial sensing is also vital for influencing the immune system maturation, as well as maintaining a healthy mucosal barrier [20]. For example, AMP and mucus secretion by IEC increases with commensal microbial sensing and PRR stimulation [16,21]. It has been shown that in the absence of these commensal signals in germ-free (GF) mice, only a thin mucus layer develops [16,42]. However, upon administration of PRR ligands to GF mice, mucus secretion increases and these mice regain the normal mucus layer thickness [16]. Furthermore, commensal derived signals also control other IEC barrier functions such as sIgA transcytosis and tight junction integrity [20,43].

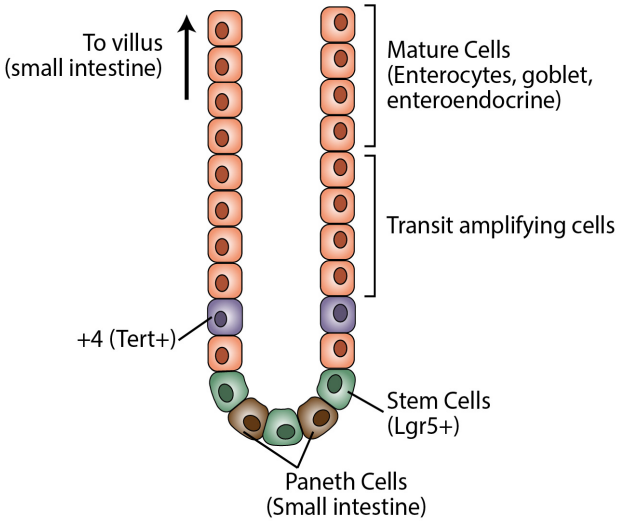


Figure 1.1 Schematic representation of intestinal epithelial crypt. At the base of the colonic and SI crypts, rapidly self-renewing Lgr-5^{+} intestinal stem cells (ISC) divide to form the TA cells, which give rise to mature IEC. TA and mature IEC are found at the mid and upper part of the intestinal crypt, +4 cells are found 4 cells above the base of the crypt (adapted from Kuratnik A, 2013) [2].

1.1.3 The intestinal microbiota

In the lower intestine dense bacterial communities that can reach up to ($\geq 10^{12}$/cm3 intestinal contents) live in close proximity to the epithelium, which lies between the luminal microbiota and the host sub epithelial tissue [44].

Over time hundreds of commensal species have evolved a symbiotic relationship with the host, providing beneficial contributions in exchange for nutrients and protection [44]. Some of these benefits include blocking pathogen colonization by competing for space and nutrients (colonization resistance), assessing nutrient acquisition through the fermentation of indigestible polysaccharides, and production of vitamin B12 and folic acid [4].

Commensal microbiota also play an essential role in preventing tissue injury, in IEC maturation and proliferation, and in intestinal and peripheral immune system maturation [39,45,46]. For example, small intestinal lymphoid follicles (ILF), which are organized intestinal lymphoid tissues composed of myeloid and lymphoid cells, fail to develop in GF mice [44]. In addition, GF mice also lack intestinal intraepithelial lymphocytes and secretory IgA [44,47].

Although these dynamic complex commensal communities are usually beneficial, their large number and proximity to the epithelium renders them a threat to the host. For that reason, several mechanisms adapted by the host to minimize bacterial epithelial contact such as the secretion of mucus by goblet cells that physically separates IEC from luminal bacteria, as well as Paneth cells AMPs that limit bacterial invasion of the mucus [44]. Furthermore, IgA secretion by lamina propria B cells and transcytosis via IEC to epithelial apical border also play an important role preventing bacterial invasion of the epithelial barrier [44]. Furthermore, a special intestinal immune system underlies the

epithelial layer in the sub-epithelial connective tissue. Within the intestinal lamina propria, specialized lymphoid tissues termed Gut Associated Lymphoid Tissue (GALT); including Peyer's patches and cryptopatches in the small intestine, as well as lymphoid follicles throughout the intestine, constitute specialized microenvironments for activation of immune responses [9,23,48].

1.1.4 Mucosal homeostasis and inflammation

Changes in the composition of commensal communities have been linked to the pathogenesis of various autoimmune and inflammatory conditions such as arthritis, airway inflammation and inflammatory bowel disease (IBD) [49-51].

Data have suggested that the host immune system can influence the composition of the dynamic microbiota community. This was illustrated in mice lacking TLR5, which developed metabolic syndrome as a result of changes in the gut microbiota [52]. In addition, GF WT mice developed a similar metabolic syndrome when receiving the $TLR5^{-/-}$ gut microbiota, suggesting a direct impact of immune deficiency on microbiota composition [52]. Therefore, a complex dynamic relationship exists between the host immune system and the commensal community that involves both entities contributing to achieve homeostasis.

The intestinal immune system has developed many adaptations to allow the coexistence of the microbiota within the gut without overstimulation. Although challenging, a balance between immune tolerance towards beneficial microbes and appropriate immune activation in response to invasive pathogens is constantly

maintained at the epithelial border. This balance is crucial for the maintenance of host-microbiota symbiotic relationship as well as intestinal homeostasis, and any disturbance can lead to chronic intestinal inflammation and neoplasia [9].

IBD is a chronic, remittent or progressive inflammation of the intestinal tract that is driven by a dysregulated mucosal immune response [53]. Two main clinical types of IBD exist, Crohn's disease (CD) and ulcerative colitis (UC), and although they share many similar characteristics, some differences exist [53]. Inflammation in CD can involve any part of the gastrointestinal tract but most commonly affects the colon and terminal ileum [53]. Histologically, CD is often characterized by transmural (involving all layers of the gut wall) skip lesions where normal tissue lie between patchy areas of inflammation, as well as ulceration and submucosal fibrosis [53]. In addition, dense cellular infiltration and granulomas are also observed in CD [53]. In contrast, UC usually involves the rectum and extends proximally without exceeding the colon [53], and is characterized by superficial lesions with ulcerations, crypt abscesses, cellular infiltration and loss of goblet cells [53]. Crohn's patients usually suffer from diarrhoea and abdominal pain, and the inflammation can be complicated with fistulisation and strictures causing bowel obstruction. However, severe bloody diarrhoea with a rigid colon is most commonly seen in UC [53].

Anti-inflammatory medications such as steroids and 5-aminosalicylic acid are usually used in active disease to induce remission [54], but these are not always effective. More recently, biologicals such as anti TNF-α monoclonal antibodies have been employed for remission induction and maintenance [54]. Despite these advances in medical management, many patients are either unresponsive or relapse following therapy and

ultimately require surgical management [54].

IBD is believed to be a multifactorial disease where environmental factors, host genetics, and immune system are all involved in the disease pathogenesis. Although the exact aetiology is unknown, many studies have suggested a strong link between dysregulated immune response towards microbiota and IBD pathogenesis [50].

1.2 Pattern recognition receptors (PRR)

Mucosal innate immunity is highly regulated by PRRs that are expressed on many leukocytes, such as intestinal DCs and macrophages, as well as non-immune cells like mucosal epithelial cells [55]. There are several families of PRR that can recognize conserved microbial-associated molecular patterns (MAMPs) or endogenous danger-associated molecular patterns (DAMPs), but the most well characterized are the Toll-like receptors (TLRs), nucleotide-binding domain and leucine-rich repeat containing receptors (NLRs), and retinoic acid-inducible gene-I (RIG-)-like receptors (RLRs) [55-57].

TLRs are membrane bound receptors that may be expressed on the cell membrane, endosomes, lysosomes and endolysosomes [58]. NLRs and RLRs on the other hand are expressed in the cytosol [12]. These receptors detect highly conserved ligands which trigger a downstream signaling cascade that induces the expression of unique genes involved in many homeostatic and pro-inflammatory responses [55].

PRR signaling at the mucosa has a critical role in regulating the epithelial immune response and ensuring mucosal barrier homeostasis, and any disturbance in this tightly regulated signaling system can lead to intestinal inflammation and pathology [12]. TLR

signaling for example has been found to be involved in epithelial restitution and repair following chemical injury induced by administration of dextran sodium sulfate (DSS) [39]. IEC-TLR signaling induced the production of tissue protective proteins such as (IL)-6 and chemokine KC-1 [39]. Furthermore, TLR2 can regulate epithelial tight and gap junctions, playing a major role in tissue healing and epithelial integrity [39,59,60]. This TLR2 protective effect was illustrated in a study that showed injured IEC treated with the TLR2 ligand Pam3Cys developed an increase in gap junction communication [60]. Additionally, it has been shown that mice deficient in TLRs were found to have high numbers of commensal bacteria in their spleen, indicating a defect in the mucosal barrier, as well as a high serum antibody against commensals and an exaggerated adaptive immune response to commensal bacteria [61,62].

1.2.1 Toll like receptors (TLRs)

Toll-like receptors are a family of type I transmembrane glycoproteins and consists of 10 or 12 functional receptors in humans and mice, respectively [63]. TLRs are formed of three domains: an outer leucin-rich repeats (LRR) ligand binding domain, a short transmembrane part, and a homologous intracellular Toll/IL-1R (TIR) domain [63].

TLR1, TLR2, TLR4, TLR5, TLR6 and TLR11 are located on the cell surface and recognize microbial lipids, lipoproteins, proteins and other microbial membrane components [55]. TLR2 forms heterodimers with TLR1 or TLR6, and recognizes bacterial lipopeptides, lipoteichoic acid and yeast zymosan [64-66]. TLR4 forms a complex with its co-receptor MD2 and needs accessory proteins, the LPS-binding protein and CD14, to attach to and recognize bacterial lipopolysaccharide (LPS) [67]. TLR5 recognizes bacterial flagella [58], and TLR11 is stimulated by uropathogenic bacteria

[68], as well as *Toxoplasma gondii* derived molecules [69].

On the other hand, TLR3, TLR7, TLR8 and TLR9 are expressed on endosomal and lysosomal compartments and are stimulated by microbial nucleic acids [55]. TLR3 senses double stranded RNA (dsRNA) and promotes the secretion of type I interferon and inflammatory cytokines that play a central role in preventing viral infection. TLR7 and TLR8 recognize single stranded RNA (ssRNA). TLR9 is activated by unmethylated 2′-deoxyribo cytidine-phosphate guanosine (CPG) DNA motifs [58].

Upon ligand binding, TLR undergo structural changes that allow the intracellular TIR domains to bind to TIR domains on signaling adaptor proteins, namely, Myeloid differentiating factor-88 (MyD88), MyD88 adaptor-like (Mal), TIR domain-containing adaptor-inducing IFN-β (TRIF), and TRIF related adaptor molecule (TRAM) [55,63,70]. MyD88 is the only adaptor protein that is used by all TLRs except TLR3, and signaling through this adaptor leads to the activation of NF-κB and MAPK (mitogen-activated protein kinases) transcription factors to produce pro-inflammatory cytokines [58]. The TIRAP adaptor protein is used by the cell to recruit MyD88 to the TLR2 and TLR4 receptors [58]. On the other hand, TRIF mediated signaling results in the production of type I IFN and inflammatory cytokines through the activation of IRF3 and NF-κB and is used by TLR3 and TLR4 [58,71]. The TRAM sorting adaptor helps recruit TRIF to TLR4 [58,72]. The diversity of adaptor proteins allows different responses to TLR ligands [58,63]. Each TLR receptor recognizes a distinct MAMP that activates a specific intracellular signaling cascade, which leads to a distinct anti-pathogen response.

1.2.2 Nod like receptors (NLRs)

NLRs are cytoplasmic innate immune receptors, structurally formed of a variable N-terminal domain, that may be a caspase recruitment domain (CARD) such as in NODs, a pryin (PYD) domain in the NLRPs, or a baculovirus-inhibitor domain in NAIP receptors [64]. In addition to the N-terminal domain, NLRs also contain a central nucleotide binding and oligomerization domain (NOD), as well as a C-terminal leucine-rich repeat (LRR) domain. Following their activation these receptors mediate intracellular signaling cascades that trigger immune and inflammatory responses [73,74].

The NLR family is composed of 23 NLR proteins identified in humans and 34 NLR genes in mice [75], and are expressed on many cells including leukocytes, such as myeloid cells and T cells, and non-immune cells such as epithelial and endothelial cells [76].

Two of the most characterized NLRs are NOD1 and NOD2 (Nucleotide- binding oligomerization domains 1 and 2). NOD1 is found in many tissues in humans, however NOD2 is only expressed in leukocytes, DCs and epithelial cells and its expression is upregulated by proinflammatory cytokines and bacterial components, via Nf-κB [77,78]. These cytoplasmic receptors sense components of bacterial cell well peptidoglycan, namely, meso-diaminopimelic acid (DAP) in the case of NOD1, and muramyl dipeptide (MDP) for NOD2 [79,80]. Ligands must be internalized into the cell before being recognized by the receptors in the cytoplasm. When NOD1 and NOD2 bind their activating ligands in the cytosol signalling complexes form which leads to nuclear translocation of Nf-κB and MAPK and the upregulation of pro-inflammatory gene expression [81].

In contrast, some NLRs, especially those belonging to the NLRP family, form complex multi-protein structures upon activation, termed inflammasomes [82]. These structures are composed of NLR, an adaptor protein called apoptosis speck-like protein (ASC), and the cytosolic protease caspase-1 [83,84]. Activation of these NLR results in multimerization of ASC and recruitment of pro-caspase-1, leading to its autocleavage and activation [83]. Active caspase-1 then cleaves pro-IL-1β and IL-18 cytokines into their active form and can also induce a form of inflammatory cell death termed pyroptosis [82].

NLR signalling has been implicated in IEC homeostasis and mucosal barrier integrity. For example, NOD2 activation in Paneth cells drive the secretion of the AMP α-defensin, as NOD2 deficient mice exhibit defects in defensin secretion as well as higher susceptibility to DSS colitis [85]. Furthermore, mice lacking NLRP3, ASC, or caspase-1 are highly susceptible to DSS colitis and show epithelial injury, leukocyte infiltration and increased chemokine production due to reduction in the NLRP3 mediated production of IL-18 cytokine [86]. The absence of NLRP3 resulted in a significant reduction in IEC proliferation and increase apoptosis during DSS-induced colitis [86].

NOD2 gene polymorphisms have been associated with susceptibility to inflammatory bowel disease. Approximately 40% of patients with Crohn's disease carry at least one NOD2 mutation in the LRR domain resulting in reduced sensing of MDP and decreased activation of Nf-κB signalling [81,87]. Additionally, NOD1 polymorphisms have also been linked to IBD susceptibility [88]. However, precisely how NLR contribute to intestinal homeostasis, especially in terms of their functions in IEC remains unclear.

1.3 Helicobacter hepaticus (*Hh*)

1.3.1 Overview

Helicobacter hepaticus (Hh) is a gram negative, spiral bacterium with bipolar sheathed flagella [89]. It was first discovered in the late 1990s, in AJ/Cr mice liver samples with chronic active hepatitis [89]. The bacterium was also found to colonize murine colonic and cecal crypts as well as the hepatic tissue (canaliculi) [90] and is the enterohepatic helicobacter species EHS prototype [91]. It is commonly found in laboratory mice and usually causes subclinical or no symptoms in immune competent WT mice, but can elicit chronic intestinal inflammation in susceptible strains [91]. It has the potential to induce colitis, colorectal cancer and extraintestinal diseases in immune compromised mice [91].

The complete *Hh* genomic sequencing lead to the identification of several virulence factors which contribute to bacterial pathogenicity [92]**.** These include cytolethal distending toxin (CDT), a multi subunit toxin comprised of CdtA, CdtB, and CdtC subunits, which has DNaseI-like activity that causes cell death upon delivery to host cell cytoplasm [93]. *Hh* CDT plays a role in persistent colonization, as a CDT deletion mutant of *Hh* failed to colonize female outbred Swiss mice, but transiently colonized male mice and caused less severe disease [94].

Another virulence factor that significantly contributes to the bacterial pathogenicity is the *HHGI1* pathogenicity island (PAI), which comprises a group of genes that encode for virulence-associated factors [92]. The *Helicobacter hepaticus* Genomic Island 1 (*HHGI1)* is a 71-kb genomic region that has been recently found to encode a type VI secretion system (T6SS) [92,95]. *HHGI1* mutants lacking 19 genes failed to cause typhlocolitis, and a milder inflammation compared to WT *Hh* was observed in IL-10$^{-/-}$ mice [96]. A T6SS is a multi-subunit complex that functions as a 'needle and syringe'

injecting effector proteins intracellularly [97]. The *IcmF* transmembrane protein, Hcp (hemolysin co-regulated protein), and three VgrG (valine glycine-repeat) proteins are known T6SS substrates [97]. This protein secretion system facilitates a molecular bacterial – host cell interaction [98]. It is believed that the HHGI1 TS66 plays a critical role in bacterial-host symbiosis through controlling colonization and limiting the host inflammatory response [95]. Thus, *Hh* T6SS mutants displayed more IEC internalization compared to WT *Hh* by the MODK-E epithelial cell line and IEC *in vivo*[95]. This indicates that the *Hh* T6SS, unlike most other enteric bacteria secretion systems that promote infection, instead limits *Hh* host cell internalization [95]. In addition, a T6SS mutant *Hh*Δ*IcmF* displayed higher levels of colonic and cecal colonization in comparison to WT *Hh* infection of mono-colonized mice [95]. Furthermore, *Hh*Δ*IcmF* induced an elevated pro-inflammatory gene expression profile in MODK-E cells infected when compared with WT *Hh* [95]. Collectively, these data suggests that the *H. hepaticus* T6SS promotes an anti-inflammatory effect on IEC [95].

Another recognized pathogenicity factor is the urease enzyme. Urease is usually utilized by gastric *Helicobacter spp.* to convert urea into ammonia and carbon dioxide and this process is important for surviving the acidic gastric milieu [99,100]. However, around 40% of enterohepatic *Helicobacter spp.* are also urease positive, including *Hh* [101]. Indeed, male A/JCr mice infected with *Hh* Urease mutants displayed lower levels of hepatic colonization and less severe hepatitis when compared to mice infected with WT *Hh* [101]. Additionally, enzymes involved in oxidative stress resistance, such as the *Hh* catalase enzyme KatA, and bacterial hydrogenase may contribute to *Hh* virulence. KatA catalyse hydrogen peroxide to water and molecular oxygen, a process that prevents bactericidal effect of the reactive oxygen species [102]. It has been shown that Hh *katA*

mutant were more sensitive to oxygen and H_2O_2 compared to WT [103]. The hydrogenase enzyme however oxidizes molecular hydrogen to yield protons and electrons, a process that is believed to contribute to the synthesis of proteins and enzymes associated with virulence [104]. Moreover, the presence of fully functional flagella is essential for *Hh* motility and colonization as flagellar mutants were non-motile and unable to colonize mice [105].

The complete genomic sequence of *Hh* helped elucidate the different virulence genes and their role in inflammation by using isogenic mutants. Further characterization of the pathogenic potential of *Hh* virulence factors and their targets could lead to new insights into the relationship between the bacteria and IEC.

1.3.2 *Hh* induced colitis

Hh has the potential to induce both inflammatory and regulatory responses by the host [106]. Upon infection of WT mice with *Hh* a strong, specific $CD4^+$T-cell and antibody response develops [106-108]. However, a strong T reg cell response that suppresses *Hh* pathogenic responses is also induced following *Hh* infection [106]. This IL-10 dependent $CD4^+$ Treg response promotes persistent *Hh* colonization without inflammation in immunocompetent WT mice [106,109]. In IL-10-deficient mice infected with *Hh*, this regulatory response is absent and potent local T cell responses drive chronic typhlocolitis [107,108]. Similarly, treatment of *Hh*-infected normal WT mice with monoclonal antibody (mAb) against the IL-10 receptor (αIL-10R mAb), triggers development of potent IL-23-driven typhlocolitis that is characterized by a robust Th1 and Th17 response in the intestine [108]. Severe inflammation with features resembling human IBD, such as

epithelial hyperplasia, edema, cellular infiltration with abscesses and ulceration were observed in this model [108].

In addition, *Hh* infection of other strains of immune compromised mice with defects in immune function and/or regulation induces intestinal inflammation with several features that resemble human IBD, such as secretion of high levels of IL-17 and Interferon gamma (IFNγ) inflammatory cytokines in response to IL-23, two cytokines that are highly implicated in CD. Furthermore, innate lymphoid cells (ILC) that are known to mediate the inflammation and secrete IL-17 and IFNγ have been identified in CD patients intestine [107,110-112].

Hh can also trigger pathological innate immune responses in the gut. Thus, when lymphocyte-deficient 129SvEv*Rag2*$^{-/-}$ mice were infected with *Hh* an IL-23-dependent innate immune mediated typhlocolitis developed [113,114]. Somewhat surprisingly, similar to the T-cell dependent inflammation models described above, disease was associated with inflammatory cytokines, such as IL-17 and IFN-γ. Subsequent investigation showed that a novel population of IL-23R^{+} innate lymphoid cells (ILC) were critical mediators of inflammation in response to IL-23 in this model [115]. The *Hh* innate immune IBD model is characterized by mucosal pathology that includes epithelial hyper-proliferation, crypt abscess formation and granulocyte mucosal infiltration [115]. This model illustrates the importance of innate immune pathways in driving *Hh* induced colitis.

Moreover, it has been shown that 129SvEv*Rag2*$^{-/-}$ mice infected with *Hh* develop colitis induced colorectal cancer (CRC), whilst 129 WT mice infected with *Hh* do not develop

CRC [116]. This indicates that carcinoma is driven by innate immune pathways and adaptive immune cells are required to prevent development of CRC. Furthermore, 129SvEv*Rag2*$^{-/-}$ mice infected with *Hh* and transferred with CD4 and CD25 regulatory lymphocytes exhibited less sever IBD and significantly lower risk of colon cancer compared to infected mice that did not receive regulatory lymphocytes. This regulatory effect was mediated by IL-10 as mice injected with regulatory cells that lack IL-10 were unable to inhibit intestinal inflammation or cancer [114,116,117]. Therefore, the *Hh* innate Immune IBD model is a useful tool for the study of bacterially-triggered intestinal inflammation that resembles human IBD and CRC.

1.3.3 *Hh* innate immune signalling

Although a central role for the innate immune activation in the *Hh* induced intestinal inflammation has been recognized, little is known about the innate immune pathways and receptors involved in *Hh* recognition by the host.

In one study, both Nf-κB and ERK intracellular signalling pathways were stimulated in bone marrow-derived macrophages (BMDM) following *Hh* infection [118,119]. Upon challenge with *Hh,* macrophages lacking the p50/p105 subunit of Nf-κB expressed more IL-12p40 compared to WT macrophages [118]. These results suggested an anti-inflammatory effect of the p50/p105 Nf-κB subunits during *Hh* infection [118,119].

Challenging 129SvEv*Rag2*$^{-/-}$ mice with *Hh* in the absence of different Nf-κB subunits showed that the activation of Nf-κB following *Hh* infection induced both anti-inflammatory and pro-inflammatory effects in these mice [120,121]. It was found that

the p50/p105 Nf-κB mediated an anti-inflammatory protective effect, which was consistent with the previous *ex vivo* BMDM studies [121]. In addition, 129SvEv*Rag2*$^{-/-}$ mice deficient with p50/p105 Nf-κB subunit were highly sensitized to *Hh* colitis [118,121]. Conversely, the c-Rel Nf-κB subunit had a pro-inflammatory effect, and the absence of c-Rel in 129SvEv*Rag2*$^{-/-}$ mice, prevented the development of *Hh* induced colitis [120]. Furthermore, macrophages lacking c-Rel failed to express IL-12/23 subunits when cultured with *Hh ex vivo* [120]. Moreover, in IL-10 deficient mice, Nf-κB activation in myeloid cells rather than intestinal epithelial cells was described to be essential for driving the chronic inflammation [122].

Although innate immune PRR have been recognized as a major player in the pathogenesis of inflammatory bowel disease [123], only a few studies have attempted to investigate the receptors involved in the inflammatory response to *Hh,* as well as bacterial recognition by distinct cellular compartments. However, MyD88 signalling in hematopoietic cells, but not in non-haematopoietic cells (intestinal epithelial cells), was found to be essential for the development of *Hh* induced typhlocolitis in both the 129SvEv*Rag2*$^{-/-}$ innate immune IBD model, as well as a T-cell dependent chronic inflammation model [124]. This suggests that TLR-mediated recognition of *Hh* by myeloid cells is pro-inflammatory. Interestingly, while epithelial MyD88 signals were not critical for the development of *Hh* induced typhlocolitis in 129SvEv*Rag2*$^{-/-}$ mice, they were essential for host survival as well as the expression of antimicrobial peptide (AMP) by IEC [124]. In contrast, both T cell immunoregulatory and pathogenic functions during *Hh* infection were MyD88-independent [124].

TLR2 and TLR4 have been suggested to have a role in *Hh* recognition by IEC. The human epithelial cell line (HEK293) transfected with TLR2, but not TLR4, were

responsive to stimulation with *Hh* bacteria [125]. However in contrast to these results, *Hh* induced colitis in both the T cell dependent and T cell independent chronic inflammation models was TLR2 independent [126].

Furthermore, *Nod2*$^{-/-}$ C57BL/6 mice were found to harbour more *Hh* in their terminal ileum compared to WT mice [127]. These data could suggest a role for Nod2 in controlling *Hh* colonization, although this was not associated with any overt pathology [127].

1.3.4 *Hh* infection of epithelial cells *ex vivo*

In vivo, H. hepaticus is intimately associated with the intestinal epithelium of the cecal and colonic crypts [128]. IEC express PRR innate immune receptors and play a major role in host-microbe recognition and influencing mucosal immune response [9]. However, few studies have investigated the nature of *Hh*-epithelial cell interaction, including the innate immune pathways and receptors involved in *Hh* recognition by epithelial cells.

Conflicting data have been reported with different epithelial cell lines. For example, only a weak activation as measured by cxcl2 secretion was seen in murine intestinal epithelial cell line mICc12 following *Hh* infection [129]. In addition, it has been shown that *Hh* activated a strong IL-8 response in TLR2 transfected human kidney epithelial cell line HEK293 [125]. In contrast, *Hh* antagonized TLR-4 mediated cxcl2 release following *E.coli* LPS stimulation in m-ICcl2 and IL-8 secretion following flagellin TLR5 stimulation in Caco-2 human colon epithelial cell line [129]. Moreover, *Hh* flagellin failed to activate human TLR5 when ovarian epithelial cell line CHO K1

transfected with TLR5 were infected with *Hh*, suggesting an immunoevasive potential of the bacterium on epithelial cells [130]. As described above, the *Hh* T6SS is believed to facilitate the bacterial molecular interaction with IEC [95]. The *Hh* TS66 has been implicated in the induction of an anti-inflammatory gene profile in MODE-K intestinal epithelial cell line, as well as limiting *Hh* colonization and epithelial cell internalization [95]. These data suggested an anti-inflammatory effect of *Hh* on IEC [95].

The reasons responsible for these discrepancies are not clear, however a common factor between all these studies is the use of epithelial cell lines, which might not truly reflect the molecular interactions between epithelial cells and *Hh*.

1.4 Growing primary IEC *ex vivo*

1.4.1 Intestinal stem cells (ISC) and the stem cell niche

Two principle ISC types are embedded in the crypt base; $Lgr5^+$ (leucine-rich repeat-containing G protein-coupled receptor-5) columnar stem cells, the most common type found, and the rare $Bmi1^+$ (B lymphoma moloney murine leukemia virus insertion region homolog-1) cells or the "+4 cells", which are found four cells above the base of the crypt (Fig.1) [8,131]. Despite their rarity, $Bmi1^+$ ISC are crucial for crypt maintenance [131,132], and it has been shown by lineage tracing that these cells give rise to the $Lgr-5^+$ ISC and can serve as a stem cell reserve in case of epithelial injury [131].

Stem cells are highly influenced by the surrounding epithelial cells and extracellular

signals forming the ISC niche at the crypt base [133]. Within the ISC niche four essential signaling pathways control ISC stemness (Fig1.2). Extracellular Wnt signals, secreted by Paneth cells in the small intestine and niche myofibroblasts in the colon, positively regulate stemness [134,135]. Activation of the Wnt pathway through binding of Wnt ligand to frizzled receptors and low-density lipoprotein receptor–related protein (LRP) co-receptors found on the cell surface, leads to the inactivation of the destruction complex [136]. The destruction complex, comprising adenomatous polyposis coli (APC), casein kinase I (CKI), glycogen synthase kinase 3 (GSK3) and axin, mediates degradation of β-catenin [136]. When the Wnt pathway is activated the destruction complex is inactivated, thus β-catenin accumulates in the cytoplasm and then eventually translocate to the nucleus [136]. In the nucleus, β-catenin binds the T cell factor/lymphocyte enhancer factor (TCF/LEF) family, forming a transcriptional complex that leads to the activation of Wnt target genes [136]. Wnt pathway activation is essential for controlling the proliferation of crypt-based columnar (CBC) and TA cells, and also for Paneth cell terminal maturation [134].

Similarly, notch pathway stimulation positively influences stemness by enhancing the proliferation of undifferentiated ISC [8]. However, inhibition of the notch pathway leads to differentiation into the secretory cell lineage [8,137]. Ligation of notch surface receptor with the notch ligands Dll1 and Dll4 expressed on Paneth cell surface leads to cleavage of the notch receptor and the formation of free notch intracellular domain (NICD) that subsequently translocate into the nucleus [8]. Within the nucleus, NICD activates target gene transcription by binding to the transcription factor RBP-Jx [8]. The main function of the notch pathway is to control absorptive versus secretory ISC differentiation [8,137]. Epidermal growth factor (EGF) extracellular signals which are

secreted by Paneth cells also positively regulate stemness through stem and TA cell epidermal growth factor receptors [134].

The only pathway repressing ISC stemness is the bone morphogenetic protein (BMP) pathway [138]. BMP is mainly expressed by stromal cells [138] and when bound to its receptor leads to phosphorylation of SMAD transcription factors that activate target genes [139]. BMP suppresses ISC proliferation, and inhibition of BMP signaling using the BMP inhibitor Noggin results in ectopic crypt formation [140].

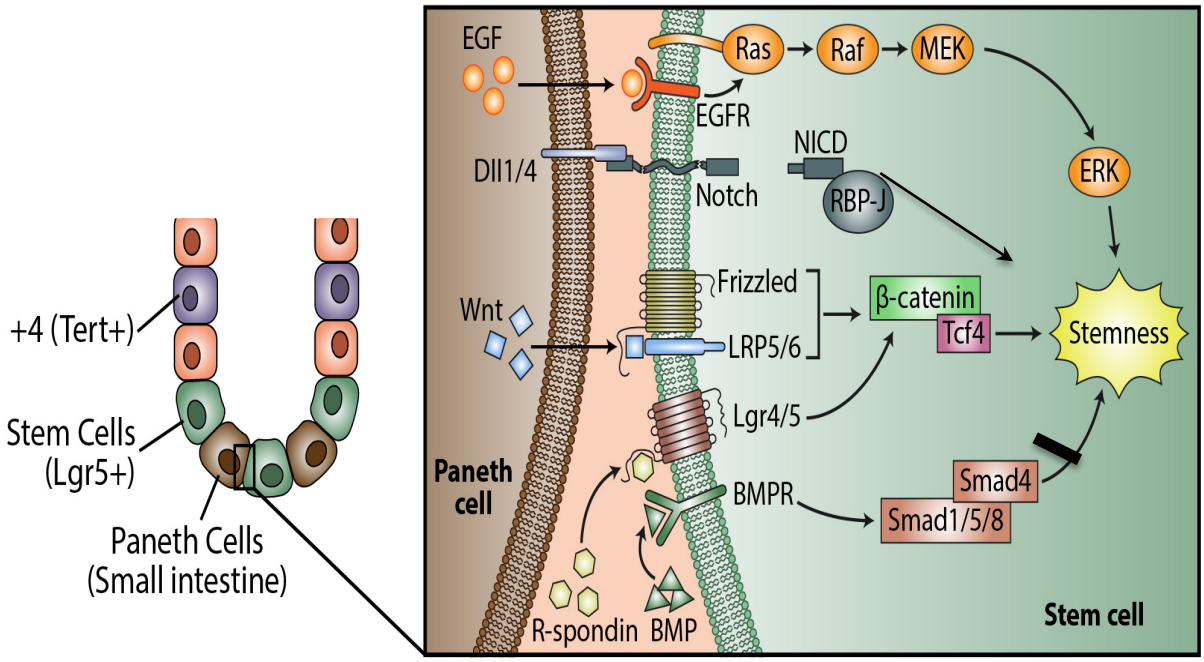


Figure 1.2 Schematic representation of intestinal epithelial crypt and ISC niche. Stem cells are highly influenced by the surrounding epithelial cells and extracellular signals forming the ISC niche at the crypt base. Within the ISC niche three essential signalling pathways (EGF, Notch, and Wnt) positively regulate ISC stemness, whereas BMP negatively regulates stemness. The Wnt agonist R-spondin enhances the Wnt pathway activation in ISC (adapted from Sato T *et al*., 2013) [3].

1.4.2 *In vitro* IEC lines

Many IEC lines have been used for *in vitro* studies of the intestinal epithelium. These have been derived from various sources including normal and cancer tissue, and from different species [141]. For example, Caco-2, T84 and the HT-29, which are among the most widely used IEC lines, were all derived from human colon cancers [141-143]. They express features of enterocytes and are useful for attachment and mechanistic studies [144].

Among the most commonly used rodent *in vitro* cell lines are the immortalized colonic epithelial cell line MCE301 [145], mouse rectal carcinoma CMT93 cells [146], the immortalized small intestine MODE-K cell line derived from mouse duodenum [147], and the immortalized mouse mIC(cl2) line derived from transgenic mice expressing the simian virus (SV40) large T-antigen gene [148].

These *in vitro* IEC lines attach and are able to form confluent and to a certain extent polarized monolayers [149] and although they have been used for many years to study intestinal epithelial biology, many limitations have been recognized. Cancer cell lines for example have numerous undefined DNA mutations that increase with increasing passage number [142,143,150], exhibit differences in the expression of differentiation parameters with increasing passage number, and are a heterogeneous population with respect to different parameters such as transport rate, brush border assembly and other differentiation characteristics [141].

Thus the need for IEC monolayer systems that exhibit fewer limitations and resemble the epithelial lining *in vivo* would offer a better alternative for *in vitro* studies of the intestinal epithelium.

1.4.3 Developing primary IEC organoid cultures

Recently, a new method enabling the isolation and maintenance of primary IEC has been developed. In 2009 Sato et al. [1] described a robust long-term methodology for culturing viable primary intestinal epithelial stem cells [1]. They were able to grow ISC using special culture conditions to generate complex structures termed organoids, which closely resemble the *in vivo* epithelial architecture [1].

Organoids can be formed from isolated intestinal crypts that contain Lgr-5^{+} stem cells, that are then embedded in Matrigel a laminin- and collagen-rich matrix that provides support for the cells [1]. Crypts start growing into three-dimensional spheres 'organoids' under special growth media and distinct media are used for different organoids depending on the source of the intestinal tissue (Fig.1.3)[3]. For example, small intestinal organoids require culture media that contains R-spondin (Wnt agonist), EGF, and noggin (BMP inhibitor), three essential factors that together enhance epithelial proliferation and stemness [1]. To prevent apoptosis that IEC usually undergo when detached from the intestinal basement membrane, organoids are cultured in Matrigel, and a Rho kinase inhibitor (Y-27632), which inhibits anoikis [151], is also added [1]. Exogenous Wnt3A is additionally required for colonic epithelial organoid culture, because Wnt-secreting Paneth cells are absent in colonic epithelium [19].

Primary IEC organoids can be passaged, expanded and maintained for many months [1]. They have been created from different tissue types within the GI tract, such as mouse or human stomach, small intestine and colonic epithelium [3]. They have been also generated from primary human adenomas and colorectal cancers [152]. In addition to organoid formation from adult ISC, they have also been generated from embryonic stem cells (ESC) and induced pluripotent stem (iPS) cells [1,152-156].

Lgr-5^{+} ISC grow to form cysts with a central lumen, lined by a single epithelial layer with multiple crypt like structures projecting outwards (Fig.1.3). The IEC covering the lumen are highly polarized, having their apical brush border oriented toward the lumen and basal surface toward the outside [1]. Using stem cell culture conditioned medium that contains Wnt3A will give rise to organoids containing predominantly ISC [19,152]. When using differentiation culture media that lack Wnt3A, organoids with differentiated epithelial cells will be formed [1,3] and similar to the *in vivo* intestinal epithelial composition Lgr-5^{+} ISC, TA cells, and all four differentiated IEC types are seen [19,152]. These include enterocytes (expressing lactase), goblet cells (Muc2^{+} PAS^{+}), enteroendocrine cells (chromogranin A^{+}), and Paneth cells (expressing lysozymes) [1,152]. Ultrastructural examination shows mucus and endocrine granules, microvilli and intracellular connections of junctional complexes [1,3,156].

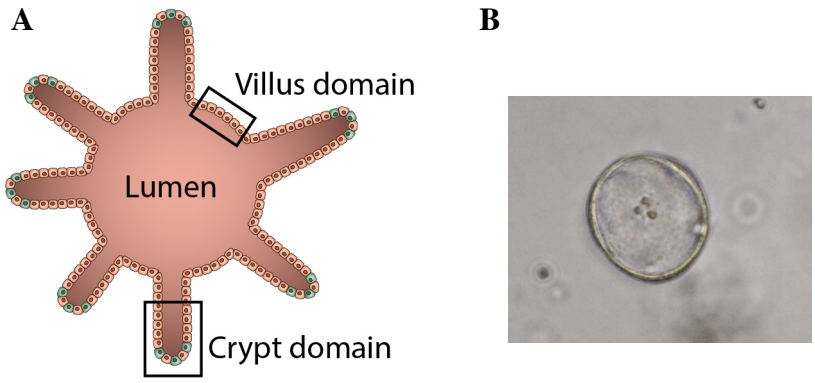


Figure 1.3 (A) Schematic of crypt organoid consisting of a central lumen lined by villus-like epithelium and several surrounding crypt-like domains (adapted from Sato T *et.al*., 2009) [1]. (B) Three-dimensional colonic organoid light microscopy image.

1.4.4 Adapting the 3D primary IEC organoid system into a 2D monolayer

The 3D organoid system is an extremely useful tool to study IEC physiology. However, the 3D architecture and embedding within the Matrigel matrix results in some limitations to study/manipulate the epithelial apical surface and brush border, which faces the lumen of the sphere. Therefore, the benefits of establishing a 2D primary IEC monolayer where both basal and apical epithelial cell surfaces were easily accessible were soon recognized [150].

Recently organoids have been used to expand primary IEC [150] that were then seeded in transwells to form a 2D primary IEC culture system [150]. Transwells are composed of an upper and lower chamber, separated by a permeable membrane upon which the cells are seeded to form the monolayer. The polarized monolayer can then be subjected to various challenges at both the apical and basal surfaces [150].

To generate 2D primary IEC monolayers, colonic organoids cultured in Matrigel were harvested after three days, then dissociated and suspended in 50% L-WRN (L cells expressing Wnt3a, R-spondin3, and Noggin) culture media along with rock inhibitor [150]. They were then seeded into the collagen coated upper compartment of a transwell and appropriate media was added to the lower compartment of the transwell [150]. Using DAPT a γ-secretase inhibitor that induces the differentiation of IEC [157], creating a functional 2D monolayer with similar architecture to the *in vivo* epithelial environment; all types of IEC were present and intercellular tight junctions, polarity, and apical brush borders were observed [150].

1.4.5 Applications of IEC organoids

Culturing viable primary IEC provides an easily accessible research tool that will facilitate the study of many epithelial cell processes, such as cell-cell interactions, host-microbiota interactions, and intracellular signaling pathways, all of which may impact on disease processes [3]. It will also provide many insights into stem cell biology [2,3].

Organoids can be stored by freezing, and can be subjected to analysis with a variety of techniques including: immunohistochemistry and confocal immunofluorescence, gene expression arrays, and mass spectrometry [3,158]. In addition, they can also be infected with recombinant retro- and lentiviruses [159], and gene expression can be manipulated using Cre recombinase-inducible retrovirus vectors [159]. In comparison to the widely used transgenic animal models this technique may provide a fast, cost-effective way to study and manipulate gene expression [159].

In addition to basic research applications, organoids should be very helpful to the medical field, for facilitating disease diagnosis and therapeutic development. For example, the CRISPR/Cas9 genome editing system was recently used to correct the cystic fibrosis transmembrane conductance regulator (CFTR) locus by homologous recombination in organoids derived from cystic fibrosis (CF) patients [160]. The organoid culture system may also be utilized to facilitate the development of intestinal tissue engineering and regenerative medicine, for example transplantation of colonic organoids to repair damaged intestinal epithelium resulted in the formation of normal crypts that replaced the impaired tissue within a few weeks [161]. This provides a promising means to generate engineered intestinal tissue that will serve in allogeneic or autologous transplantation [162].

Finally, by using this technology, organoids from patient samples or biopsies can be

propagated and used to diagnose disease, to test responsiveness to certain medications, and to generate biobanks [3].

1.5 Project aims

The overall aim of this study is to investigate the nature of IEC innate immune response to *Hh* and PRR ligands (PAMPs) in an *ex vivo* setting. 2D primary IEC monolayer system will be used to assess whether IEC are immunologically responsive to *Hh*. IEC have been recently recognized to play a critical role in mucosal immune hemostasis and microbial sensing through the expression of innate immune PRRs. The murine pathogen *Hh* colonizes cecal and colonic epithelial cells and induces both pro- and anti-inflammatory responses without eliciting inflammation in immunocompetent mice, however it can cause severe colitis in susceptible strains. Little has been done to examine the nature of IEC-*Hh* interaction, and its contribution to the host immunological response. It is not clear if or how IEC normally respond to *Hh*, and whether signals arising from IEC in response to *Hh* could be involved in the host subsequent immunological response to the bacteria. Therefore, I have attempted to investigate the IEC-*Hh* interaction *ex vivo* to determine whether isolated primary IEC retain their immune function and are immunologically responsive to *Hh* and PAMPs.

The inability to culture primary IEC *in vitro* in the past limited their use in *ex vivo* functional studies. However, a method for culturing primary IEC in cyst-like 3D structure has been recently described. Therefore, my aim was to develop a 2D-monolayer system that highly resembles the *in vivo* epithelial lining using the 3D organoid culture system, followed by characterization and optimization of these monolayers. The 2D-monolayer system will be used to provide an accessible and controlled *in vitro* co-culture system for investigating the primary IEC response to *Hh* and different PAMPs in isolation of other immune cells.

Chapter 2 – Material and methods

2.1 Conditioned medium

2.1.1 Production of Rspo1-Fc or Noggin-Fc conditioned medium

R-spondin-1 and Noggin conditioned medium were produced in the lab using Human epithelial cell line (HEK293) stably transfected with Rspo1-Fc or Noggin-Fc (kind gift from Prof. Gijs van den Brink). In HEK293T R-spondin1, the R-spondin1 is fused to the mouse IgG 1 Fc- fragment, and in HEK293T Noggin cell line, the Noggin is attached to a Human IgG1 Fc-fragment. HEK293T R-spondin1 cells were cultured in FCS free Advanced DMEM/F12 (Invitrogen) medium and supernatant was collected on the 7th day. The conditioned medium from HEK293T Noggin cells cultured in 5% FCS Advanced DMEM/F12 (Invitrogen) medium and was harvested after 3-4 days. FCS was used to enhance attachment of the cells. Collected supernatant was centrifuged at 3000 rpm (1800g) for 5 minutes. Supernatant from all batches were then filtered using 0.22µm filters (Sigma-Aldrich), and then tested for R-spondin1-Fc and Noggin-Fc using a spotblot analysis technique that detects Fc-coupled proteins.

2.1.2 Spotblot analysis for detection of Fc-coupled proteins

The spotblot technique was used to estimate the concentration of Fc-proteins in the conditioned medium. Samples from each batch of collected R-spondin1-Fc and Noggin-Fc containing conditioned medium were diluted at 1:2, 1:4, 1:8, and 1:16, and then spotted on a nitrocellulose membrane (732-4007, VWR). Mouse IgG (M0725, Dako) was used as a standard for R-spondin with the following concentrations: 200, 100, 50, 25, 12.5, and 6.25 µg/ml. And human IgG1 (M0725, Dako) was used as a standard for Noggin with the following concentrations: 200, 100, 50, 25, and 12.5

ng/µl. Once the membrane was dried, 3% BSA/TBS (3% BSA, 60.58 g/L Tris-HCl, 87.66 g/L NaCl pH 7.6) was used to block nonspecific sites. The membrane was then washed, and incubated with the appropriate HRP conjugated antibody; goat anti-mouse IgG-HRP 1:1000 (170-6516, Bio-Rad) for Rspo1-Fc, and Rabbit anti-human IgG-HRP 1:1000 (P0214, Dako) for Noggin-Fc at room temperature for 30 minutes. After 3 washes (10 minutes each) with TBS-T (0.025% Tween-20), membranes were developed with ECL western blotting substrate (Thermo Scientific). Signals from samples were compared to signals from standard to estimate the concentration of the Rspo1-Fc and Noggin-Fc in the conditioned medium.

2.1.3 Wnt-3A conditioned medium

To produce Wnt-3A conditioned medium, L Wnt-3A (ATCC CRL-2647) cells transfected with a Wnt-3A expression vector were used. Cells were cultured in Dulbecco's modified Eagle's medium (DMEM, Invitrogen) containing 10% fetal bovine serum. The first batch of Wnt-3A conditioned medium was collected on day 4, and on day 7 the second batch was collected. Both collected batches were mixed and sterile filtered. β-catenin stabilization assay was used to measure Wnt-3A bioactivity in the conditioned medium.

2.1.4 β-catenin stabilization assay

β-catenin stabilization assay was used to measure Wnt-3A bioactivity in the conditioned media. The assay is based on the effect of Wnt intracellular signalling which leads to the stabilization of β-catenin. L929 cells seeded in 48-well plate were stimulated with 100%, 50%, 20%, 5% and 1% Wnt-3A containing conditioned medium. Recombinant Wnt-3A (rWnt3a, Peprotech) was used as a standard (at a concentration of: 200 ng/ml, 20 ng/ml, 2 ng/ml). After 2 h and 4 h of incubation at

37°C, cells were washed and lysed using 50 µl RIPA buffer (50mM Tris HCL pH 8, 150mM NaCl, 1% Igepal, 0.5% sodium deoxycholate, 0.1% SDS) containing a protease inhibitor cocktail (Roche). Cell lysates were centrifuged at 13000rpm (14000g), 4°C, for 10 min. Protein concentrations were determined by the BCA protein assay kit (Thermo scientific) according to manufacturer's instructions. Sample concentrations were normalised to35µg and sample buffer (60 mM Tris HCl pH 6.8, 2% SDS, 0.02% Bromophenol Blue, 5% β-Mercaptoethanol, all from Sigma Aldrich) was added. Samples were boiled at 95°C for 5 min and stored at -20°C. Samples were then blotted with Mouse Anti-β-Catenin antibody (BD biosciences 610154) as described in 2.9.2. For loading control α-tubulin antibody (1:2000, rabbit α-tubulin, Cell Signalling) was used.

2.2 Organoid culture

2.2.1 Mice

C57/BL6 (B6) and B6*MyD88*$^{-/-}$ mice were bred and maintained under specific pathogen-free (SPF) conditions in accredited animal facilities at the University of Oxford.

2.2.2 Crypt isolation and cell culture

Harvested mouse colons were flushed once with cold PBS. The whole colon was opened longitudinally, and washed with cold PBS. The tissue was cut into 2-4 mm pieces, and further washed 10 - 20 times by pipetting up and down cold PBS using 10-ml pipette. Tissue was washed until supernatant was clear. The tissue fragments were incubated in 2 mM EDTA/ PBS at 4C for 90 minutes under constant shacking. After removal of EDTA/ PBS, the tissue fragments were vigorously suspended by using a 10-ml pipette with ice cold 10% FCS/ PBS. The first fraction of the supernatant was discarded; the sediment was resuspended again for three more times with ice cold 10%FCS/PBS and supernatant was collected after vigorous suspension. The supernatant collected was passed through a 70-µm cell strainer (BD Falcon) to remove residual material. Isolated crypt fractions were centrifuged at 800 rpm for 5 minutes to separate crypts from single cells. The final fraction consisted of enriched crypts and was used for culture. The supernatant was removed and the pellet resuspended in Advanced DMEM/F12 (Invitrogen) media and centrifuged once more. The crypts were resuspended in 20 µl/ well Matrigel (BD 356231, Corning) and plated in 24-well plates. After polymerization of Matrigel, 400 ml of crypt culture medium was added. The medium is composed of 10% R-spondin, 20% Noggin, and 20% Wnt3-A conditioned medium in Advanced DMEM/F12 (Ad-Df) with 1x Pen/Strep, 10mM Hepes, 1x Glutamax (Invitrogen) supplemented with 50ng/ml epidermal growth factor (EGF) (PMG8043, Invitrogen), 10µM Rock-Inhibitor (Y-27632 dihydrochloride monohydrate, Sigma Aldrich), 1mM N-Acetyl-L-Cysteine (A9165, Sigma Aldrich), 1X B27 supplement (17504-044, Invitrogen) and 1X N2 supplement (17502-048 , Invitrogen). Culture medium was changed every 2-3 days.

2.2.3 Passaging of organoids

For organoid passage, organoids were resuspended in TrypLE (12605-036, Invitrogen), and after 2-4 minutes incubation at room temperature they were mechanically dissociated by vigorous pipetting into small cell aggregates. Dissociated crypts were then resuspended in fresh Matrigel (BD 356231, Corning) and seeded into 24 well plates. Passage was performed every 4-6 days with a 1:3 split ratio.

2.3 2D-Monolayers

2.3.1 Developing 2D-monolayers

To form monolayers of primary intestinal epithelial cells, spheroids were first expanded in 3D cultures, and then dissociated into single cells and seeded on collagen coated wells. Wells were collagen coated by adding Collagen I, Rat tail (Thermo Fisher Scientific A10483-01) according to manufactures instructions (85µl into 5ml Acetic Acid 0.02M; 200 µl/ well), and incubated for 1 h at room temperature. They were washed 3 times with PBS. Spheroids were recovered from Matrigel (BD 356231, Corning) by first washing with PBS, and then dissociated using TrypLE (12605-036, Invitrogen) by vigorous pipetting (using a 1,000 ml pipette) for 2 minutes at RT. The trypsin was then inactivated using Advanced Dulbecco's modified Eagle's medium/F12 media (Invitrogen). The cells were then re-suspended in crypt culture medium. On average, spheroids from three wells of a 24-well plate were plated into a single well (24-well plate) in 800 µl of media.

2.3.2 Monolayer treatments and infection

On day 1 post seeding fresh media was added, according to the type of cells needed: Supplemented advanced DMEM/F12 (Ad-Df) (Invitrogen) without conditioned medium to differentiate the cells containing following supplements: 50ng/ml (EGF) (PMG8043, Invitrogen), 10μM Rock-Inhibitor (Y-27632 dihydrochloride monohydrate) (Y0503-5MG , Sigma Aldrich), 1mM N-Acetyl-L-Cysteine (A9165-5G , Sigma Aldrich), 1X B27 supplement (50X), serum free (17504-044, Invitrogen) and 1X N2 supplement (100X) (17502-048 , Invitrogen) or full supplemented medium that additionally contains 10% R-spondin, 20% Wnt3-A, 20% Noggin conditioned medium to maintain stemness. On day 2 post seeding, experiments were performed. Additional treatments included: DAPT γ-secretase inhibitor (565784, Calbiochem) was added prior to MUC2 staining.

Prior to infecting monolayers with *H. hepaticus*, fresh media without antibiotics (Pen/Strep) was added on day 1 post seeding. Monolayers were infected on 2nd day post seeding. At the time of infection, bacteria were added at a multiplicity of infection (MOI) of 100:1. Plates were centrifuged at 1200 rpm (300g) for 5 min to synchronize the infection. After coincubation for the indicated time points, the supernatants were removed, cleared by centrifugation, and stored at -20°C for further analysis. For RNA preparation, cells were scraped from the incubation plates in 200μL/ per well of RLT (QIAGEN) with 2-mercaptoethanol.

2.3.3 Assays of innate immune activation through PRRs

Innate immune PRRs stimulation was examined by coincubating the cells with various well-defined PRR ligands, including pure bacterial flagellin from S. *typhimurium* FLA-ST a TLR5 ligand (InvivoGen), the lipopeptide structural analogue Pam3CSK4 a TLR1/2 ligand (InvivoGen), and ODN 1668 CpG oligonucleotide with the sequence 5'-TCCATGACGTTCCTGATGCT-3' a mouse-specific TLR9 ligand (InvivoGen), ultrapure *E. coli* LPS (ALX-581-007, Enzo) a TLR4 ligand, poly (I:C) (Sigma Aldrich, P1530), and the synthetic NOD2 ligand muramyl di-peptide (MDP) (InvivoGen). Monolayers were generated as described above. After this, the stimuli were added at the concentrations and for the times indicated in the figure legends. After coincubation, supernatants and cells were harvested as described above for qPCR and ELISA.

2.4 Immunostaining

Primary IECs were seeded in 24-well plates on round 13-mm coverslips (Thermo Scientific) pre coated with collagen I, Rat tail (A10483-01, Thermo Fisher Scientific). Monolayers were washed with phosphate-buffered saline (PBS) and fixed with 4% paraformaldehyde (PFA) in PBS for 20 min at RT. The cells were then washed three times (5 minutes each) with cold PBS. The cells were then blocked and permeabilized with PBS containing 10% donkey or goat serum, 5% bovine serum albumin and 0.5% saponin for 1 hour at RT. Monolayers were washed three times and incubated with primary antibody for 1-2 hour at RT (Table 1). Monolayers were washed 3 times (5 minutes each) with PBS and then incubated with Alexa Fluor conjugated species specific secondary antibodies for 1 h at room temperature (Table 1). Cover slips were washed three times in PBS and then stained with 4', 6 Diamidino-2-phenylindole

dihydrochloride (DAPI, Sigma Aldrich) to visualize nuclei and mounted with Vectashield mounting media (P36935, Thermo Fisher Scientific). Staining was visualized with an Inverted Olympus FV1200.

2.4.1 *Hh* internalization immunostaining

Monolayers seeded on coverslip were coincubated with *Hh* at an MOI of 100:1 for the indicated time points and plates were centrifuged at 1200 rpm (300g) for 5 min to synchronize the infection. After coincubation, nonadherent bacteria were removed, by washing with PBS (3 times), and cells were fixed for 20 minutes with 4% PFA in PBS. To stain external *Hh,* monolayers were first blocked and stained without Saponin. Cells were blocked with 10% goat serum/5% bovine serum albumin in PBS for 1 hour at room temperature. Adherent surface *Hh* were stained with primary antibody Rabbit anti-*H. hepaticus* antiserum (1:300) and the secondary antibody goat anti-rabbit immunoglobulin G antiserum coupled to Alexa Fluor 555 (1:400) without saponin. Monolayers were then blocked and stained again with saponin to permeabilize the cells and stain internalized *Hh*. Monolayers were blocked with 10% goat serum/5% bovine serum albumin/ 0.5% saponin in PBS for 1 hour at room temperature. Internalized *Hh* were stained with primary antibodies including: Rabbit anti-*H. hepaticus* antiserum (1:300), and lysosomal stain Rat anti-lamp-1 (1:200). Secondary antibodies include: goat anti-rabbit immunoglobulin G antiserum coupled to Alexa Fluor 488 (1:400) and goat anti-rat coupled to Alexa Fluor 633 (1:400). Cells were counterstained for DNA using DAPI (1:25,000 in PBS) and were mounted on microscope slides. The specimens were examined using an Inverted Olympus FV1200.

.

2.4.2 Antibodies and stains

A summary of antibodies and stains used for Immunostaining are displayed in Table 1.

Antibody	**Source**	**Dilution**
Rabbit -α-ZO-1	Invitrogen	1:100
Mouse- α-E-cadherin	BD Biosciences	1:100
Rabbit- α-*Hh*	In-house	1:300
Rabbit-α-mouse Ki67	Abcam	1:200
Rat-α-LAMP-1	Santa Cruz Biotechnology	1:200
Rabbit-α-Mucin-2	Santa Cruz Biotechnology	1:200
WGA AF647	Invitrogen	1:250
Goat-α -mouse-AF488	Invitrogen	1:400
Goat-α-rabbit-AF555	Invitrogen	1:400
Goat-α-rabbit-AF488	Invitrogen	1:400
Goat-α-rat-AF633	Invitrogen	1:400
Stains	**Source**	**Dilution**
DAPI	Sigma Aldrich	1:25,000
Phalloidin-AF647	Cell Signaling	1:100

Table 1 Summary of antibodies and stains

2.5 Helicobacter hepaticus

2.5.1 Culture

Culture of *H. hepaticus* NCI-Frederick isolate 1A (Hh1A; strain 51449; American Type Culture Collection) was achieved on blood agar plates containing trimethoprim (5μg/ml), vancomycin (10 μg/ml) and polymyxin B (25 IU/ml) (TVP; all from Oxoid, UK) in ajar placed under microaerophilic conditions (10% H2, 10% CO2, balance N2) at 37°C for two days (D.71 Maloy KJ. 2006). For liquid cultures, *H. hepaticus* was inoculated at OD600 of 0.05 into vented Erlenmeyer flasks (Corning) containing liquid growth media (TSB supplemented with TVP and 10% FCS (Gibco, Invitrogen)). The flask was then transferred into an anaerobic jar and placed under microaerophilic conditions and incubated at 37°C on a shaking platform (150rpm). Fluorescent Live/Dead™ assay kit (Molecular Probes) was used to assess viability according to the manufacturer's instructions.

2.6 Chemokine detection in cell supernatant using ELISA

MIP-2 (cxcl2) mouse ELISA development kit (900-K152; PeproTech) was used according to the manufacturer's instructions. Nunc maxisorp plates were coated with 100 μL of capture antibody in PBS. Plates were incubated at room temperature overnight and then washed 3 times with PBS/0.05%Tween. Plates were blocked with 300 μL of 1%BSA/PBS for 1h at room temperature. Plates were incubated with samples for 2h at room temperature. Plates were then washed, incubated with detection antibody for 2h, followed by washing (3 times) and then incubated with Avidin-HRP conjugate for 30 minutes. After incubation with Avidin-HRP plates were washed 4 times and incubated with ABTS substrate (A3219, Sigma Aldrich). A colour reaction

developed after 15-20 min, the reaction was stopped with 2M H_2SO_4 and plates were read at 405nm with wavelength correction set at 650nm.

2.7 Analysis of mRNA expression by qPCR

2.7.1 RNA extraction from cell isolates

For RNA isolation, cell isolates were resuspended in 200µl RLT lysis buffer (QIAGEN) with 2-mercaptoethanol, and processed using the QIAGEN RNeasy Mini Kit (Cat.: 74104). Lysates were mixed with ethanol (70%) and loaded onto RNeasy mini column (QIAGEN). RNA was isolated according to the manufacturer's instructions, including a DNase digest. RNA was eluted in water and amounts were quantified using a NanoDrop (Thermo Scientific). RNA was stored at -20°C. cDNA was synthesized through reverse transcription, using oligo-dT primers (Sigma) and Superscript III reverse transcriptase (Invitrogen).

2.7.2 Quantitative PCR (qPCR)

Quantitative PCR analysis was performed using the Taqman system. 4µL of cDNA were used for a final reaction volume of 20µL. For Taqman qPCRs, Eurogentec qPCR MasterMix reagents (RT-QP2X-03) were used. *Hprt1, cxcl2* primer and Taqman probes were obtained from Applied Biosystems. Taqman assays were performed according to the manufacturer's instructions and detected using a Chromo4 detection system (MJ Research). Gene expression was normalized to *Hprt1* expression and gene expression levels were calculated using the Pfaffl method [163] (D.135 Pfaffl M, Nucleic acid res. 2001).

2.8 Western blot

2.8.1 Sample preparation

Cells were lysed in 50 µl RIPA buffer (50mM Tris HCL pH 8, 150mM NaCl, 1% Igepal, 0.5% sodium deoxycholate, 0.1% SDS) containing a protease inhibitor cocktail (Roche). Cell lysate were centrifuged at 13000rpm (~14000g), 4°C, for 10 min. Protein concentrations were determined by the BCA protein assay kit (Thermo scientific) according to manufacturer's instructions. Sample concentrations were normalized and sample buffer (60 mM Tris HCl pH 6.8, 2% SDS, 0.02% Bromophenol Blue, 5% β-Mercaptoethanol, all from Sigma Aldrich) was added. Samples were boiled at 95°C for 5 min and stored at -20°C.

2.8.2 Western blot

15µl of samples were loaded in a 10% SDS-PAGE gel and transferred onto a PVDF membrane (GE-Healthcare), which had been pre-activated in methanol. Membranes were blocked in 5% milk/PBS/0.5% Tween-20 (Sigma Aldrich) for 1 hr at room temperature. Membranes were then incubated with primary antibody (1:1000 mouse anti-β-catenin antibody (610154, BD biosciences), or 1:1000 phospho-p44/42 MAPK Rabbit antibody (9101, Cell Signaling), or 1:1000 phospho- NF-kB p65 Rabbit mAb (3033, Cell Signaling) at 4°C overnight. The next day, the membrane was washed thoroughly with PBS 0.5% Tween-20 (3 times, 10 minutes each) before incubating with peroxidase conjugated secondary antibody anti-Rabbit IgG (1:5000, Santa Cruz) or anti-Mouse IgG (1:3000, Cell Signaling) for 1-2 h at room temperature. After extensive washing to remove non-specifically bound secondary antibody samples were incubated with SuperSignal West Femto (Thermo Scientific) according to the manufacturers's instructions. Membranes were developed using medical X-ray film

(Fuji) and a XOGraph (XOGraph healthcare). Membranes were washed 4 times in PBS/0.5% Tween-20 for 10 min each. Membranes were then blocked as described above and incubated with loading control antibody (1:2000, rabbit α-tubulin, Cell Signaling) at 4°C overnight. Membranes were washed and incubated with secondary antibody as described above. Finally, membranes were developed with ECL Western blotting substrate (Thermo Scientific).

2.9 Statistical analysis

Statistical analysis was performed using Prism (GraphPad software, La Jolla CA USA). The nonparametric Mann–Whitney test was used for all statistical comparisons. Differences were considered statistically significant at a *p*-value of less than 0.05.

Chapter 3 – Culturing primary IEC in an *ex vivo* system

3.1 Introduction

Until recently, intestinal epithelial cell (IEC) lines have been the only available system to study host-microbial interactions between IEC and intestinal bacteria *in vitro*. These cell lines have been derived from different species and various sources, including normal and cancer tissue [141]. Although some colonic epithelial cell lines form confluent polarized monolayers that resemble primary IEC *in vivo*, major differences with the *in vivo* epithelial cell lining exist [141]. Cancer cell lines for example exhibit many undefined DNA mutations, and variations in the expression of differentiation parameter such as transport rate and brush border assembly with increasing passage number [142,143]. Therefore, the need for improved primary IEC culture models has long been recognized [1,150].

Sato et al. recently described a robust long-term culture model for developing intestinal crypt-like structures of primary mouse or human IEC. The method involves culturing Lgr-5^+ intestinal stem cells (ISC) with a selection of growth factors that enable the generation of crypt-villus structures, called organoids. This technique has greatly advanced the IEC biology research field, and allowed long-term culture and passage of primary IEC [1].

Although the organoid culture system provides a novel tool to culture IEC *ex vivo*, the luminal orientation of IEC brush border makes it difficult to manipulate/access the cell apically. Thus, the need for a 2D primary IEC monolayer system was recognized.

Primary IEC undergo anoikis and die as soon as they are separated from the epithelium, as they lose their cell-to-cell contact and anchorage protein interactions

[18]. Thus, developing primary IEC monolayers has proven to be challenging, and was only possible with seeding a substantial number of viable cells to allow the formation of cell-to-cell contact and overcome anoikis [18].

In a recent study, primary IEC monolayers were created through adaptation of the 3D-organoid culture system [150]. This model is based on the expansion of primary ISC in the 3D organoid system using 50% L-WRN (L cells expressing Wnt3a, R-spondin3, and Noggin) conditioned media (CM) as source for the 2D monolayers [150]. They managed to develop functional, differentiated IEC monolayers on a transwell system that displayed marked transepithelial electrical resistance (TER) [150]. The IEC attached and polarized appropriately, and stained positively for the IEC markers villin and E-cadherin, as well as the ZO1 tight junction marker and differentiated epithelial cell markers, such as the enteroendocrine cell marker chromogranin A and goblet cell marker lectin UEA-1 [150]. In addition to displaying features of *in vivo* polarized colonic epithelium these functional IEC monolayers were responsive to immunological stimuli, such as TNF-α, IL-1β and heat-killed *E. coli*, which stimulated pIgR expression and IgA transcytosis [150].

Studies of IEC-microbe interactions have been limited by the lack of appropriate primary IEC monolayer models *ex vivo.* Therefore, the main aims of this chapter were first, to establish the primary IEC 3D organoid culture system, and second, to develop and optimize 2D primary IEC monolayers that could be used as a model to study innate immune response of primary IEC *ex vivo* to bacterial pathogen, *Helicobacter hepaticus* (*Hh)* as well as PRR ligands (PAMPs).

3.2 Results

3.2.1 Growing primary IEC *ex vivo*

Wnt is considered the main pathway controlling stemness and stem cell proliferation at the crypt base intestinal stem cell niche *in vivo* [164]. The localized production of Wnts at the crypt base by Paneth cells (small intestine) and mesenchymal tissue to support the crypt base columnar (CBC) stem cells creates a Wnt-gradient along the crypt axis, which allows the differentiation of cells as they migrate away from the crypt base [136]. Small intestinal organoids that were derived from a Wnt reporter mouse (Axin2-LacZ) managed to form crypt-villus structures with a differentiated and heterogeneous stem cell population, even when cultured in Wnt-deprived media, due to the strong Wnt signal at the crypt base created by Paneth cells [19]. When the same organoids were cultured in Wnt3-rich media the crypt-villus structure was lost and rounded organoids with a homogenous stem cell population developed instead [19].

In colonic organoid culture however, the Wnt-producing niche cells are absent and Wnt is provided in the culture media, which promotes stemness rather than differentiation, and smooth rounded organoids with a homogenous population of stem and progenitor cells form [3,19]. In the absence of Wnt-rich media colonic organoids lose their rounded shape and start budding, as the IEC lose their stemness and differentiate, they eventually die [3]. In the absence of homogenous Wnt signaling the crypt like structures bud away from the lumen and stem cells localize to the crypt base [3].

Primary IEC were grown and expanded *ex vivo* using the organoid culture system method originally developed by the Clevers lab [1]. Colonic crypts were cultured in Advanced DMEM/F12 medium containing growth factors; R-spondin1, Noggin, Wnt3-A and EGF, along with the Rho kinase inhibitor Y-27632 that inhibits anoikis

[151]. Wnt signaling is vital for the crypt proliferation [164,165], R-spondin-1 enhances the Wnt pathway through binding the Lgr-5 receptor, augmenting crypt proliferation [166] and EGF also promotes ISC proliferation [167]. Noggin is a bone morphogenetic protein (BMP) antagonist and is essential to maintain stemness in long-term cultures of the organoids [140].

R-spondin-1 and Noggin growth factors were produced in the lab using stably transfected HEK293T cell lines (kind gifts from Prof. Gijs van den Brink). The cells were either transfected with R-spondin1-Fc, where R-spondin1 is fused to the mouse IgG1 Fc fragment, or Noggin-Fc, where Noggin is fused to a Human IgG1 Fc-fragment (Prof. Gijs van den Brink lab). R-spondin1 and Noggin concentrations in culture supernatants were evaluated using a spotblot analysis technique that detects Fc-coupled proteins (Fig 3.1). Thus, two-fold dilutions of samples and standards (mouse IgG or human IgG1, respectively) were spotted on a nitrocellulose membrane and detected using the appropriate HRP conjugated antibody. Membranes were developed with ECL substrate and sample signals were compared to signals from the standard to estimate the concentration of the R-spondin1-Fc and Noggin-Fc in the conditioned medium.

For R-spondin1, spotblot analysis showed a similar protein signal to the standard protein signals in all samples, with a 1:1 R-spondin1 dilution found to correspond to approximately 100μg/ml mouse IgG (Fig 3.1). Similarly, spotblot analysis of recombinant Noggin produced a strong signal, with a 1:8 Noggin dilution corresponding to approximately 100ng/μl human IgG1 (Fig 3.1).

To produce Wnt-3A, L cells transfected with a Wnt-3a expression vector were used (L-Wnt3A) [168]. A β-catenin stabilization assay was used to measure Wnt-3A

bioactivity in the conditioned media, as Wnt intracellular signaling leads to the stabilization of β-catenin [136]. L929 cells were seeded in 48-well plates and stimulated with 100%, 50%, 20%, 5% and 1% conditioned media or recombinant Wnt-3A standards (200, 20 or 2 ng/ml). After two hours of incubation cells were washed, lysed using RIPA buffer and samples were blotted with anti-β-catenin antibody (Fig 3.2). The results of the blot suggest that 5% conditioned medium equates to approximately 200ng/ml rWnt3a (Fig.3.2).

Murine colonic crypts containing $Lgr5^{+}$ - CBC cells from wild type C57BL/6 (WT) mice were isolated and cultured as described in the materials and methods chapter (materials and methods 2.1.6). After harvesting murine colons, tissue was cut into 2-4mm pieces and crypts were isolated using EDTA based chelation and vigorous pipetting. Supernatant was collected and passed through a 70-µm cell strainer then centrifuged to acquire pure single cells /crypts fraction. These crypts were then embedded in a laminin-containing matrix termed Matrigel [1]. Laminin is naturally found at the crypt base supporting IEC *in vivo* [169], and hence it provides the mechanical support needed by IEC to overcome anoikis *in vitro* [1]. 20µl of crypt-containing Matrigel was seeded in 24-well plates and incubated at 37°C, which leads to the polymerization of the Matrigel. 50% conditioned media (50% CM) that contains 10% R-spondin, 20% Noggin, 20% Wnt3-A, as well as 50% Advanced DMEM/F12 (Ad-Df) with supplements (EGF, Rock-Inhibitor) was used in the colonic organoid culture system.

In culture, the IEC crypts form cyst-like structures with a central cavity that resembles the intestinal lumen [1]. The cyst is formed of a single polarized epithelial layer, with the apical brush border facing the inside and the basolateral site in contact with the

Matrigel (Fig 3.3 B). Stem cells at the base of the crypt proliferate in the presence of stem cell maintenance growth factors (Fig 3.3 B). Stem cell proliferation pushes the differentiated cells upward until they die via apoptosis and are shed into the central cavity (Fig 3.3 B). Therefore, the IEC organoid process highly resembles the *in vivo* crypt dynamics.

In the presence of stem cell maintenance factors (50%CM), uniformly rounded organoids mainly composed of proliferating stem cells form. In the absence of stem cell maintenance factors (0%CM) cells start differentiating resulting in organoid budding (Fig 3.3 B). Using the stem cell maintenance factor cocktail (containing R-spondin, Noggin and EGF with or without Wnt3a), primary IEC stem cell organoids can be cultured for a long periods of time without losing their phenotype and karyotype [1,3]. They are usually passaged every 3-4 days, and fresh media is added every second day to maintain the stemness [1]. During passage, organoids are dissociated into single crypt domains that seal and form new organoids, therefore a constant expansion of primary IEC growth is maintained (Fig 3.3 A).

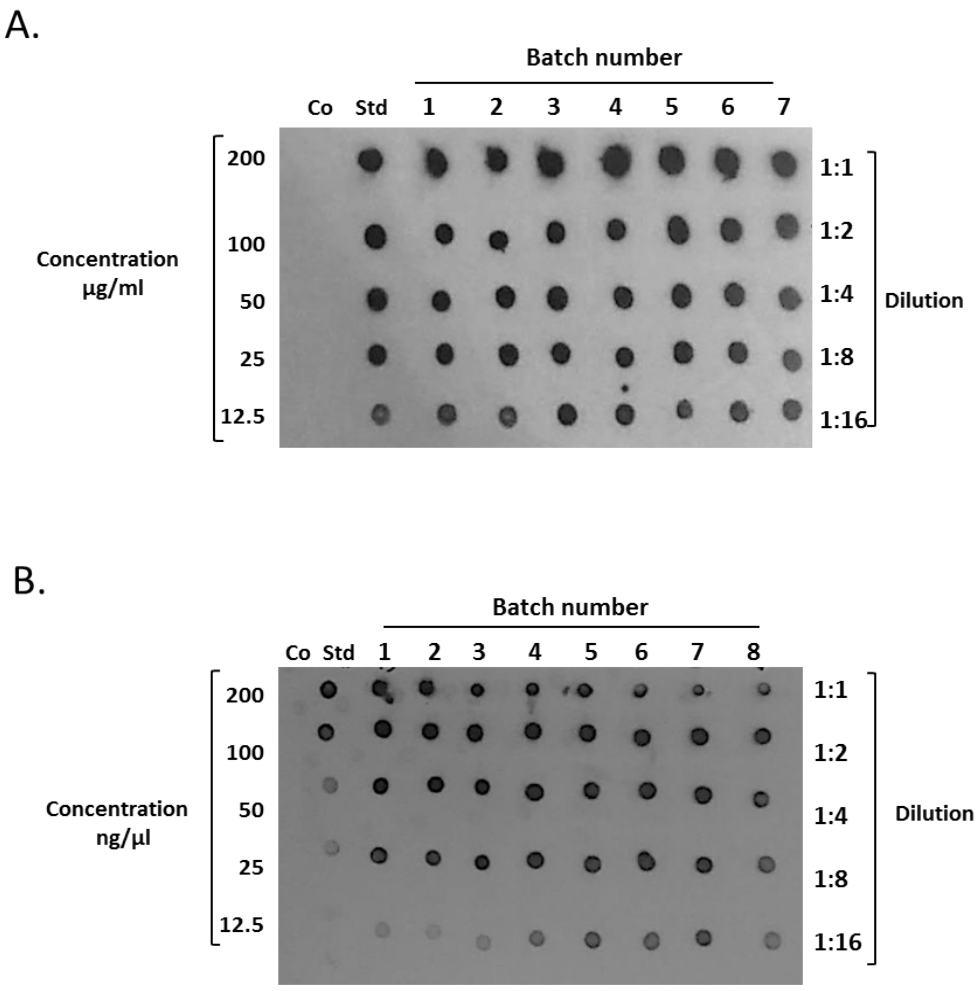


Figure 3.1 Stably transfected HEK293T produce R-spondin, and Noggin. HEK293 R-spondin1 cells were cultured in Ad-Df without FCS and supernatant was collected after 7 days (A). Hek293T Noggin cells were cultured in 5% FCS Ad-DF and supernatant harvested after 3-4 days (B). Collected supernatants from all batches were filtered and tested for R-spondin1 and Noggin using a spotblot analysis (A) and (B), using anti-mouse IgG-HRP for R-spondin1, and anti-Human IgG-HRP for Noggin. Control: TBS-T/BSA, standard: Mouse IgG (for R-spondin), Human IgG1 (for Noggin). Membranes were developed with ECL western blotting substrate and signals from samples were compared to signals from standard to estimate the concentration of the Rspondin1-Fc and Noggin-Fc in the conditioned media. Results are representative of 6 similar experiments.

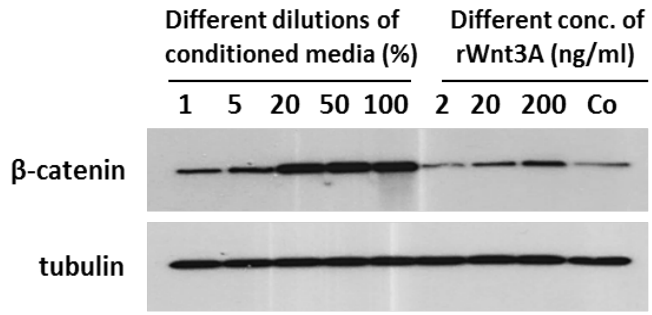
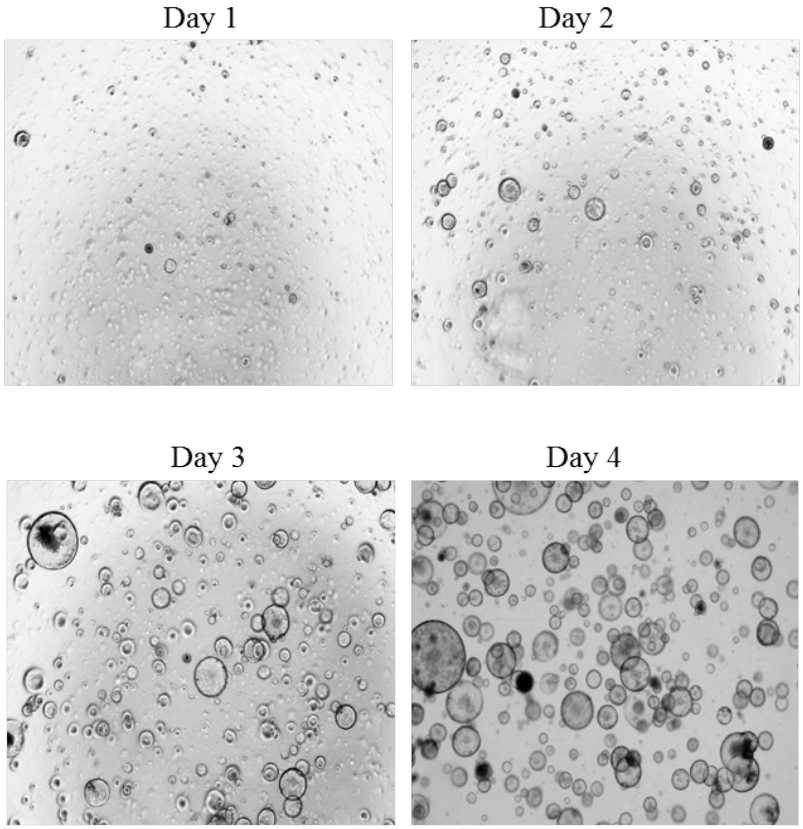


Figure 3.2 L Wnt-3A cells express Wnt3A. L929 cells were stimulated with different dilutions (100%, 50%, 20%, 5% and 1%) of Wnt-3A conditioned media, and different concentrations (2, 20, 200 ng/ml) of recombinant Wnt-3A were used as a standard. After 2h of stimulation samples were lysed using RIPA buffer and protein concentrations were normalized. Equivalent amounts of total protein were loaded on SDS-PAGE gel and blotted for active β-catenin (top bands). Signals from different sample dilutions were compared with signals from standard. As a loading control, α-tubulin reactivity was measured (bottom bands). Results are representative of 6 similar experiments.

A.



B.

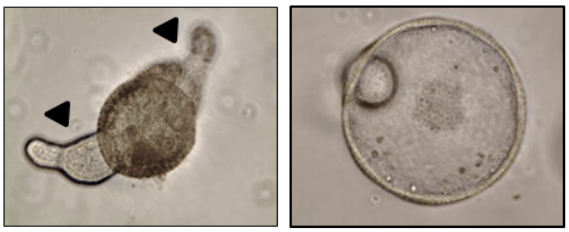


Figure 3.3 Time course of colonic organoid growth. Primary IEC colonic organoids from WT C57BL/6 mice cultured in Matrigel with 10% R-spondin, 20% Wnt3a, and 20% Noggin. Magnification in (A) 4x (B) single organoid, 40x. Arrows indicate budding crypts.

3.2.2 Adapting 3D organoid culture system to form 2D-monolayers

The 3D organoid culture system is a tool that enables the growth of primary IECs *ex vivo* for extended periods of time. However, within the 3D organoids the epithelium polarizes with the apical side facing towards the inside of the sphere, which makes the apical surface rather inaccessible for manipulation. *In vivo, H. hepaticus* colonizes the mucus layer of the cecum and colonic epithelium, in close proximity to the apical border of the IEC [128]. Hence, accessing the apical side of IEC is crucial to understand how *H. hepaticus* interacts with the epithelium. Therefore, the 3D organoid culture system was adapted to form 2D monolayers, which allowed the accessibility of the IEC apical border.

To create IEC monolayers, 3D organoids were cultured with 50% CM for 3-4 days. Spherical organoids were then harvested, washed, and then mechanically disrupted to obtain single crypts/cells. Single crypts/cells were re-suspended in 50% CM, and then seeded onto a collagen-coated 24-well plate. 50% CM was used for stem/progenitor cell monolayers, whereas 0% conditioned media, with or without specific treatments, were utilized to push seeded cells into differentiation. Using this protocol, we found that IEC exhibited good attachment onto the collagen-coated wells at day 1 post seeding (Fig 3.4).

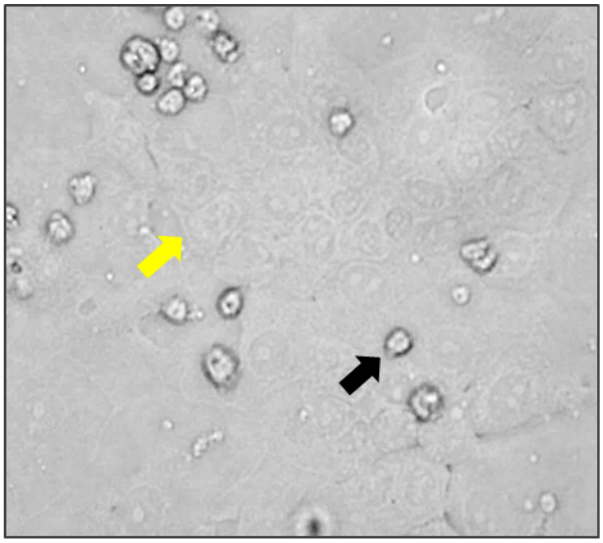


Figure 3.4 Adapting 3D organoid culture system to form 2D monolayers. 3D Organoids were cultured in 50% CM for 3-4 days, then harvested and mechanically disrupted. Single cells were re-suspended in 50% conditioned media before seeding onto a collagen coated surface. A representative image taken day 1 post seeding. Cells attached to the surface (yellow arrow); floating detached cells (black arrow). Magnification (10x).

3.2.3 Characterization and optimization of the 2D monolayers

Next we assessed if the IEC grown in 2D monolayers could polarize and differentiate after losing the 3D architecture and Matrigel support of the organoid culture. In order to use these monolayers in functional *ex vivo* studies, characterization and optimization of the model was required, and further work on determining the optimal growth conditions and organoid numbers required to generate confluent monolayers was needed. Immunofluorescent staining was used to assess epithelial cell markers, monolayer composition (differentiated IEC), polarization (location of key tight junction and apical and basolateral markers), as well as IEC proliferation and expansion capacity post seeding.

Monolayer cells were grown on collagen-coated cover slips and immunostained with different epithelial cell markers. The fungal toxin Phalloidin binds and stabilize F-actin filaments of the cell cytoskeleton [170]. These cytoskeleton microfilaments play an important role in the assembly of intestinal tight junctions as well as maintaining epithelial cell shape [171]. Phalloidin-FITC conjugate were used to stain and visualize F-actin filaments organization in IEC. Confocal images demonstrate a normal epithelial distribution of the F-actin [172-174], as cross-linked fibers of the actin cortex on the inner side of the cell membrane and long stress fibers traversing the cytosol are seen (Fig 3.5 A).

Furthermore, confocal images show near-confluent IEC monolayers expressing E-cadherin, an epithelial adhesion molecule which stains the basolateral epithelial membrane, and Zonula Occludens1 (ZO1), a tight junction protein [175], at the expected location (Fig3.6). Wheat germ agglutinin (WGA) lectins selectively bind N-acetylglucosamine and N-acetylneuraminic acid (sialic acid) glycoproteins, and are rapidly internalized into the cytoplasm of IEC [176,177]. It is known that IEC apical

surface express complex glycoconjugates such as glycoproteins that are involved in microbial adhesion [178]. Therefore, surface sialic acid can be an important determinant of cellular interactions with bacteria [179]. As shown in (Fig.3.5 B), WGA stained cell surface as well as internalized cytoplasmic glycoproteins, indicating high expression of N‑acetylglucosamine and sialic acid by primary IEC which could facilitate bacterial adhesion. Collectively, these data show that primary colonic IEC seeded to form 2D monolayers, attached basolaterally to the collagen-coated surface and formed cell-to-cell contact through adhesion molecules and tight junction proteins. Thus, polarized IEC monolayers that express appropriately distributed epithelial markers develop.

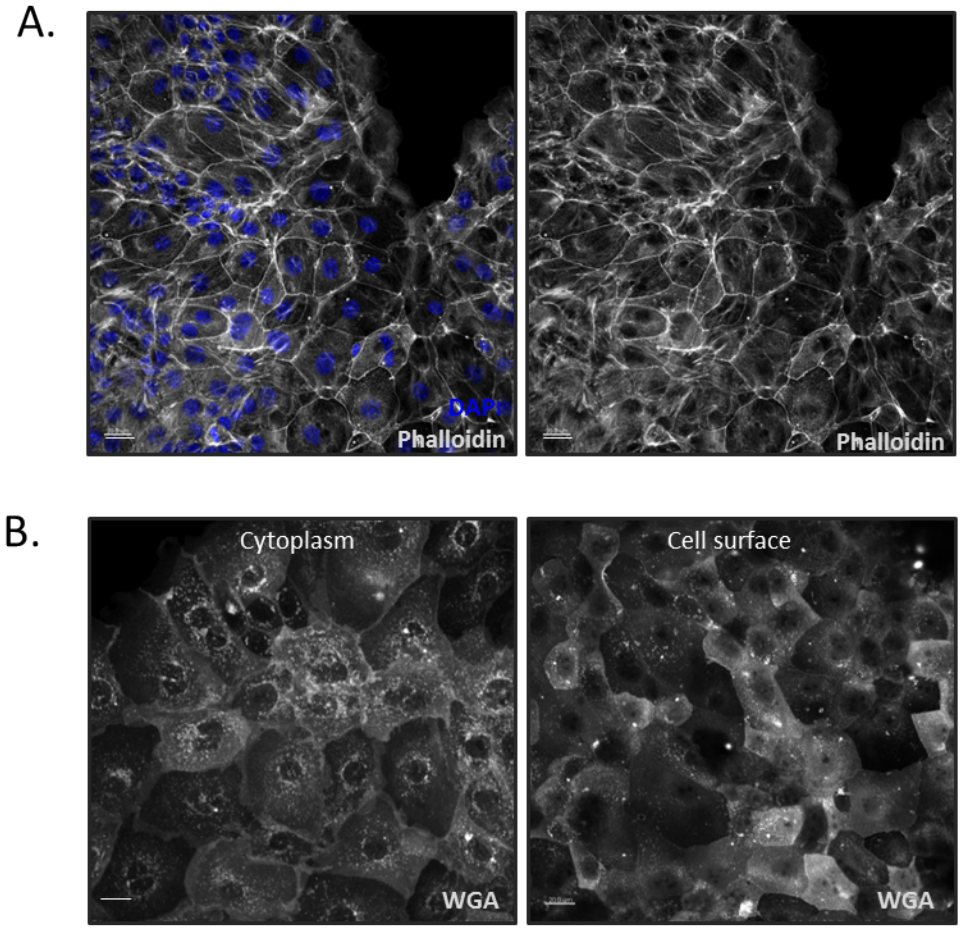


Figure 3.5 Primary IEC monolayers stain for Phalloidin and WGA. Primary colonic IEC organoids were disrupted and seeded onto a collagen coated cover slip. On day 2 post-seeding, cells were fixed and stained with (A) DAPI (blue) and Phalloidin (grey), (B) Wheat Germ Agglutinin (WGA) (grey). Magnification: 40x. Scale bar: 20µm. Representative images from 2 repeats for each condition. Results are representative of 3 similar experiments.

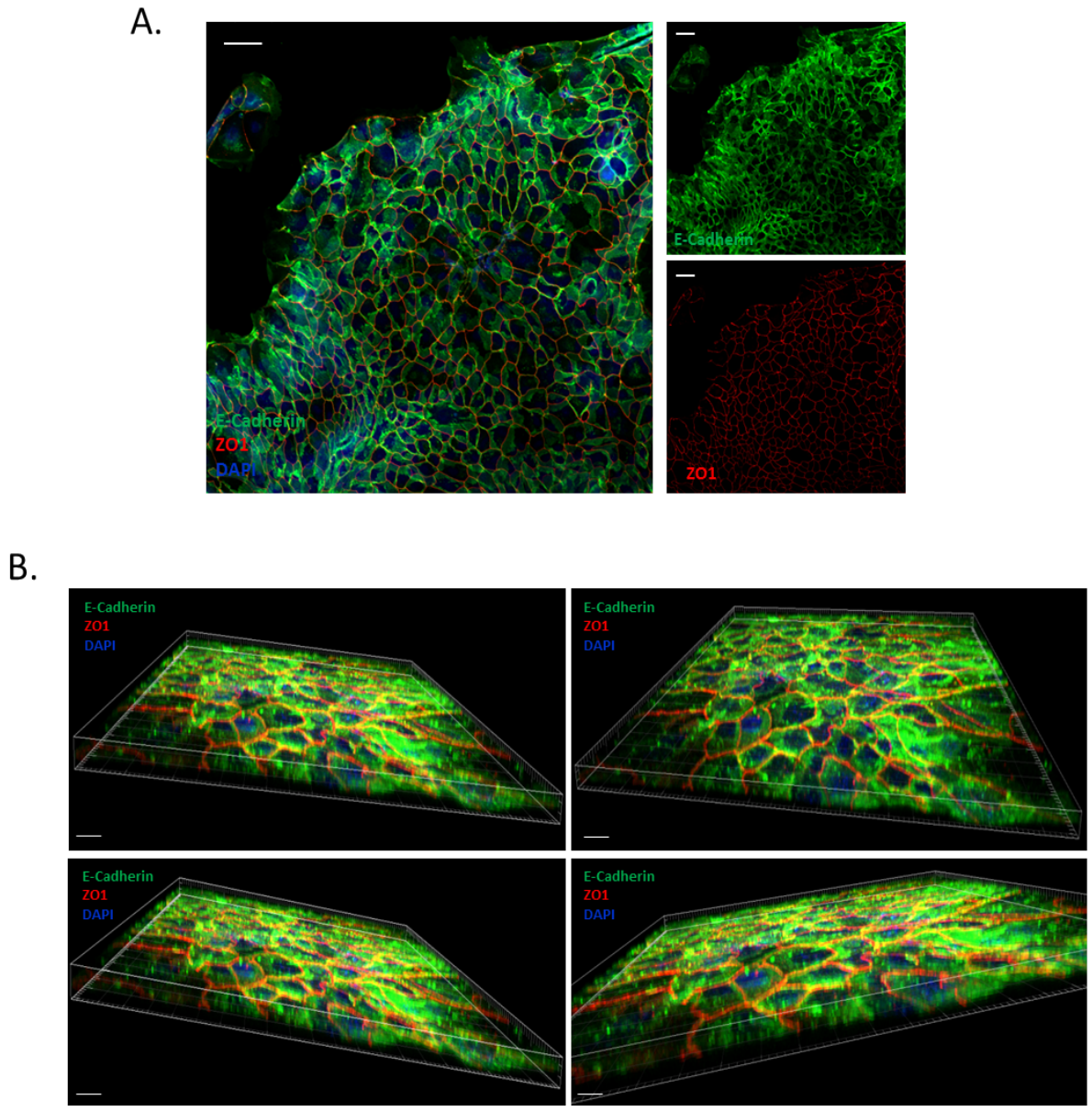


Figure 3.6 Monolayer polarization expressing apical and basolateral markers. WT primary IEC were seeded on a collagen coated cover slip. On the second day post seeding cells were fixed and stained with ZO-1 (red), E-cadherin (green) and DAPI (blue) (A) and (B). Magnification: 20x, Scale bar: 50µm (A). Z-stacks reconstructed from confocal images. Magnification: 60x, Scale bar: 10µm (B) Representative images from 2 repeats. Results are representative of 3 similar experiments.

3.2.3.1 Optimizing the 2D monolayer system

To determine the optimal number of crypt cells derived from 3D organoid cultures needed to give rise to confluent 2D IEC monolayers, different numbers of organoids (generated following 3-4 days of culture in 24-well plates as outlined above) were seeded onto collagen-coated coverslips and were immunostained with DAPI to allow cell density comparison. All 2D monolayers were treated with 50% CM at the time of seeding, then 0% CM on day 1 post-seeding to allow differentiation. 2D IEC monolayers were fixed and stained on day 2 post-seeding. We found that seeding three wells of a 24-well organoid culture gave rise to near-confluent 2D monolayers, which could not be achieved by seeding 1 or 2 wells of organoid-derived crypt cells (Fig 3.7).

To find out if primary IEC maintained their proliferative capacity within the 2D monolayer cultures, cell proliferation was evaluated by Ki67 staining. Monolayers were treated with 50% CM at the time of seeding, and were either switched to 0% CM or maintained with 50% CM at day 1 post-seeding, in order to compare proliferative capacity between the two conditions. Proliferating $Ki67^+$ IECs were present in both 50% and 0% CM monolayers (Fig 3.8). However, 50% CM-treated monolayers displayed significantly more proliferating $Ki67^+$ IEC, suggesting that a higher proportion of progenitor/stem cells were present in these monolayers (Fig 3.8).

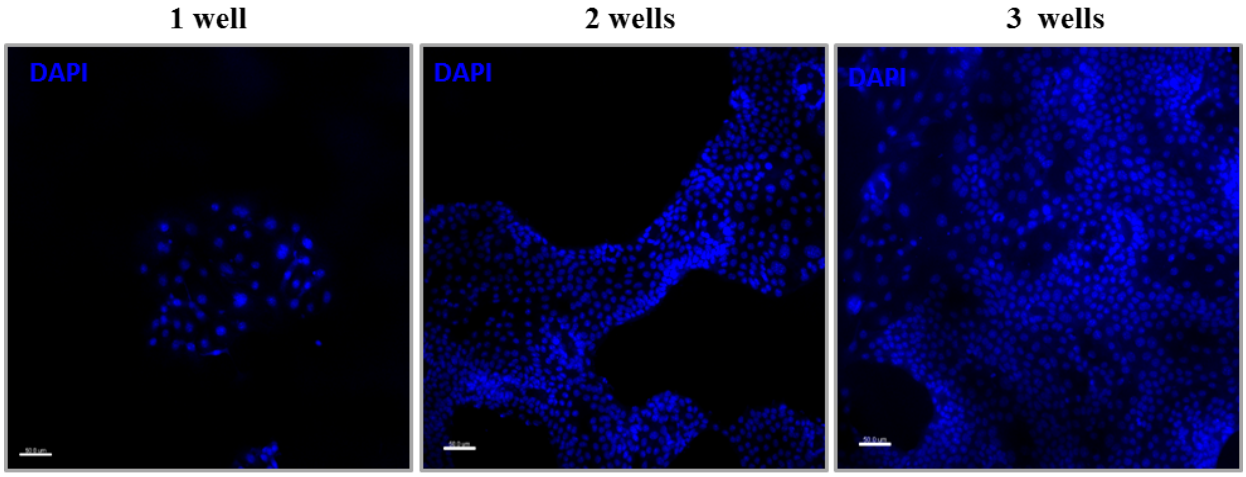


Figure 3.7 Seeding 3 wells (24-well plate) of 3D organoids achieves near-confluent 2D IEC monolayers. Different numbers of 3D organoids (1, 2 or 3 wells of the 24-well organoid cultures) were disrupted and seeded onto a collagen-coated cover slip. Two days post-seeding cells were fixed and stained with (DAPI) (blue) to evaluate monolayer confluence. Magnification: 20x. Scale bar: 50µm. Representative images from 2 repeats for each condition. Results are representative of 3 similar experiments.

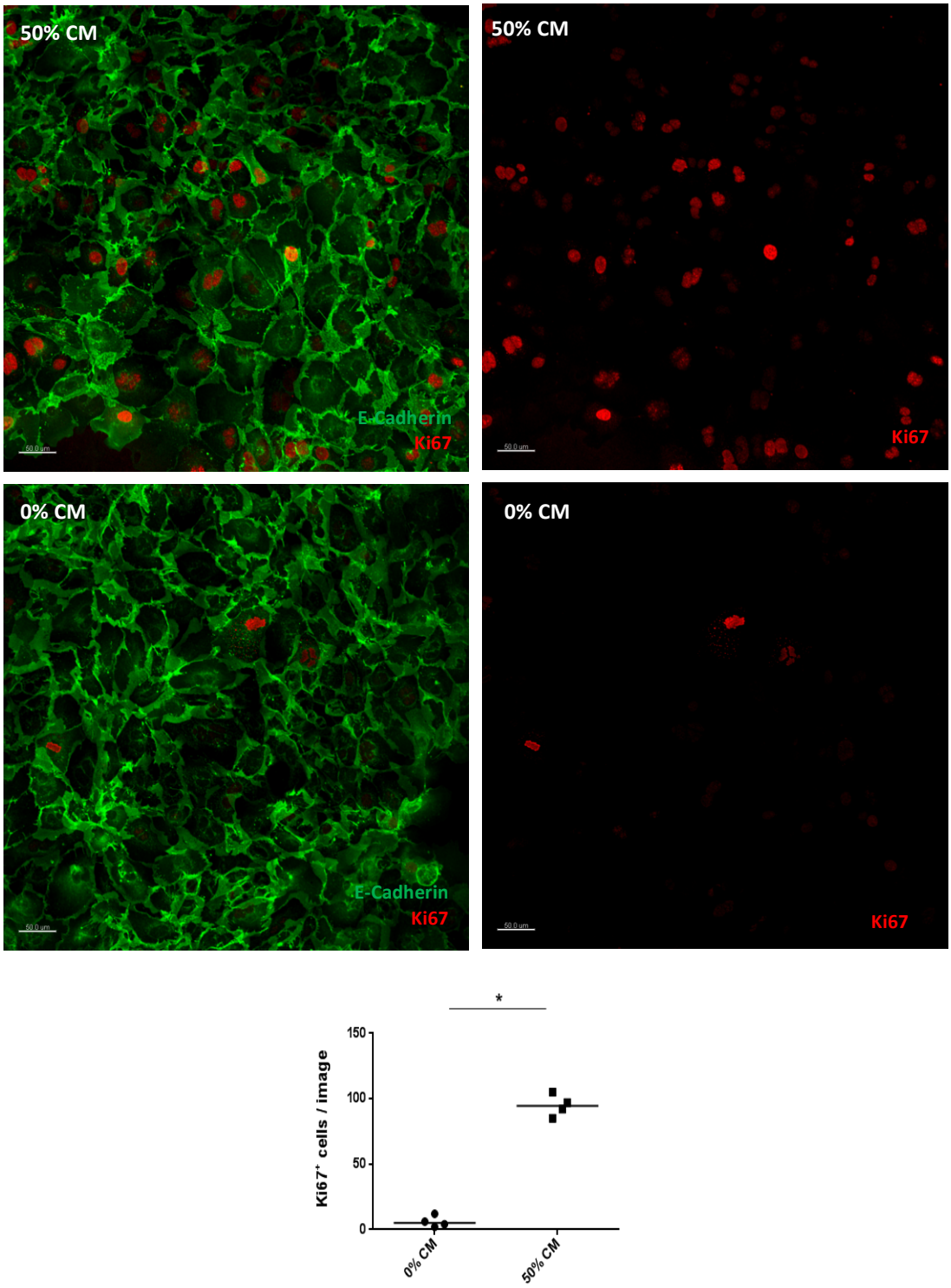


Figure 3.8 Primary IEC maintain their proliferative capacity post-seeding when treated with 50% conditioned media. Monolayers were treated with 0% or 50% CM and, on day 2 post-seeding, monolayers were fixed and stained for Ki67 (red) and E-cadherin (green). Magnification: 20x. Scale bar: 50µm. Representative images from 2 repeats for each condition. Staining was done 3 times. Cells positive for Ki67 were enumerated in on average of 4 field images from each condition. Each symbol represents a single field and horizontal lines represent medians. Statistical analysis was performed using the non-parametric Mann-Whitney test, *P<0.05.

3.2.3.2 Monolayers contain differentiated epithelial cells

Mucus constitutes an integral part of the epithelial niche *in vivo* [20]. *H. hepaticus* has been shown to colonize the inner mucus layer reaching the mid upper part of the colonic crypt where it resides in close proximity with the intestinal epithelial cells [128]. We therefore assessed the presence of mucus and mucus-secreting goblet cells in the primary IEC cultures. Staining for MUC2, one of the major proteins present in mucus, was performed to find out if monolayers had differentiated goblet cells, and to visualize the mucus layer. On day 1 post-seeding onto collagen-coated wells, 50% CM was replaced with 0% CM with or without DAPT (γ- secretase inhibitor). DAPT was used as it inhibits notch pathway, leading to secretory lineage cell differentiation [157]. We found that, under both conditions, monolayers exhibited patchy staining for MUC2 (Fig 3.9). However, relative to control cultures, DAPT-treated monolayers showed significantly more mucus stained goblet cells, and, at higher magnification, the presence of discrete mucus-containing vesicles was apparent (Fig 3.9B). In contrast, mRNA expression levels of MUC2 showed no difference between 2D monolayers cultured in the presence and absence of DAPT (Fig 3.9C). Moreover, a mucus layer could not be visualized on the 2D monolayers with the MUC2 stain.

Taken together, these data indicate that our 2D monolayer model contains MUC2 expressing goblet cells and that the differentiation of goblet cells from primary IEC may be enhanced by treatment with DAPT.

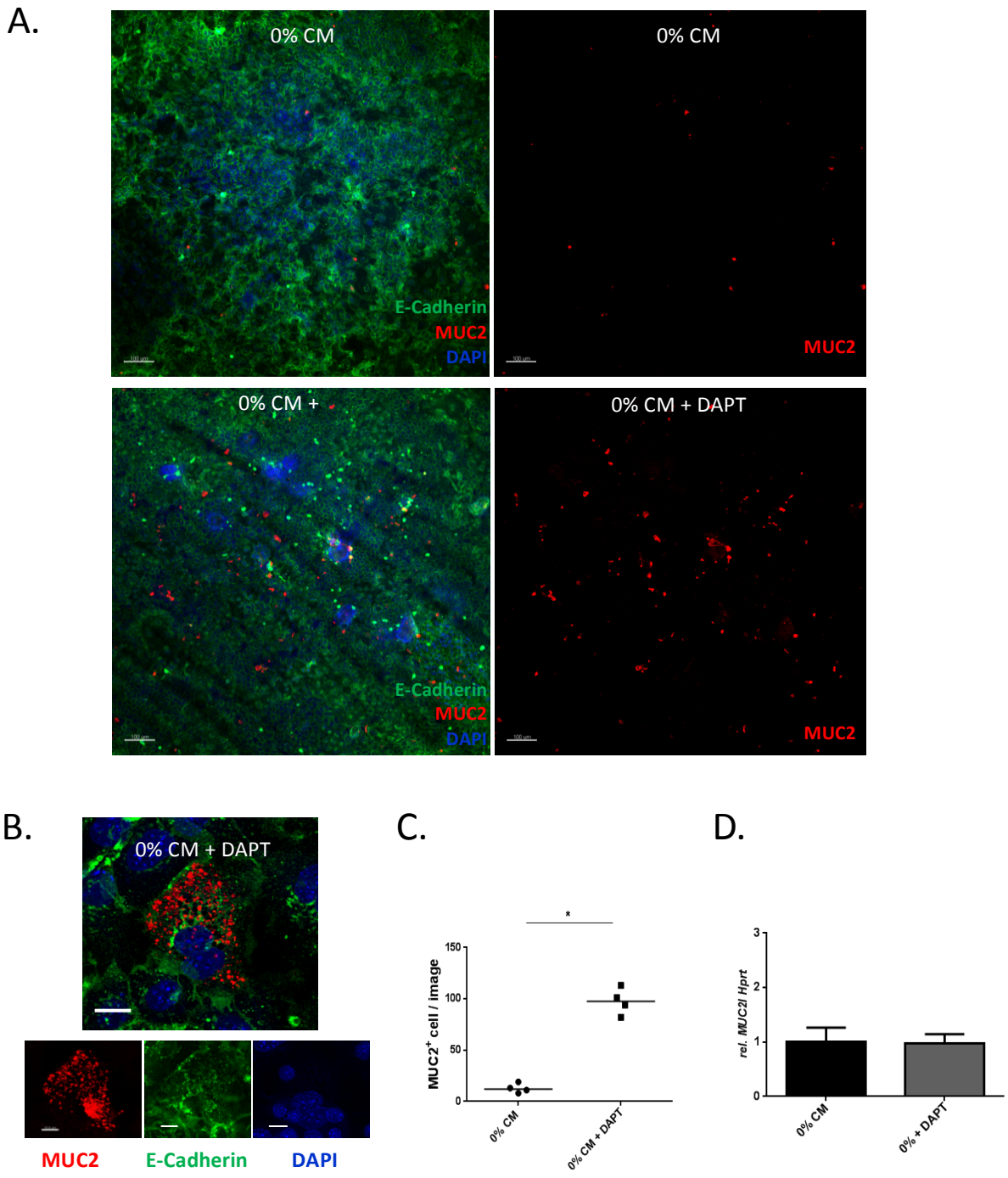


Figure 3.9 IEC monolayers contain differentiated goblet cells. (A,B) 2D primary IEC monolayers were cultured in 0% CM from day 1 post-seeding, with or without DAPT (γ- secretase inhibitor). On day 2 post-seeding, monolayers were fixed and stained for MUC2 (red), E-cadherin (green), and DAPI (blue). Magnification: (A) 10x, (B)100x. Scale bar: (A) 100µm (B) 15µm. Representative images from 2 repeats for each condition. Staining was done 2 times. (C) Cells positive for MUC2 were enumerated in on average of 4 fields from each condition. Each symbol represents a single field and horizontal lines represent medians. All statistical analysis was performed using the non-parametric Mann-Whitney test, *P<0.05. (D) mRNA expression levels of MUC2 were measured by qPCR and normalized to *Hprt1*. Error bars represent ± SD of mean (pooled data from 2 independent experiments, n=5 per group).

3.3 Discussion

Significant progress has been made in culturing primary IEC. Short term enterocyte culturing has been reported in previous studies [180,181], but a long term primary IEC culturing system was not possible before Sato et al. and described the 3D organoid culture system [1,156]. To overcome rapid enterocyte apoptosis *ex vivo*, this system is based on three main components. First, the use of intestinal crypts that contain self-renewing $Lgr5^{+}$-stem cells capable of expanding while still retaining their original characteristics. *In vivo*, $Lgr5^{+}$-CBC stem cells replenish dying epithelial cells, and Lgr4 and -5 depletion affects crypt survival as *Lgr5* and *Lgr4* gene deletion in murine gut leads to rapid demise of crypts due to a defect in *Wnt* target gene expression [182,183]. Second, a collagen-based 3D matrix scaffold (Matrigel) provides cell support and allows the formation of the crypt 3D structure *ex vivo*. Finally, culturing these cells in a unique growth factor cocktail and addition of a Rho kinase inhibitor provides the essential factors required for stem cell maintenance in culture.

We managed to isolate and grow primary IEC crypts in Matrigel with the necessary growth factors. They underwent budding and, with further expansion, organoids developed. Spheroids were seen in culture just a few days after crypts were isolated and cultured, which indicates their responsiveness to the growth factors produced using transfected cells.

Although the 3D organoid culture system provides a novel method to propagate primary IEC *ex vivo* for long periods of time, it does not allow easy accessibility of the apical epithelial surface. Epithelial monolayers are therefore desirable to enable the analysis of the nature of *H. hepaticus* interaction with IEC *in vitro*. Using a

modification of the organoid protocol, we managed to create primary 2D IEC monolayers that displayed typical features of colonic epithelial cells.

Confluence has a major impact on monolayer functionality and differentiation state. In a recent study, cell density was found to affect IgA transcytosis, and less cellular differentiation correlated with lower cell density [150]. In order to use this model in functional studies, confluent monolayers had to be achieved. Organoids harvested from 3 wells of a 24-well plate were found to be the optimum number required to create near-confluent monolayers. Characterization of the monolayers revealed a single cell layer when stained with E-cadherin.

We further evaluated whether these 2D monolayers retained characteristic markers of polarized epithelial tissue. Cells were found to express the epithelial marker E-cadherin, and the tight junction marker ZO1 at the appropriate location. Enterocytes cell surface and actin filaments were stained using WGA and Phalloidin. Our data showed a normal epithelial F-actin filament distribution as well as a high expression of N‑acetylglucosamine and sialic acid by primary IEC which could potentially serve as microbial receptors facilitating bacterial adhesion. It has been shown that colonic epithelial sialic acid play a role in Salmonella enterica serovar Typhi (S. Typhi) IEC adherence, as the treatment of Caco-2 epithelial cell line with neuraminidase, that significantly reduced surface sialic acid by cleaving the sialyl residues, diminished the adherence of S. Typhi by 41% [179]. Thus, surface carbohydrate moieties might play a role in *Hh* adhesion.

A recent report showed that primary IEC 2D monolayers seeded on transwells, stained positively for goblet cells and other differentiated epithelial cell markers [150]. Further characterization using staining MUC2 indicated that monolayers had differentiated

goblet cells that produce mucus. We also observed that the treatment with DAPT, a γ-secretase inhibitor that inhibits the notch pathway promoting secretory epithelial cell differentiation, increased the number of goblet cells. However, no extracellular mucus was seen with MUC2 florescent images. This may be due to the fragile nature of mucus that makes it difficult to stain *in vitro*, or it may have been washed away during staining. Another possibility would be that not enough mucus was secreted to form a mucus layer due to the low frequency of goblet cells or possibly because these cells lacked the ability to secrete it.

These results illustrate the potential of primary IEC to grow as polarized 2D monolayers on a collagen-coated surface. We were able to show that these monolayers express epithelial cell markers and typical structural features of the colonic epithelium, as well as differentiated goblet cells. Together, these data suggest that our model system may provide a good tool to study the nature of *Hh* – IEC interaction *ex vivo*.

Chapter 4 – *Helicobacter hepaticus (Hh)* infection of primary IEC

4.1 Introduction

Helicobacter hepaticus (Hh) was first isolated from liver of mice with chronic hepatitis and was identified as the cause of liver tumors in A/JCr mice [89,184]. This microaerophilic, enteric bacterium is a common constituent of the murine enteric microflora that naturally colonizes the cecum and colon and causes a lifelong, persistent colonization without any pathology in WT mice [185,186].

Hh is a spiral, flagellated bacterium, which penetrates the mucus reaching the deeper inner mucus layer where it lies in close proximity to the apical surface of IEC [128]. Although it lives in close proximity without eliciting inflammation in most immunocompetent mouse strains, *Hh* is not considered a commensal species because it elicits potent, specific antibody and T cell responses, both locally and systemically [106-108]. In addition, it can trigger severe pathological immune responses in the large intestine and liver of immune-deficient or IL-10-deficient mouse strains [107,108,113,114]. *Hh* has therefore been described as a 'pathobiont' with pathogenic potential [95].

In WT mice infected with *Hh,* a balance between strong pro-inflammatory and immune regulatory T cell responses develops. The bacterium elicits a specific $CD4^+$ Th1 and Th17 inflammatory response that is controlled by a Treg mediated anti-inflammatory response in an IL-10 dependent manner [106]. When this IL-10 anti-inflammatory response is lost such as in IL-10 deficient mice, a severe $CD4^+$ T cell mediated intestinal inflammation develops [107,110,111,187]. Furthermore, *Hh* infection of lymphocyte deficient 129SvEv*Rag2*$^{-/-}$ mice also elicits an innate immune

typhlocolitis [114], showing that *Hh* triggers potent innate inflammatory responses in the gut.

Despite its ability to elicit such potent intestinal inflammation, little is known about the intracellular signaling pathways and receptors involved in the inflammatory response to *Hh.* Strong inflammatory responses, as measured by cxcl2 secretion, were seen following the culture of murine macrophages J77 with live *Hh* or soluble *Hh* components [129]. *Hh* has been reported to activate both the Nf-κB and ERK signaling pathways in BMDM, however activation of the p50/105 and c-Rel Nf-κB subunits have been linked to differential responses to *Hh* [118,119]. Indeed, *Rag*$^{-/-}$ mice lacking p50/105 subunit developed exacerbated *Hh* induced colitis, suggesting an anti-inflammatory role, whereas, *Rag*$^{-/-}$ mice lacking c-Rel exhibited reduced intestinal inflammation, which suggests a pro-inflammatory effect of the c-Rel subunit [119-121].

TLRs are believed to play an important role in *Hh* recognition by the host, mediating the inflammatory response against the bacterium. The development of *Hh* induced intestinal inflammation was dependent on the TLR adaptor protein MyD88 signaling in myeloid cells in both the 129SvEv*Rag2*$^{-/-}$ innate immune model as well as the T-cell dependent chronic inflammation model [124]. This suggests a TLR-mediated recognition of *Hh* in myeloid cells is essential for chronic inflammation. Although non-haematopoietic (IEC) MyD88 signaling was insufficient to induce intestinal inflammation following *Hh* infection of 129SvEv*Rag2*$^{-/-}$ mice, their potential contribution to disease remains unclear [124].

IEC form a crucial part of the mucosal barrier and have been described to play a major role in the microbial immune recognition and triggering of subsequent responses [9]. Because *Hh* can induce both inflammatory and anti-inflammatory responses by the host, and although it has a pathogenic potential, it still manages to colonize the epithelium without eliciting an inflammation in immunocompetent mice, thus it provides a good tool to dissect IEC immune responses. However, the nature of *Hh* – IEC interactions and the signaling pathways and immune receptors involved has not been thoroughly investigated.

Few previous studies described the interaction of *Hh* with IEC *in vitro,* however these studies were mainly done using murine and human IEC lines, such as MODE-K, m-IC_{cl2} and HEK923 cells [95,125,129]. Furthermore, different data have been reported with different cell lines as some described *Hh* to activate IEC, while others described an anti-inflammatory effect of *Hh* on IEC. Thus, there are conflicting accounts of the consequences of innate immune recognition of *Hh* by IEC and a better understanding of the innate immune signals and receptors involved in *Hh* recognition could provide further insight into microbiota-induced colitis.

The aim of this chapter was to investigate the nature of IEC immune responses towards *Hh* using a primary IEC *ex vivo* culture model. Whether *Hh* is internalized into IEC and whether IEC are immunologically responsive to *Hh* and PAMPs were the main questions we addressed in this chapter.

4.2 Results

4.2.1 *Hh* surface adhesion and internalization into WT primary IEC

In vivo, *Hh* is known to be closely associated with murine cecal and colonic epithelial cells [128]. In order to investigate the effects of *Hh* on IEC, we had to first assess whether the bacterium exhibited good adhesion with our *in vitro* derived primary IEC, simulating the *in vivo Hh* environment. Hence, primary IEC 2D-monolayers were seeded onto coverslips, and then infected with *Hh* at an MOI of 100:1. At the time of infection, plates were centrifuged at 1200 rpm for 5 min to synchronize the infection. After 4h, monolayers were washed with PBS to remove any non-adherent bacteria then IEC were fixed and stained with antibodies against *Hh* and E-cadherin and with WGA. Cells stained for WGA were not permeabilized, hence only *Hh* attached to the cell surface were stained (Fig 4.1A). However, monolayers stained for E-cadherin were treated with saponin to permeabilize the cells, so both internal and surface *Hh* were stained (Fig 4.1B).

Confocal images revealed that *Hh* exhibited strong adhesion to primary IEC monolayers, suggesting that this system provides a good model to study *Hh*-IEC interactions (Fig 4.1 A, B). Z-stack images showed cell surface associated *Hh* in monolayers stained with WGA (Fig 4.1A). However, in monolayers stained with E-cadherin, internalized versus surface *Hh* could not be distinguished. For that reason we had to use another method to look for internalization of *Hh*.

Although *Hh* is typically found as an extracellular bacterium, it was reported that *Hh* could be actively internalized into cultured MODE-K epithelial cells, through a process requiring actin rearrangement [95]. To determine if *Hh* could enter primary IEC, we infected primary IEC 2D-monolayers with *Hh* at an MOI 100:1 for 4h. As a positive control for this assay, we used RAW macrophages, which are highly phagocytic [188].

To discriminate between *Hh* bound to the cell surface and internalized *Hh*, we first fixed the cells and then stained with primary and secondary antibodies coupled to Alexa Fluor 555 for surface *Hh* without permeabilizing the cells. Monolayers were then washed and the cell membranes were permeabilized with saponin. Cells were re-stained with anti-*Hh* for a second time together with the lysosomal-associated membrane protein 1 (LAMP-1). The secondary antibody used in the second stain was coupled to Alexa Fluor 488 making the internalized *Hh* appear green and surface *Hh* appear orange.

Analyses using confocal microscopy demonstrated that *Hh* were associated with the cell surface (orange) of RAW macrophages and IEC (Fig. 4.2). Internalized *Hh* (green) was also seen in RAW 264.7 macrophages and to a lesser extent in IEC (Fig. 4.2). Therefore, these data illustrates that *Hh* exerts good attachment to IEC in our model and appears to be internalized into cultured primary IEC. However, as expected, fewer bacteria were internalized into IEC compared to the highly phagocytic RAW macrophages. Collectively, these data indicate that *Hh* intimately interacts with IEC in our 2D monolayer model making it a good *in vitro* system to analyze IEC innate immune responses to *Hh*.

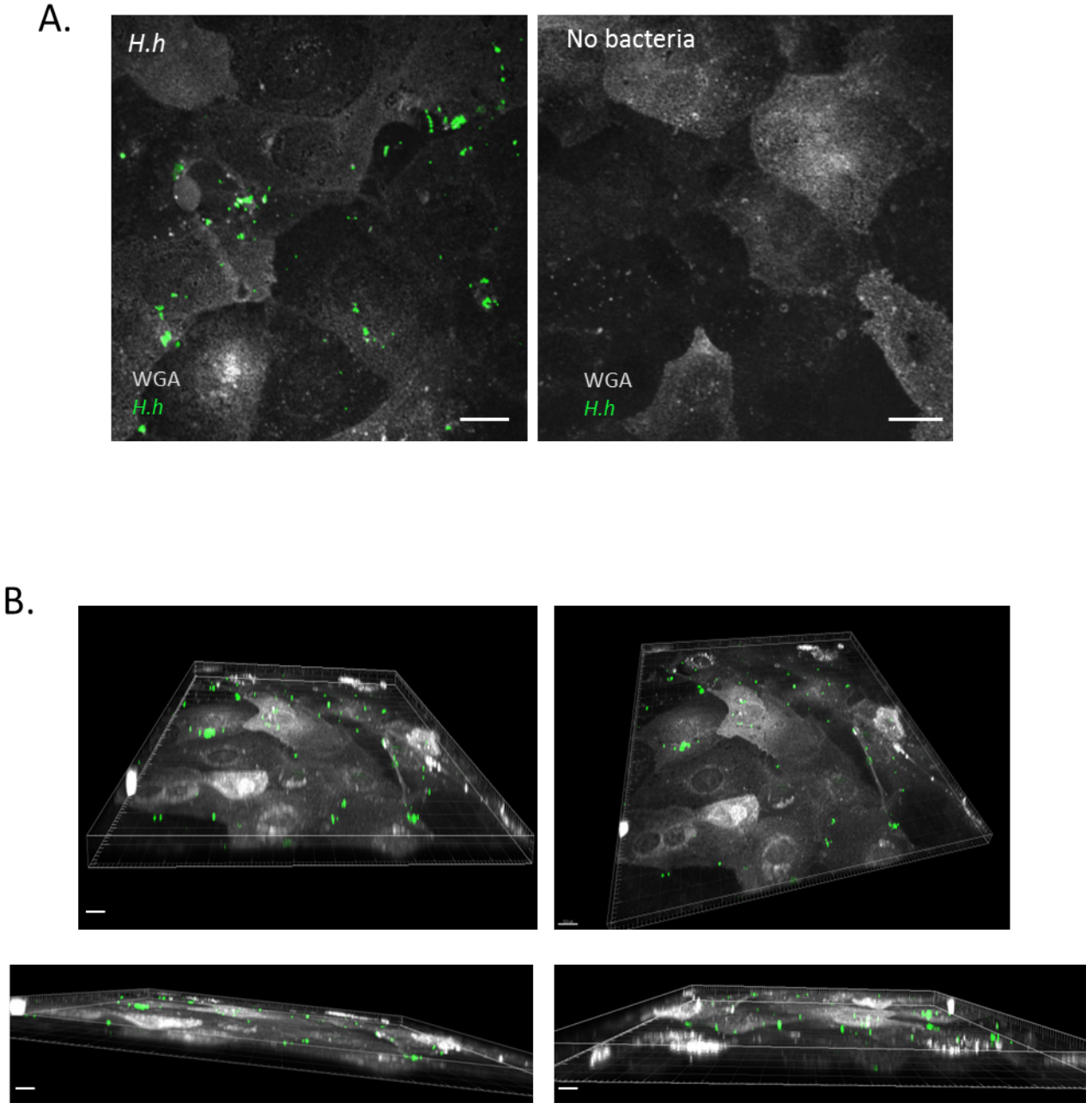


Figure 4.1 *Hh* exhibits adherence to primary IEC *ex vivo*. Monolayers were coincubated with *Hh* at an MOI of 100:1 for 4h, then non-adherent bacteria were removed by washing. Monolayers were stained with wheat germ agglutinin WGA (grey) and antibodies against *Hh* (green) (A) (B), or with antibodies against E-cadherin (green) and *Hh* specific stain (red) (C). Z-stacks reconstructed from confocal images (B). Right panel in (C) shows magnified image of the area in the white box. Original magnification:60x. Scale bar represent 15µm (A) (B), 20µm and 5µm (zoomed in image) (C). Representative images from2 repeats for (A) (B) and (C). Results are representative of 3 similar experiments.

C.

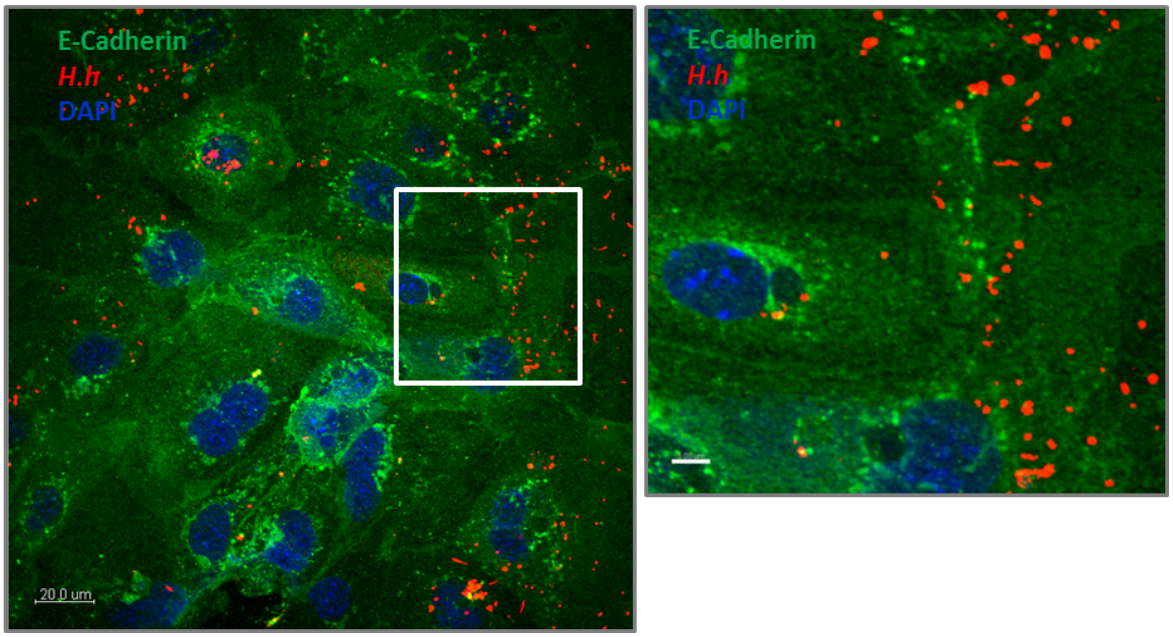
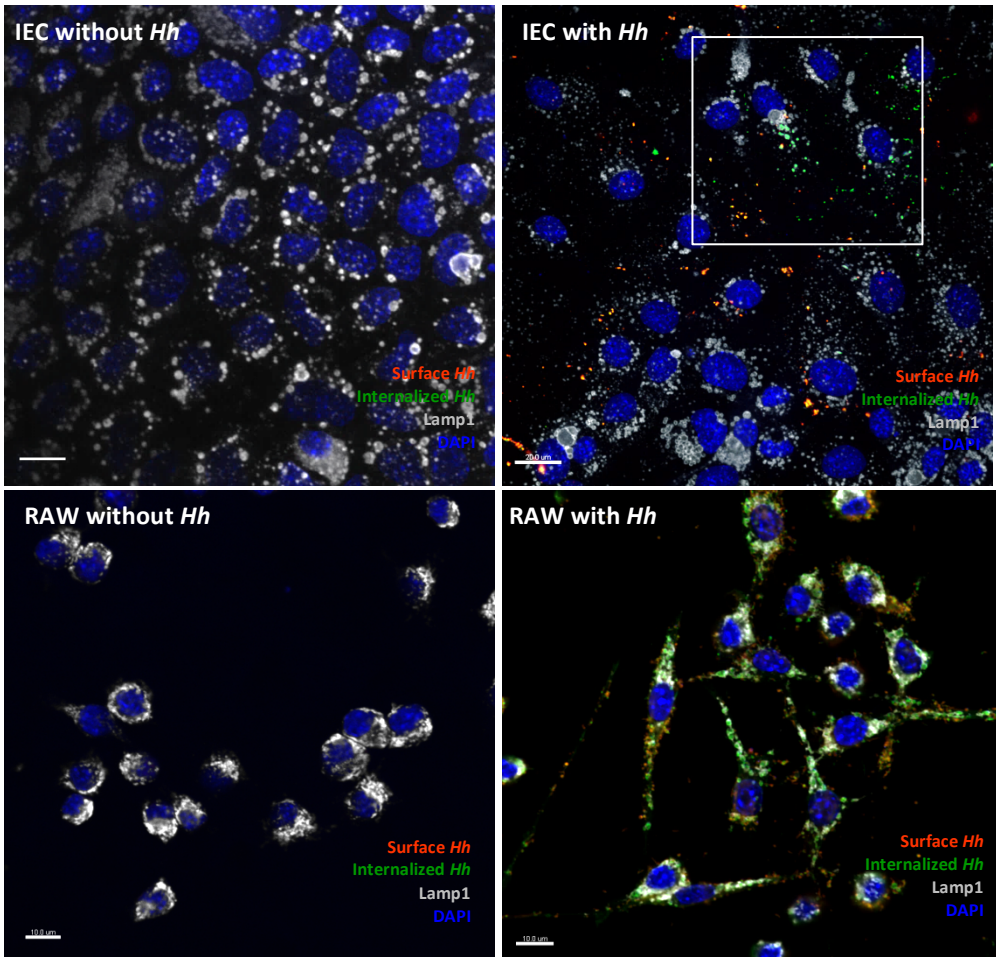


Figure 4.1 *Hh* exhibits adherence to primary IEC *ex vivo*. Monolayers were coincubated with *Hh* at an MOI of 100:1 for 4h, then non-adherent bacteria were removed by washing. Monolayers were stained with wheat germ agglutinin WGA (grey) and antibodies against *Hh* (green) (A) (B), or with antibodies against E-cadherin (green) and *Hh* specific stain (red) (C). Z-stacks reconstructed from confocal images (B). Right panel in (C) shows magnified image of the area in the white box. Original magnification:60x. Scale bar represent 15µm (A) (B), 20µm and 5µm (zoomed in image) (C). Representative images from2 repeats for (A) (B) and (C). Results are representative of 3 similar experiments.

A.



B.

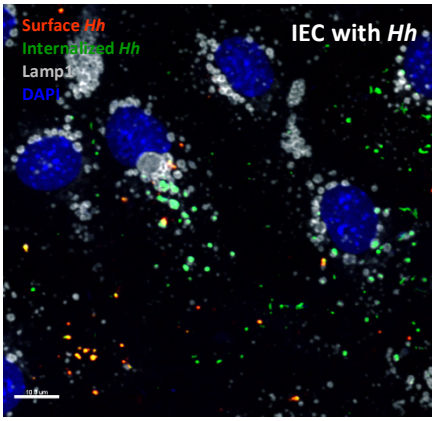


Figure 4.2 *Hh is* internalized into cultured primary IEC following 4h of infection. Primary IEC monolayers and RAW macrophages (used as a control) were coincubated with *Hh* at an MOI of 100:1 for 4h (A) and (B). Cells were washed with PBS to remove any non-adherent bacteria, fixed in 4% PFA, and stained for surface *H. hepaticus* (red) in the absence of saponin without permeabilizing the cell membrane. Cells were then permeabilized with saponin and stained with the lysosomal stain LAMP-1 (grey), and a 2nd *Hh* stain (green) to stain both surface and internalized *Hh*. (B) shows magnified image of the area in the white box in (A). Representative images from 2 repeats from 3 independent experiments are shown. Original magnification: 60x. Scale bars represent 20µm IEC, 10µm RAW (A), 10µm (B).

4.2.2 Response of WT IEC to *Hh* and chemokine secretion

As *Hh* has been reported to activate the Nf-κB and ERK pathways in macrophages [118,119], we next investigated the intracellular signaling pathways stimulated by *Hh* challenge of primary IEC. Therefore, primary IEC 2D-monolayers were infected with *Hh* at an MOI of 100:1 for time points ranging from 15' to 4h, with *E. coli* LPS used as a positive control. At the indicated time points, samples were homogenized and equivalent amounts were loaded onto an SDS-PAGE gel and blotted for phosphorylated p65 (p-p65) and ERK (p-ERK). We found that upon *Hh* challenge, p-ERK activation was seen in primary IEC as early as 15' post-infection, and that p-ERK levels gradually subsided over the 4h time course (Fig. 4.3B). In contrast, stimulation with *E.coli* LPS for 4h or 30' did not activate p-ERK in primary IEC (Fig. 4.3B and data not shown). In addition, *Hh* infection also activated p-65 at 15' and 30' as well as the positive control LPS (Fig. 4.3A and data not shown).

Consistent with the activation of these innate signaling pathways, we also found that primary IEC expressed significantly higher levels of *cxcl2* and secreted more cxcl2 after 6h or 24h stimulation with *Hh* (Fig.4.4A). The magnitude of the *Hh*-induced cxcl2 response was comparable to that induced following stimulation with *E.coli* LPS (Fig.4.4A), but was several orders of magnitude lower than the cxcl2 response of RAW 264.7 macrophages following infection with *Hh* (Fig. 4.4B).

Collectively, these data suggest that *Hh* activates primary IEC inducing a pro-inflammatory chemokine secretion. However, primary IEC seem to have a low immune activation potential as stimulation with high doses of either *Hh* or *E. coli* LPS led to only modest increases in cxcl2 expression and secretion.

Naturally, the IEC apical surface is exposed to luminal microbes, whereas the basolateral surface is isolated from non-invasive, luminal microbes. In order to determine if IEC were hyporesponsive to apical stimuli but had strong innate immune potential that was activated by pathogen invasion, 3D primary IEC organoids were also infected with *Hh* at the basolateral surface. To examine this, 3D IEC organoids were infected with *Hh* at an MOI of 100:1 for 6 or 24h. Although data was collected from a single experiment, we found that basolateral infection of primary IEC with *Hh* led to increased *cxcl2* gene expression and cxcl2 secretion (Fig.4.5). These *Hh*-induced cxcl2 responses were comparable to those observed following basolateral stimulation with *E. coli* LPS (Fig.4.5) and they were also comparable in magnitude to those elicited by apical infection with *Hh* (Fig.4.4).

Together, our data suggests that primary IEC are weakly activated by *Hh* in a similar manner both apically and basolaterally. However, a reduced cxcl2 response to *E. coli* LPS is seen following basolateral stimulation when compared to apical IEC response to *E. coli* LPS. Collectively, these data could indicate a low innate immune activation potential of IEC possibly due to a low TLR expression and or activation in primary IEC.

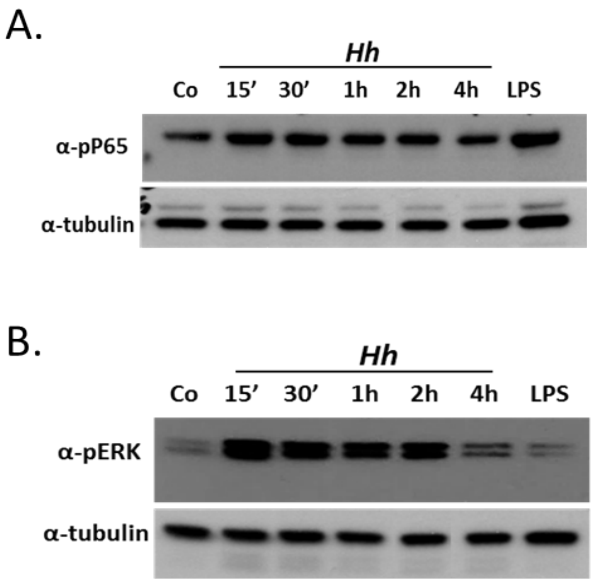
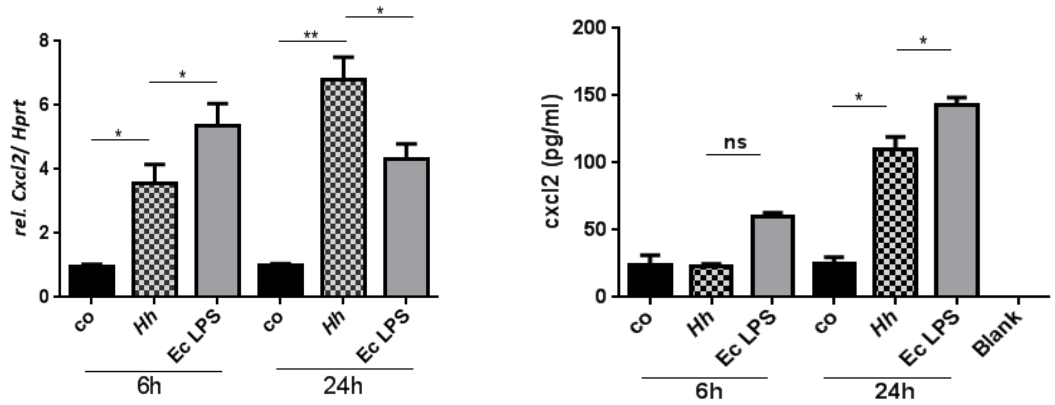


Figure 4.3 *H. hepaticus* stimulates both MAPK and Nf-kB intracellular signalling cascades in primary IEC. Primary IEC monolayers were infected with *Hh* at MOI 100:1 for the indicated time points (LPS (1µg/ml), control at 4h). Samples were homogenized and 15µl were loaded on SDS-PAGE gel and blotted for p-p65 (A) and pERK (B). After washing, membranes were developed with ECL western blotting substrate. For loading control α-tubulin reactivity was measured. A representative blot from 3 independent experiments is shown.

A.



B.

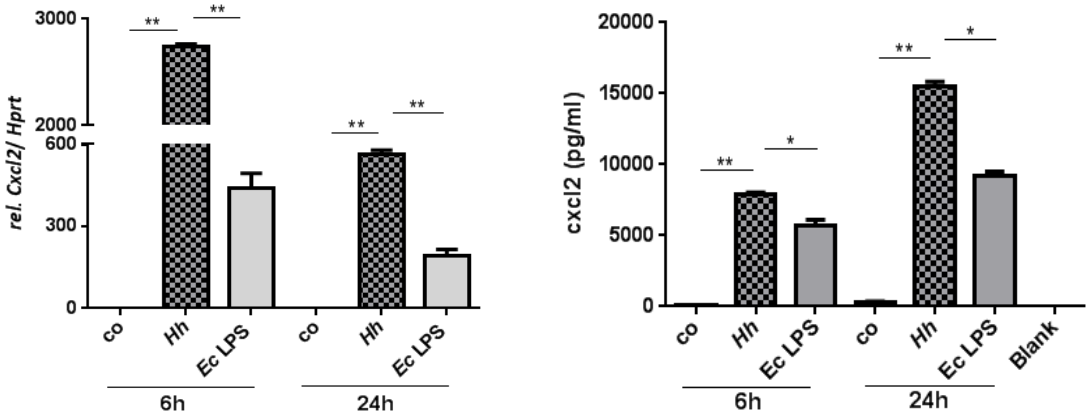


Figure 4.4 Cxcl2 secretion is induced following *Hh* infection of primary IEC. WT primary IEC monolayers (A) and RAW macrophages (B) were infected for 6h or 24h with *Hh* (MOI: 100:1 for IEC and 10:1 RAW, or stimulated with 1µg/ml of *E. coli* LPS. Cxcl2 release into the cell supernatant after 6h and 24h of coincubation was measured by ELISA and total RNA was isolated and mRNA expression levels were measured by qPCR and normalized to *Hprt1*. Error bars represent group means ± SD (pooled data from 3 independent experiments (A) and 2 independent experiments (B), n=6-8 per group). All statistical analysis was performed using the non-parametric Mann-Whitney test, *P<0.05, **P<0.01.

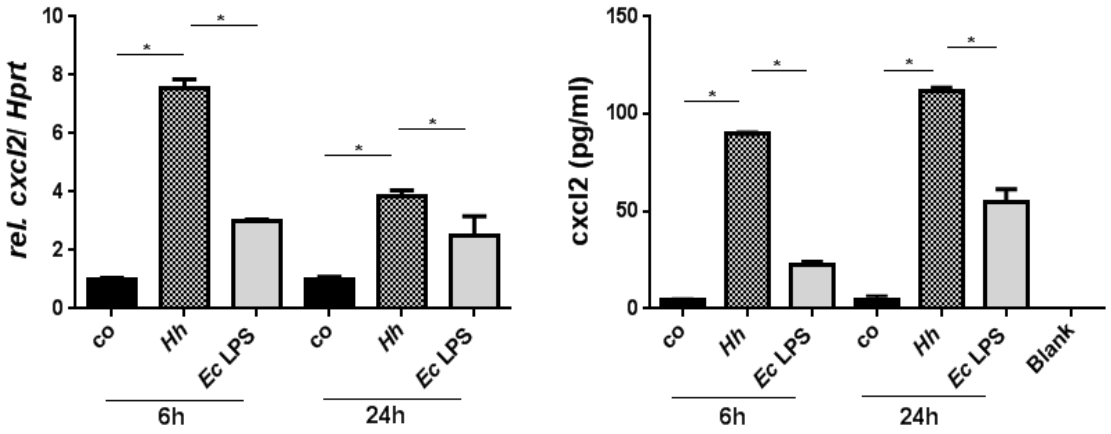


Figure 4.5 Cxcl2 production following *Hh* infection of IEC basolaterally (3D organoids). Primary IEC organoids were infected with *Hh* (MOI: 100:1) or stimulated with *E. coli* LPS (1µg/ml) for 6 or 24h. Cxcl2 release into the cell supernatant was measured by ELISA. Total RNA was isolated and mRNA expression levels were measured by qPCR and normalized to *Hprt1*. Error bars represent group means ± SD (1 experiment, n=3-4 per group). All statistical analysis was performed using the non-parametric Mann-Whitney test

4.2.3 Innate immune receptor expression by primary IEC

IEC may recognize luminal microbes through innate immune receptors (PRRs), a process that leads to the secretion of effector proteins such as cytokines and AMPs, that together promote the recruitment of immune cells, limit microbial growth and enforce the mucosal barrier. IEC exhibit highly regulated expression and restricted localization of innate PRRs, which controls recognition of microbes [9]. For example, very little or no TLR2 and TLR4 are expressed apically at steady state in primary IEC *in vivo* and in various IEC cell lines [189-191]. In addition, although the TLR4/MD2 receptor complex has been detected in fetal, neonatal and adult IEC *in vivo*, activation of TLR4 is only seen in fetal cells and adult IEC acquire hypo-responsiveness to LPS, facilitating host-microbe coexistence and homeostasis [191]. TLR5 has been reported to be expressed by IEC basolaterally *in vitro* and *ex vivo* [192]. Furthermore, TLR3, TLR7, TLR8 & TLR9 are located on endosomal membranes intracellularly [55].

In addition to TLR, IEC have been reported to express a range of cytosolic NLRs, including NOD1, NOD2 [77,78], as well as an array of inflammasomes-associated NLRs and inflammasome components, including NLRP3, NLRC4, NLRP6, caspase-1, ASC, and IL-18 [193-196]. Thus, IEC express a diverse range of PRRs that can sense distinct types of microbes and danger signals.

To investigate the expression and activation of innate immune receptors by primary IEC in our 2D monolayers, we examined cxcl2 chemokine expression and secretion following stimulation with various PRR agonists. After 6h of stimulation with different PRR agonists, supernatant was collected to measure cxcl2 secretion and total RNA was isolated to measure *cxcl2* expression levels by qPCR. A modest increase in *cxcl2* expression and secretion was seen after stimulation with the TLR4 ligand

lipopolysaccharide (*E. coli* LPS) (Fig. 4.6). However, primary IEC monolayers did not exhibit any increased *cxcl2* expression or cxcl2 secretion in response to stimulation with other TLR agonists that were tested, including; Pam3CSK4 (TLR2), *S. typhimurium* flagellin (TLR5), poly (I:C) (TLR3) or CpG oligonucleotide 1668 (TLR9) (Fig. 4.6). In addition, there was no increase in *cxcl2* expression or cxcl2 secretion by primary IEC monolayers following stimulation with the NOD2 agonist MDP (Fig. 4.6). In contrast, RAW 264.7 macrophages, which were used as controls, showed dramatically increased expression and secretion of cxcl2 in response to LPS, Pam3CSK4, and poly (I:C) and more moderate, but significantly increased cxcl2 production in response to MDP or flagellin (Fig. 4.6 B). Thus, primary IEC monolayers were largely unresponsive to common microbial PAMPs, with the exception of LPS, which elicited a modest response.

As basolateral infection of IEC with *Hh* also induced a modest cxcl2 response, we therefore tested whether 3D IEC organoids could respond to PRR agonists that were encountered basolaterally. However, primary IEC organoids basolateral stimulation with PAMPs revealed no significant actiavtion of IEC following stimulation with Pam3CSK4, *S. typhimurium* flagellin, poly (I:C) or CpG oligonucleotide 1668, as well as muramyl di-peptide (MDP) (Fig. 4.7). Only a weak activation, as measured by cxcl2 release was seen following *E. coli* LPS stimulation (Fig. 4.7).

These data collectively indicates that primary IEC respond only to TLR4 ligand both apically and to a lesser extent basolaterally, implying the expression and activation of the receptor. However, primary IEC did not respond to other PAMPs, suggesting either low levels of PRR expression or impaired signaling through these receptors.

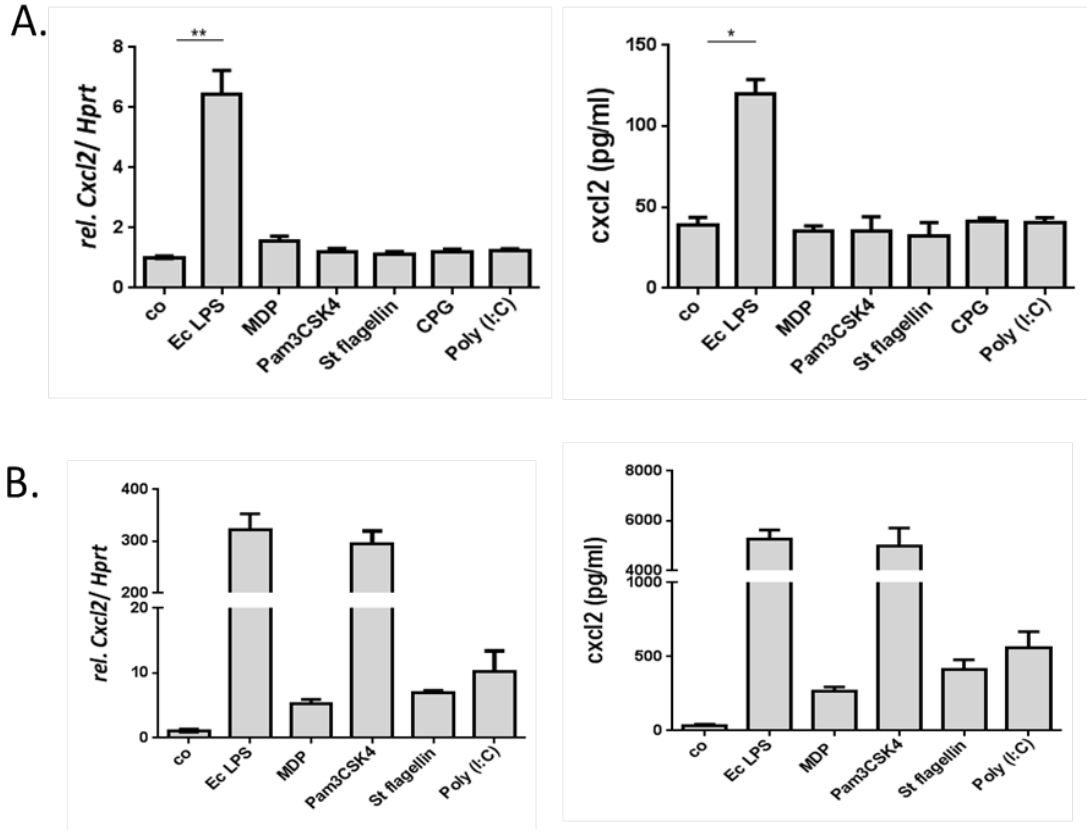


Figure 4.6 Primary IEC monolayers respond to LPS, but not to other PRR agonists. Primary IEC monolayers (A) and RAW macrophages (B) were stimulated with the following substances: *E.coli* LPS (1µg/ml for IEC and 100ng/ml for RAW), Muramyl dipeptide - MDP (10µg/ml)**,** *S. typhimurium* flagellin (St flagellin) (100ng/ml), Pam3CSK4 (10ng/ml), Poly (I:C) (1µg/ml), CpG oligonucleotide 1668 (2 µM). Cxcl2 release into the cell supernatant after 6h was measured by ELISA. Total RNA was isolated and mRNA expression levels were measured by qPCR and normalized to *Hprt1*. Error bars represent group means ± SD (pooled data from 2 independent experiments, n=6-7 per group)

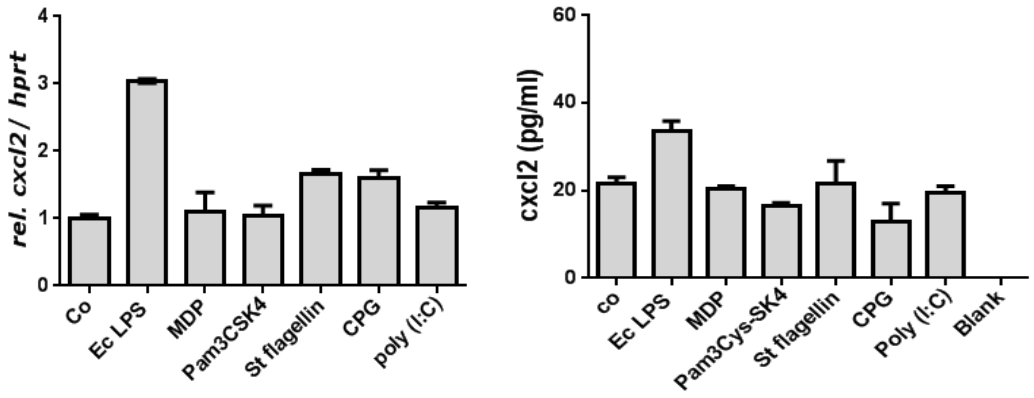


Figure 4.7 Responses of primary IEC organoids to basolateral stimulation with PAMPs. Primary IEC organoids were stimulated with different PAMPs: *E.coli* LPS (1µg/ml), Muramyl dipeptide MDP (10µg/ml)**,** *S. typhimurium* flagellin (St flagellin) (100ng/ml), Pam3CSK4 (10ng/ml), Poly (I:C) (1µg/ml), CpG oligonucleotide 1668 (2 µM). Cxcl2 release into the cell supernatant after 6h was measured by ELISA. Total RNA was isolated and *cxcl2* expression levels were measured using qPCR and normalized to *Hprt1*. Error bars represent group means ± SEM (pooled data from 2 independent experiments n=6-7 per group)

4.2.4 PRR receptors involved in *Hh* recognition

TLR receptors are believed to play a critical role in *Hh* recognition by IEC [125]. TLR2 transfected HEK293 epithelial cells exhibited a strong IL-8 inflammatory response when infected with *Hh* [125]. Furthermore, the ablation of shared TLR adaptor protein MyD88 in hematopoietic cells hindered the development of *Hh* induced colitis, however IEC MyD88 signaling contribution to disease remains unclear [124]. To further investigate the innate immune receptors involved in *Hh* recognition by primary IEC, and to highlight the role that MyD88 play in this process, organoids derived from MyD88$^{-/-}$ mice were used. Thus, 2D monolayers from MyD88$^{-/-}$ or WT mice were infected with *Hh* at an MOI of 100:1 for 6h. Our data show no *cxcl2* expression or cxcl2 secretion following *Hh* infection or TLR4 ligand (*E.coli* LPS) stimulation of primary MyD88$^{-/-}$ IEC (Fig. 4.8). In contrast, a moderate cxcl2 response was seen following *Hh* infection or *E.coli* LPS stimulation of the WT IEC (Fig. 4.8). These results suggest that IEC MyD88 and TLR signaling is involved in *Hh* recognition and subsequent cell activation.

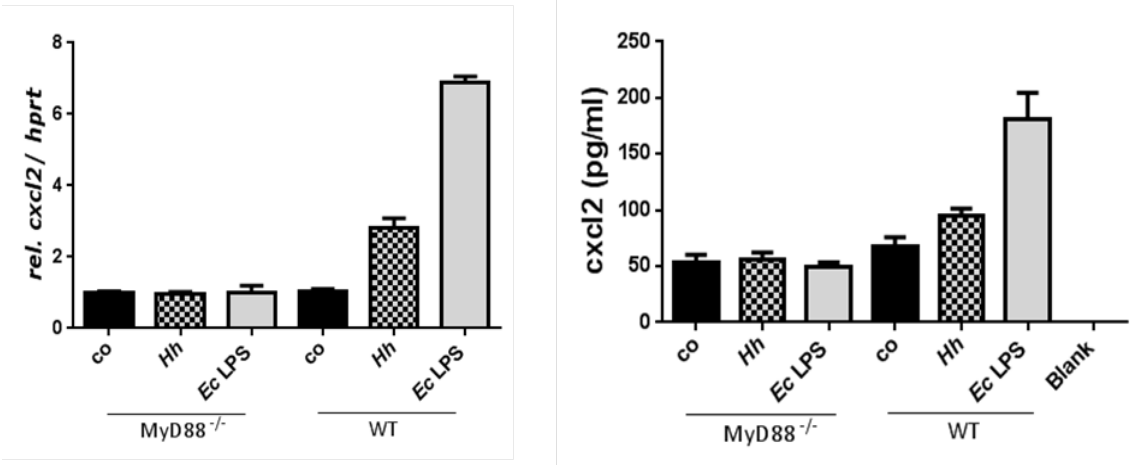


Figure 4.8 Primary IEC responses to *Hh* and LPS are MyD88-dependent. Primary IEC monolayers from WT or MyD88$^{-/-}$ mice were infected for 6h with *Hh* (MOI: 100:1), or stimulated with *E. coli* LPS (1µg/ml). Cxcl2 release into the cell supernatant after 6h was measured by ELISA. Total RNA was isolated and *Cxcl2* expression levels were measured by qPCR and normalized to *Hprt1*. Error bars represent group means ± SEM (pooled data from 2 independent experiments n=5-7 per group).

4.3 Discussion

Although *Hh* live in close proximity with IEC, little is known about the interactions that this bacterium has with IEC and how these interactions impact on persistent *Hh* colonization and on the initiation of host immune responses. Using the primary IEC culture systems described in the previous chapter, we have investigated the effects of *Hh* infection on primary IEC *in vitro*.

Before infecting monolayers with *Hh*, cells were pushed to differentiation through the removal of the stem cell enhancing condition media (R-spondin, Noggin, and Wnt-3A). In 0% CM, monolayers develop into a mix of differentiated as well as progenitor/stem cells

Although *Hh* is an extracellular bacterium, MODE-K cells, an immortalized intestinal epithelial cell line, have been reported to be able to internalize *Hh* [95]. In order to visualize *Hh* attachment and internalization by IEC we co-stained for E-cadherin and *Hh*, and although these images stained positively for *Hh*, we could not identify if any *Hh* uptake by IEC occurred (Fig. 4.1). The double *Hh* staining technique, first without cellular permeabilization and then following permeabilization, allowed us to stain both surface and internalized *Hh* with different secondary antibodies, enabling us to distinguish between these two. Our data showed that *Hh* were able to form attachments to the apical surface of primary IEC monolayers *in vitro* and appeared to be internalized into cultured primary IEC. Collectively these results suggested that our IEC 2D-monolayers could be used to mimic natural *Hh* infection of primary IEC, in the absence of any effects from other immune and mucosal cells, thus allowing the analysis of isolated IEC responses to *Hh.*

Consistent with previous reports that describe the activation of both Nf-κB and ERK signaling pathways in BMDM following *Hh* infection [118,119], we have found that *Hh* induced an early ERK as well as p65 activation in IEC, which suggests an early recognition of *Hh* by IEC. As different Nf-κB subunits have been linked to differential responses to *Hh* in $Rag^{-/-}$ mice suggesting both an anti-inflammatory and pro-inflammatory effects of Nf-κB signaling, it would be interesting to further characterize the Nf-κB responses in IEC following *Hh* infection. The extent of epithelial signaling involvement in driving *Hh* induced pathology is still not yet fully understood. It is however known that epithelial MyD88 signaling is insufficient to drive *Hh* induced intestinal inflammation in the absence of MyD88 signaling in myeloid cells [124].

We found that although primary IEC were generally weakly activated by *Hh* or LPS as measured by cxcl2 production, our data suggests a pro-inflammatory effect of *Hh* on primary IEC. Consistently, *Hh* strongly activated murine monocyte/macrophage cell line RAW 264.7, confirming the strong pathogenic potential of *Hh* and its capacity to induce innate immune activation. These weak primary IEC responses to *Hh* and LPS could be explained by low TLR expression and activation in primary IEC. In support of this idea it has been reported that very little or no TLR2 and TLR4 are expressed apically at steady state in primary IEC *in vivo* and in various IEC cell lines [189-191].

In addition, adult IEC acquire hypo-responsiveness to LPS which is believed to be involved in host-microbe coexistence and homeostasis [191]. Nevertheless, although weak, it is possible that these pro-inflammatory signals arising from IEC could be involved in potentiating innate or adaptive immune activation following *Hh* infection. Additional investigations to determine whether other chemokines and cytokines are

involved in *Hh* – IEC activation could further help understand the nature of the IEC contribution to *Hh* driven colitis.

Interestingly, our data showed that primary IEC were also weakly activated by *Hh* and LPS encountered basolaterally, which could possibly indicate a low innate immune activation potential of IEC. Another possible explanation would be low or no innate immune receptor expression and activation on the basolateral surface of IEC. Consistent with this idea, we observed reduced Cxcl2 responses following stimulation with LPS basolaterally when compared to apical stimulation (Figs 4.6, 4.7). Similarly, primary IEC stimulated with a range of PAMPs at the apical surface showed no activation as measured by cxcl2 production, with only a moderate response seen following LPS stimulation. Similar responses were seen when cells stimulated basolaterally, but with slightly less activation observed with TLR4 ligand. Again, IEC unresponsiveness to the different PAMPs could be possibly explained by the lack of PRR expression on apical and basolateral borders. One way to answer these questions would be through expression analysis of the different PRRs in primary IEC. It is noteworthy that IEC have been reported to express TLR2 and TLR4, TLR5, endosomal TLR3, TLR7, TLR8 & TLR9 as well as a range of cytosolic NLRs [9]. This suggests that primary IEC derived *in vitro* may have altered expression of PRR relative to their *in vivo* counterparts.

We found that cells lacking TLR signaling adaptor protein MyD88 failed to respond to *Hh,* suggesting TLR involvment in *Hh* recognition and activation by IEC. Furthermore, as expected MyD88$^{-/-}$ cells were unresponsive to the TLR4 ligand *E.coli* LPS. A previous study showed that although *Hh* LPS activated HEK293 cells via TLR4, the response to the whole bacteria was dependent on TLR2 which suggests that

non-LPS bacterial components may drive the immune response. This could imply that different *Hh* components might be recognized by different IEC TLR receptors. Thus, it would be interesting to test *Hh* as well as *Hh* LPS effect on IEC derived from different TLR KO transgenic mice.

Chapter 5: General Discussion

The results presented in this thesis have investigated the effect of the murine intestinal bacterium *Helicobacter hepaticus (Hh)* on primary intestinal epithelial cells *ex vivo* in the absence of any immune cells. It is well recognized that gut microbiota influence the host immune system, and changes in the bacterial composition termed dysbiosis has been strongly linked to inflammatory disorders such as inflammatory bowel disease [44,197].

Although *Hh* colonizes mice intestine and is rarely found in humans, other enterohepatic *Helicobacter* species have occasionally been reported in human IBD. For example, *H. pullorum and H. fennelliae* were more frequently found in gut samples from Crohn's and ulcerative colitis patients compared to controls [198]. Therefore, understanding the epithelial-*Hh* relationship and the underlying molecular dynamics may help identify new host-pathogen interactions at the level of the epithelium and the role they play in protection against disease.

H. hepaticus infection models have advanced our understanding of the inflammatory and immunoregulatory pathways involved in the pathogenesis of chronic intestinal inflammation [91]. In particular, *Hh*-induced IBD models have illustrated the importance of innate immune pathways in driving chronic colitis. This is seen in lymphocyte-deficient 129SvEv*Rag2*$^{-/-}$ mice following *Hh* infection, where an innate immune mediated typhlo-colitis develops [113,114]. A novel population of IL-23R^{+} innate lymphocytes was found to drive inflammation in response to IL-23 in this model [115]. Furthermore, the Nf-κB signaling pathway has been described to play a major role in the innate immune model following *Hh* infection. Infection of 129SvEv*Rag2*$^{-/-}$ mice lacking either p50/p105 or c-Rel Nf-κB subunits with *Hh* indicated that activation of the Nf-κB pathway could have pro- or anti-inflammatory effects during *Hh* infection [118,120,121].

Moreover, MyD88 signaling in myeloid cells was found to be crucial for *Hh* induced colitis in 129SvEv*Rag2*$^{-/-}$ mice suggesting a critical role for the TLR innate immune receptors in *Hh* mediated intestinal inflammation [124]. These data strongly suggest a critical role for innate immune pathways and PRRs in driving *Hh* induced colitis. However, the potential involvement of IEC in these responses remained unclear.

Parallel data suggested TLR2 and TLR4 involvement in *Hh* recognition by epithelial cells [125]. However, it has been shown that *Hh*-induced colitis in both the T cell dependent and T cell independent chronic inflammation models *in vivo* were TLR2-independent [126]. Other innate immune PRRs have been also suggested to be involved in *Hh* recognition. For example, more *Hh* was found in the terminal ileum of C57BL/6 *Nod-2*$^{-/-}$ mice compared to WT mice, suggesting a Nod-2 involvement in controlling *Hh* colonization, although this did not appear to affect pathology [127]. Whilst most previous studies were focused on leukocyte responses to *Hh*, little is known about the innate immune signaling and receptors involved in *Hh* recognition by the intestinal epithelium. Thus, the aim of this thesis was to investigate the innate immune responses of primary IEC to *Hh* infection *ex vivo* in the absence of immune cells, using the organoid *ex vivo* IEC culture system as a model of infection.

The intestinal epithelial cell layer forms the first-line of mucosal immune system defense and is situated between the luminal microbiota and the underlying sub-epithelial tissue that is richly populated by leukocytes. IEC have a central role in discriminating between harmless versus pathogenic bacteria, making them a key player in regulating the appropriate host response towards intestinal bacteria [9]. Furthermore, IEC have the ability to sample luminal microbes, as well as express a range of PRR that recognize conserved Microbial Associated Molecular Patterns (MAMPs), and can secrete pro-

inflammatory mediators such as cytokines and chemokines in response to PRR stimulation [9,13].

Since *H. hepaticus* is intimately associated with the upper crypt IEC in the murine large intestine, we decided to study the impact of *Hh* on primary IEC innate immune responses. In order to experimentally investigate the isolated effect of *Hh* on primary IEC, we had to first develop a model mimicking *H. hepaticus* infection *in vivo*. We first used the 3D organoid culture method that enabled the propagation of primary IEC *ex vivo* in the presence of cell supporting matrix and growth factors. However, in order to be able to study the interactions of *Hh* with primary IEC, we had to adapt the spherical organoid system into 2D IEC monolayers that allowed access of the apical surface. Similar to primary IEC seeded on transwell described in a recent study [150], our monolayers expressed appropriately distributed epithelial markers and contained differentiated epithelial cells. However, unlike the transwell system our monolayers were attached basolaterally to a collagen-coated surface where the basolateral border was not accessible. Thus, one advantage of the transwell system over our method is the accessibility of both apical and basolateral surfaces that enables us to selectively infect either apical or basolateral surface of the polarized epithelial layer. Therefore, it would be interesting to identify the primary IEC basolateral chemokine and cytokine secretion in response to apical *Hh* stimulation in a transwell system.

Recently, another method that utilizes microinjection of small intestinal organoids to investigate the interaction of enteric pathogen *Salmonella enterica serovar Typhimurium* (STM) and small IEC was described [199]. One prominent advantage of this model is an intact organoid lumen that is accessible by microinjection, which separates apical stimuli and epithelial secretions from the basolateral border [199].

Whilst this approach offers a novel method for studying IEC-pathogen interaction, it is however time consuming and exhibits some limitations. For example, only a limited number of cells are stimulated at the same time. In addition, only restricted volumes can be injected into the organoid lumen [199]. Our method however, enabled us to stimulate many cells at the same time, with large bacterial volumes.

Although our study provide novel insight into primary IEC-*Hh* interaction it is important to recognize its limitations. While more physiologically relevant than other intestinal epithelial cell lines our culture system lack some important physiological features that might influence the survival of *Hh* within the culture system such as the absence of a mucus layer, which normally provides an important niche for the bacteria *in vivo*. In our study bacterial viability was determined by immunofluorescent staining only at the beginning but not by the end of the assay. Cell viability however was not determined. In addition, the lack of lamina propria immune cells in our system excludes any effect these cells may normally have on the intestinal epithelium *in vivo* that can influence the IEC response to *Hh.* Furthermore, although previous studies report both pro- and anti-inflammatory effects of *Hh* on the host, we have mainly focused on the pro-inflammatory response of IEC to *Hh* in our study. It would be interesting to examine the production of anti-inflammatory factors such as TSLP and TGF-β by IEC in response to *Hh* that might contribute to the tolerogenic mucosal environment seen in *Hh* infection. Considering these limitations the data presented in this study should be interpreted cautiously.

Following infection of monolayers with *Hh*, the bacteria exhibited adherence to primary IEC in our model. In agreement with our results, previous studies have

described attachment of *Hh* to IEC cell lines, such as mICc12 and MODE-K cells [95,129]. *Hh* close association and attachment to IEC might be critical for maintaining a balanced relationship through *Hh* T6SS mediated secretion of effector proteins into epithelial cells, that may exert anti-inflammatory effects [95].

Pathogenic enteric bacteria such as *Listeria monocytogenes*, *S. typhimurium* and *Shigella* spp. have been previously described to express virulence factors that allow them to adhere and internalize within IEC leading to internalization-dependent innate immune activation of IEC [200-202]. Thus, bacteria that are able to invade the epithelial barrier and disseminate into sub-epithelial tissue are preferentially recognized by the host immune system, a process that may enable discrimination between pathogenic and commensal bacteria [200-202]. In response to invasive enteric pathogens, IEC may secrete pro-inflammatory mediators such as IL-8, IL-25, Cxcl2, IL-18 [9].

Furthermore, previous data suggested an important role for TLR4 in gram negative *Escherichia coli* internalization into epithelial cells. Bacterial uptake was seen in HEK-293 cells transfected with MD2/TLR4 but not in non-transfected HEK-293 cells [203]. In addition, the internalization of this gram negative bacterium *in vivo* was significantly higher in WT compared to TLR4-deficient mice [203].

H. hepaticus was described to be actively internalized into MODE-K IEC through a process that was controlled by actin rearrangement and was limited by the T6SS [95]. Additionally, *in vivo* internalization of *Hh* by IEC was reported following *Hh* infection of specific pathogen free (SPF) C57Bl/6 mice [95]. Furthermore, in the same study they demonstrated that although both WT and T6SS deletion mutants exhibited similar internalization at 30 min, *Hh* T6SS deletion mutants demonstrated a significantly

higher level of internalization by MODE-K cells following 6h of co-incubation [95]. These data could imply that the T6SS prevents further *Hh* internalization once bacteria get initial access to IEC. In addition, GF mice mono-colonized with *Hh* T6SS mutants exhibited higher colonization levels compared to mice infected with WT *Hh* [95]. Thus, these data suggests *Hh* colonization and internalization in IEC is limited via the T6SS. The T6SS effects might explain why so few bacteria appeared to be internalized by our cultured primary IEC and this could have explained the weak innate immune activation. It would therefore be interesting to test T6SS mutant internalization by primary IEC using our culture method.

It is not known how *H. hepaticus* manages to avoid eradication by the host and, although a strong pro-inflammatory response develops following *Hh* infection, most immune competent mice do not exhibit overt disease [91]. This suggests that *Hh* engages in a dialogue with the host to ensure that a balanced, regulated immune response is maintained. *Helicobacter* species are known to have some immune evasive features, for example, they have been shown to have alterations in their flagellin that remove agonistic activity for TLR5 [130]. However, the *Hh* flagellar hook protein FlgE is known to be a strong T-cell antigen [204], showing that flagellar antigens are recognized as immunogenic by the host . Furthermore, another study reported that *Hh* has an inhibitory effect on TLR4-mediated immune responses in mICc12 cells, and on TLR5-induced proinflammatory responses in the human epithelial cell line Caco-2 [129]. The recent discovery of *Hh* T6SS demonstrated a molecular relationship between the bacteria and epithelial cells and an anti-inflammatory gene expression profile was induced in MODE-K epithelial cells in a T6SS-dependent manner [95]. This tolerogenic effect on the epithelium is believed to contribute to the host-bacterial homeostatic relationship, facilitating the bacterial persistent colonization. However,

conflicting results were seen with different IEC lines. Thus, *Hh* was found to only weakly activate innate immune responses in mICc12 and MODE-K murine intestinal epithelial cell lines [95,129], however *Hh* induced a strong IL-8 response in HEK293 human epithelial cells via activation of TLR2 [125]. The reasons responsible for these discrepancies are not clear, but a key limitation of all previous studies was that they relied on IEC cell lines and it was unclear whether these results were truly reflective of the molecular interactions between *Hh* and primary IEC.

Our data showed some innate immune activation of primary IEC in response to *Hh* infection, as measured through secretion of cxcl2, which was of a similar magnitude as the response elicited by *E. coli* LPS. Nevertheless, as expected the primary IEC responses were markedly less than those observed from RAW macrophages following stimulation with *Hh* and *E.coli* LPS. Unlike IEC however, macrophages are known to retain a potent phagocytic and bactericidal activities [205]. One reason for this difference in response is probably due to the fact that more *Hh* was internalized by the highly phagocytic RAW macrophages. Another factor contributing to the strong inflammatory reaction seen by RAW macrophages could be a higher level of PRR expression [206].

In terms of intracellular signaling cascades induced in primary IEC, we found that both ERK as well as p-65 activation was seen as early as 15 minutes following *Hh* infection, but that this response gradually diminished over time. This agrees with previous data that showed *Hh* induced IκB degradation and nuclear translocation of κb, indicative of activation of the Nf-κB intracellular signaling pathway [118]. In addition, challenging BMDM with *Hh* also induced rapid phosphorylation of ERK1/2 and MEK1/2 through a pathway dependent upon the p105 subunit and Tpl-2 [119].

However, previous data demonstrated that Nf-κB activation in myeloid but not epithelium drives *Hh* induced colitis in a T-cell dependent model [122].

Furthermore, MODE-K epithelial cells infected with WT *Hh* exhibited a reduced level of Nf-κB expression, as well as other innate immunity mediators such as IL-17 receptor, TLR3, and TLR4 when compared to infection with *Hh* T6SS deletion mutants, indicating an inhibitory effect of T6SS on the epithelial Nf-κB mediated activation following *Hh* infection [95]. Thus, this suggests that the limited activation of innate immune pathways in primary IEC in response to *Hh* infection may be due to the inhibitory effects of the T6SS. It would be interesting to assess whether T6SS affects primary IEC-*Hh* innate immune activation, using *Hh* T6SS deletion mutants

Another potential explanation for the weak innate immune reaction observed in our primary IEC after *Hh* infection could be a low steady state expression and/or activation of the innate PRRs, a mechanism that is believed to be used by IEC to tolerate constitutive exposure to luminal microbiota without being overstimulated [9]. In support of this, it has been reported that although TLR4/MD receptor are detected in fetal, neonatal and adult IEC, the activation of the receptor is only seen in fetal cells, and adult IEC acquire hypo-responsiveness to LPS, facilitating host-microbe coexistence and homeostasis [191]. This concept is further supported by our data demonstrating that primary IEC 2D-monolayers failed to respond to a range of PRR ligands, including TLR2, TLR3, TLR5, TLR9, and NOD2 agonists. Other IEC lines such as the mouse intestinal crypt cell (mICc12) have been also previously shown to be unresponsive to the various bacterial components (PAMPs), and only exhibited a response to the TLR4 ligand [129]. On the other hand, another study reported that the mouse small intestinal cell line (IEC-1) exhibited a strong, dose-dependent secretion of

cxcl2 and cxcl5 in response to the TLR4 and TLR5 ligands, *E.coli. LPS* and flagellin, respectively [207]. In contrast, only a weak cxcl2 response was detected in response to the TLR2/TLR1 ligand Pam3Cys, and no response was elicited following exposure to the TLR3 ligand poly (I:C) or to the TLR9 ligand CpG DNA [207].

Although little is known about the response of primary IEC to bacterial PAMPs, one recent study assessed the effect of NOD1, NOD2, TLR2, TLR4, TLR5, and TLR9 ligands on organoid number and growth [208] . The data showed that organoids stimulated with NOD1 and NOD2 ligands, i.e peptidoglycan (PGN) or muramyl-dipeptide (MDP), respectively, exhibited a 5-fold increase in organoid number compared to controls, however other PAMPs had no effect [208]. These results suggest that stimulation of NOD2 expressing $Lgr5^{+}$ cells with MDP triggers stem cell survival generating more organoids [208]. Moreover, another study demonstrated that infecting primary IEC monolayers with heat killed *E. coli* stimulated IgA transcytosis and pIgR expression indicating a primary IEC innate immune response to *E. coli* [150]. In conclusion, our data demonstrate that isolated *ex vivo* IEC retained their immune function and were weakly responsive to *Hh* and *E.coli* LPS, but were hyporesponsive to other PRR ligands. Although previous studies done on epithelial cell line HEK293 have suggested a critical role for TLR2 and TLR4 in *Hh* recognition [125], we observed no response to TLR2 ligand and a modest response to TLR4 ligand by primary IEC. These results, which might be related to low receptor expression or activation, could explain the epithelial hypo-responsiveness towards *Hh* infection. In fact, one possible explanation for how *Hh* manages to persistently colonize the epithelium and escape eradication *in vivo*, could be the restricted expression of TLR2 and TLR4 by IEC. Further studies are needed to match the functional assays with the availability of receptors in IEC, for example using RT-PCR to characterize expression

of TLR, NLR and other PRR by primary IEC, both at steady state and in the presence of activating stimuli.

Related to this idea, our data showed a lack of Cxcl2 secretion in response to *Hh* in MyD88$^{-/-}$ IEC, strongly suggesting TLR involvement in *Hh* recognition by primary IEC. Further analyses, using primary IEC isolated from TLR2 and TLR4 knockout mice, could indicate whether these receptors are likely to be involved in *Hh* recognition by epithelial cells *in vivo*.

The cytoplasmic innate immune receptors NOD1 and NOD2 detect components of the bacterial cell wall peptidoglycan once internalized into the cell [79,80]. One way to study the involvement of NLRs in *Hh* recognition would be by using primary IEC derived from RIP2$^{-/-}$ mice lacking a key kinase involved in NOD signaling. Finally, the inflammasome-activating NLR should also be considered, especially since the secretion of IL-1b was shown to play a pathogenic role during *Hh*-triggered innate immune colitis [209]. As these NLR detect cytosolic disturbances during invasion or infection-associated damage, these receptors could play a role in sensing effector proteins secreted into host cell by the *Hh* T6SS or in response to secreted toxins such as Cdt. The impact of inflammasomes on IEC responses to *Hh* could be analyzed using primary IEC derived from mice lacking the shared inflammasome adaptor molecule, ASC.

In summary, the primary IEC culture system described in this thesis provides a platform for further study into the interactions of IEC with *Hh,* which could indicate how this influences the activation of innate and adaptive immunity during chronic intestinal inflammation.

References

1. Sato, T.; Vries, R.G.; Snippert, H.J.; van de Wetering, M.; Barker, N.; Stange, D.E.; van Es, J.H.; Abo, A.; Kujala, P.; Peters, P.J.*, et al.* Single lgr5 stem cells build crypt-villus structures in vitro without a mesenchymal niche. *Nature* **2009**, *459*, 262-265.

2. Kuratnik, A.; Giardina, C. Intestinal organoids as tissue surrogates for toxicological and pharmacological studies. *Biochem Pharmacol* **2013**, *85*, 1721-1726.

3. Sato, T.; Clevers, H. Growing self-organizing mini-guts from a single intestinal stem cell: Mechanism and applications. *Science* **2013**, *340*, 1190-1194.

4. Ley, R.E.; Lozupone, C.A.; Hamady, M.; Knight, R.; Gordon, J.I. Worlds within worlds: Evolution of the vertebrate gut microbiota. *Nat Rev Microbiol* **2008**, *6*, 776-788.

5. Hansson, G.C.; Johansson, M.E. The inner of the two muc2 mucin-dependent mucus layers in colon is devoid of bacteria. *Gut Microbes* **2010**, *1*, 51-54.

6. Hooper, L.V.; Macpherson, A.J. Immune adaptations that maintain homeostasis with the intestinal microbiota. *Nat Rev Immunol* **2010**, *10*, 159-169.

7. Van der Sluis, M.; De Koning, B.A.; De Bruijn, A.C.; Velcich, A.; Meijerink, J.P.; Van Goudoever, J.B.; Büller, H.A.; Dekker, J.; Van Seuningen, I.; Renes, I.B.*, et al.* Muc2-deficient mice spontaneously develop colitis, indicating that muc2 is critical for colonic protection. *Gastroenterology* **2006**, *131*, 117-129.

8. van der Flier, L.G.; Clevers, H. Stem cells, self-renewal, and differentiation in the intestinal epithelium. *Annu Rev Physiol* **2009**, *71*, 241-260.

9. Artis, D. Epithelial-cell recognition of commensal bacteria and maintenance of immune homeostasis in the gut. *Nat Rev Immunol* **2008**, *8*, 411-420.

10. Shen, L.; Turner, J.R. Role of epithelial cells in initiation and propagation of intestinal inflammation. Eliminating the static: Tight junction dynamics exposed. *Am J Physiol Gastrointest Liver Physiol* **2006**, *290*, G577-582.

11. Abreu, M.T. Toll-like receptor signalling in the intestinal epithelium: How bacterial recognition shapes intestinal function. *Nat Rev Immunol* **2010**, *10*, 131-144.

12. Fukata, M.; Arditi, M. The role of pattern recognition receptors in intestinal inflammation. *Mucosal Immunol* **2013**, *6*, 451-463.

13. Philpott, D.J.; Girardin, S.E. The role of toll-like receptors and nod proteins in bacterial infection. *Mol Immunol* **2004**, *41*, 1099-1108.

14. Bjerknes, M.; Cheng, H. Intestinal epithelial stem cells and progenitors. *Methods Enzymol* **2006**, *419*, 337-383.

15. Barker, N.; van Es, J.H.; Kuipers, J.; Kujala, P.; van den Born, M.; Cozijnsen, M.; Haegebarth, A.; Korving, J.; Begthel, H.; Peters, P.J.*, et al.* Identification of stem cells in small intestine and colon by marker gene lgr5. *Nature* **2007**, *449*, 1003-1007.

16. Kim, Y.S.; Ho, S.B. Intestinal goblet cells and mucins in health and disease: Recent insights and progress. *Curr Gastroenterol Rep* **2010**, *12*, 319-330.

17. Schonhoff, S.E.; Giel-Moloney, M.; Leiter, A.B. Minireview: Development and differentiation of gut endocrine cells. *Endocrinology* **2004**, *145*, 2639-2644.

18. Frisch, S.M.; Francis, H. Disruption of epithelial cell-matrix interactions induces apoptosis. *J Cell Biol* **1994**, *124*, 619-626.

19. Sato, T.; van Es, J.H.; Snippert, H.J.; Stange, D.E.; Vries, R.G.; van den Born, M.; Barker, N.; Shroyer, N.F.; van de Wetering, M.; Clevers, H. Paneth cells constitute the niche for lgr5 stem cells in intestinal crypts. *Nature* **2011**, *469*, 415-418.

20. Peterson, L.W.; Artis, D. Intestinal epithelial cells: Regulators of barrier function and immune homeostasis. *Nat Rev Immunol* **2014**, *14*, 141-153.

21. Gallo, R.L.; Hooper, L.V. Epithelial antimicrobial defence of the skin and intestine. *Nat Rev Immunol* **2012**, *12*, 503-516.

22. Mabbott, N.A.; Donaldson, D.S.; Ohno, H.; Williams, I.R.; Mahajan, A. Microfold (m) cells: Important immunosurveillance posts in the intestinal epithelium. *Mucosal Immunol* **2013**, *6*, 666-677.

23. Mowat, A.M. Anatomical basis of tolerance and immunity to intestinal antigens. *Nat Rev Immunol* **2003**, *3*, 331-341.

24. Hase, K.; Kawano, K.; Nochi, T.; Pontes, G.S.; Fukuda, S.; Ebisawa, M.; Kadokura, K.; Tobe, T.; Fujimura, Y.; Kawano, S.*, et al.* Uptake through glycoprotein 2 of fimh(+) bacteria by m cells initiates mucosal immune response. *Nature* **2009**, *462*, 226-230.

25. McDole, J.R.; Wheeler, L.W.; McDonald, K.G.; Wang, B.; Konjufca, V.; Knoop, K.A.; Newberry, R.D.; Miller, M.J. Goblet cells deliver luminal antigen to cd103+ dendritic cells in the small intestine. *Nature* **2012**, *483*, 345-349.

26. Rescigno, M.; Urbano, M.; Valzasina, B.; Francolini, M.; Rotta, G.; Bonasio, R.; Granucci, F.; Kraehenbuhl, J.P.; Ricciardi-Castagnoli, P. Dendritic cells express tight junction proteins and penetrate gut epithelial monolayers to sample bacteria. *Nat Immunol* **2001**, *2*, 361-367.

27. Chieppa, M.; Rescigno, M.; Huang, A.Y.; Germain, R.N. Dynamic imaging of dendritic cell extension into the small bowel lumen in response to epithelial cell tlr engagement. *J Exp Med* **2006**, *203*, 2841-2852.

28. Zeuthen, L.H.; Fink, L.N.; Frokiaer, H. Epithelial cells prime the immune response to an array of gut-derived commensals towards a tolerogenic phenotype through distinct actions of thymic stromal lymphopoietin and transforming growth factor-beta. *Immunology* **2008**, *123*, 197-208.

29. Xu, W.; He, B.; Chiu, A.; Chadburn, A.; Shan, M.; Buldys, M.; Ding, A.; Knowles, D.M.; Santini, P.A.; Cerutti, A. Epithelial cells trigger frontline immunoglobulin class switching through a pathway regulated by the inhibitor slpi. *Nat Immunol* **2007**, *8*, 294-303.

30. He, B.; Xu, W.; Santini, P.A.; Polydorides, A.D.; Chiu, A.; Estrella, J.; Shan, M.; Chadburn, A.; Villanacci, V.; Plebani, A.*, et al.* Intestinal bacteria trigger t cell-

independent immunoglobulin a(2) class switching by inducing epithelial-cell secretion of the cytokine april. *Immunity* **2007**, *26*, 812-826.

31. Rimoldi, M.; Chieppa, M.; Salucci, V.; Avogadri, F.; Sonzogni, A.; Sampietro, G.M.; Nespoli, A.; Viale, G.; Allavena, P.; Rescigno, M. Intestinal immune homeostasis is regulated by the crosstalk between epithelial cells and dendritic cells. *Nat Immunol* **2005**, *6*, 507-514.

32. Taylor, B.C.; Zaph, C.; Troy, A.E.; Du, Y.; Guild, K.J.; Comeau, M.R.; Artis, D. Tslp regulates intestinal immunity and inflammation in mouse models of helminth infection and colitis. *J Exp Med* **2009**, *206*, 655-667.

33. Schulz, O.; Jaensson, E.; Persson, E.K.; Liu, X.; Worbs, T.; Agace, W.W.; Pabst, O. Intestinal cd103+, but not cx3cr1+, antigen sampling cells migrate in lymph and serve classical dendritic cell functions. *J Exp Med* **2009**, *206*, 3101-3114.

34. Coombes, J.L.; Siddiqui, K.R.; Arancibia-Cárcamo, C.V.; Hall, J.; Sun, C.M.; Belkaid, Y.; Powrie, F. A functionally specialized population of mucosal cd103+ dcs induces foxp3+ regulatory t cells via a tgf-beta and retinoic acid-dependent mechanism. *J Exp Med* **2007**, *204*, 1757-1764.

35. Hadis, U.; Wahl, B.; Schulz, O.; Hardtke-Wolenski, M.; Schippers, A.; Wagner, N.; Müller, W.; Sparwasser, T.; Förster, R.; Pabst, O. Intestinal tolerance requires gut homing and expansion of foxp3+ regulatory t cells in the lamina propria. *Immunity* **2011**, *34*, 237-246.

36. Macpherson, A.J.; Uhr, T. Induction of protective iga by intestinal dendritic cells carrying commensal bacteria. *Science* **2004**, *303*, 1662-1665.

37. Cheroutre, H.; Lambolez, F.; Mucida, D. The light and dark sides of intestinal intraepithelial lymphocytes. *Nat Rev Immunol* **2011**, *11*, 445-456.

38. Cepek, K.L.; Shaw, S.K.; Parker, C.M.; Russell, G.J.; Morrow, J.S.; Rimm, D.L.; Brenner, M.B. Adhesion between epithelial cells and t lymphocytes mediated by e-cadherin and the alpha e beta 7 integrin. *Nature* **1994**, *372*, 190-193.

39. Rakoff-Nahoum, S.; Paglino, J.; Eslami-Varzaneh, F.; Edberg, S.; Medzhitov, R. Recognition of commensal microflora by toll-like receptors is required for intestinal homeostasis. *Cell* **2004**, *118*, 229-241.

40. Podolsky, D.K.; Gerken, G.; Eyking, A.; Cario, E. Colitis-associated variant of tlr2 causes impaired mucosal repair because of tff3 deficiency. *Gastroenterology* **2009**, *137*, 209-220.

41. Brandl, K.; Sun, L.; Neppl, C.; Siggs, O.M.; Le Gall, S.M.; Tomisato, W.; Li, X.; Du, X.; Maennel, D.N.; Blobel, C.P.*, et al.* Myd88 signaling in nonhematopoietic cells protects mice against induced colitis by regulating specific egf receptor ligands. *Proc Natl Acad Sci U S A* **2010**, *107*, 19967-19972.

42. Deplancke, B.; Gaskins, H.R. Microbial modulation of innate defense: Goblet cells and the intestinal mucus layer. *Am J Clin Nutr* **2001**, *73*, 1131S-1141S.

43. Johansen, F.E.; Kaetzel, C.S. Regulation of the polymeric immunoglobulin receptor and iga transport: New advances in environmental factors that stimulate pigr expression and its role in mucosal immunity. *Mucosal Immunol* **2011**, *4*, 598-602.

44. Hooper, L.V.; Littman, D.R.; Macpherson, A.J. Interactions between the microbiota and the immune system. *Science* **2012**, *336*, 1268-1273.

45. Macpherson, A.J.; Harris, N.L. Interactions between commensal intestinal bacteria and the immune system. *Nat Rev Immunol* **2004**, *4*, 478-485.

46. Hooper, L.V.; Wong, M.H.; Thelin, A.; Hansson, L.; Falk, P.G.; Gordon, J.I. Molecular analysis of commensal host-microbial relationships in the intestine. *Science* **2001**, *291*, 881-884.

47. Umesaki, Y.; Setoyama, H.; Matsumoto, S.; Okada, Y. Expansion of alpha beta t-cell receptor-bearing intestinal intraepithelial lymphocytes after microbial colonization in germ-free mice and its independence from thymus. *Immunology* **1993**, *79*, 32-37.

48. Lorenz, R.G.; Chaplin, D.D.; McDonald, K.G.; McDonough, J.S.; Newberry, R.D. Isolated lymphoid follicle formation is inducible and dependent upon lymphotoxin-

sufficient b lymphocytes, lymphotoxin beta receptor, and tnf receptor i function. *J Immunol* **2003**, *170*, 5475-5482.

49. Packey, C.D.; Sartor, R.B. Commensal bacteria, traditional and opportunistic pathogens, dysbiosis and bacterial killing in inflammatory bowel diseases. *Curr Opin Infect Dis* **2009**, *22*, 292-301.

50. Kaser, A.; Zeissig, S.; Blumberg, R.S. Inflammatory bowel disease. *Annu Rev Immunol* **2010**, *28*, 573-621.

51. Cario, E. Microbiota and innate immunity in intestinal inflammation and neoplasia. *Curr Opin Gastroenterol* **2013**, *29*, 85-91.

52. Vijay-Kumar, M.; Aitken, J.D.; Carvalho, F.A.; Cullender, T.C.; Mwangi, S.; Srinivasan, S.; Sitaraman, S.V.; Knight, R.; Ley, R.E.; Gewirtz, A.T. Metabolic syndrome and altered gut microbiota in mice lacking toll-like receptor 5. *Science* **2010**, *328*, 228-231.

53. Bouma, G.; Strober, W. The immunological and genetic basis of inflammatory bowel disease. *Nat Rev Immunol* **2003**, *3*, 521-533.

54. Baumgart, D.C.; Sandborn, W.J. Inflammatory bowel disease: Clinical aspects and established and evolving therapies. *Lancet* **2007**, *369*, 1641-1657.

55. Lavelle, E.C.; Murphy, C.; O'Neill, L.A.; Creagh, E.M. The role of tlrs, nlrs, and rlrs in mucosal innate immunity and homeostasis. *Mucosal Immunol* **2010**, *3*, 17-28.

56. Uematsu, S.; Fujimoto, K. The innate immune system in the intestine. *Microbiol Immunol* **2010**, *54*, 645-657.

57. Zelenay, S.; Reis e Sousa, C. Adaptive immunity after cell death. *Trends Immunol* **2013**, *34*, 329-335.

58. Akira, S.; Uematsu, S.; Takeuchi, O. Pathogen recognition and innate immunity. *Cell* **2006**, *124*, 783-801.

59. Cario, E.; Gerken, G.; Podolsky, D.K. Toll-like receptor 2 enhances zo-1-associated intestinal epithelial barrier integrity via protein kinase c. *Gastroenterology* **2004**, *127*, 224-238.

60. Ey, B.; Eyking, A.; Gerken, G.; Podolsky, D.K.; Cario, E. Tlr2 mediates gap junctional intercellular communication through connexin-43 in intestinal epithelial barrier injury. *J Biol Chem* **2009**, *284*, 22332-22343.

61. Slack, E.; Hapfelmeier, S.; Stecher, B.; Velykoredko, Y.; Stoel, M.; Lawson, M.A.; Geuking, M.B.; Beutler, B.; Tedder, T.F.; Hardt, W.D.*, et al.* Innate and adaptive immunity cooperate flexibly to maintain host-microbiota mutualism. *Science* **2009**, *325*, 617-620.

62. Macpherson, A.J.; Slack, E.; Geuking, M.B.; McCoy, K.D. The mucosal firewalls against commensal intestinal microbes. *Semin Immunopathol* **2009**, *31*, 145-149.

63. Kawai, T.; Akira, S. The role of pattern-recognition receptors in innate immunity: Update on toll-like receptors. *Nat Immunol* **2010**, *11*, 373-384.

64. Creagh, E.M.; O'Neill, L.A. Tlrs, nlrs and rlrs: A trinity of pathogen sensors that co-operate in innate immunity. *Trends Immunol* **2006**, *27*, 352-357.

65. Jin, M.S.; Kim, S.E.; Heo, J.Y.; Lee, M.E.; Kim, H.M.; Paik, S.G.; Lee, H.; Lee, J.O. Crystal structure of the tlr1-tlr2 heterodimer induced by binding of a tri-acylated lipopeptide. *Cell* **2007**, *130*, 1071-1082.

66. Kang, J.Y.; Nan, X.; Jin, M.S.; Youn, S.J.; Ryu, Y.H.; Mah, S.; Han, S.H.; Lee, H.; Paik, S.G.; Lee, J.O. Recognition of lipopeptide patterns by toll-like receptor 2-toll-like receptor 6 heterodimer. *Immunity* **2009**, *31*, 873-884.

67. Akashi-Takamura, S.; Miyake, K. Tlr accessory molecules. *Curr Opin Immunol* **2008**, *20*, 420-425.

68. Zhang, D.; Zhang, G.; Hayden, M.S.; Greenblatt, M.B.; Bussey, C.; Flavell, R.A.; Ghosh, S. A toll-like receptor that prevents infection by uropathogenic bacteria. *Science* **2004**, *303*, 1522-1526.

69. Yarovinsky, F.; Zhang, D.; Andersen, J.F.; Bannenberg, G.L.; Serhan, C.N.; Hayden, M.S.; Hieny, S.; Sutterwala, F.S.; Flavell, R.A.; Ghosh, S.*, et al.* Tlr11 activation of dendritic cells by a protozoan profilin-like protein. *Science* **2005**, *308*, 1626-1629.

70. O'Neill, L.A.; Bowie, A.G. The family of five: Tir-domain-containing adaptors in toll-like receptor signalling. *Nat Rev Immunol* **2007**, *7*, 353-364.

71. Sakaguchi, S.; Negishi, H.; Asagiri, M.; Nakajima, C.; Mizutani, T.; Takaoka, A.; Honda, K.; Taniguchi, T. Essential role of irf-3 in lipopolysaccharide-induced interferon-beta gene expression and endotoxin shock. *Biochem Biophys Res Commun* **2003**, *306*, 860-866.

72. Fitzgerald, K.A.; Rowe, D.C.; Barnes, B.J.; Caffrey, D.R.; Visintin, A.; Latz, E.; Monks, B.; Pitha, P.M.; Golenbock, D.T. Lps-tlr4 signaling to irf-3/7 and nf-kappab involves the toll adapters tram and trif. *J Exp Med* **2003**, *198*, 1043-1055.

73. Tschopp, J.; Martinon, F.; Burns, K. Nalps: A novel protein family involved in inflammation. *Nat Rev Mol Cell Biol* **2003**, *4*, 95-104.

74. Inohara; Chamaillard; McDonald, C.; Nuñez, G. Nod-lrr proteins: Role in host-microbial interactions and inflammatory disease. *Annu Rev Biochem* **2005**, *74*, 355-383.

75. Shaw, M.H.; Reimer, T.; Kim, Y.G.; Nuñez, G. Nod-like receptors (nlrs): Bona fide intracellular microbial sensors. *Curr Opin Immunol* **2008**, *20*, 377-382.

76. Fritz, J.H.; Ferrero, R.L.; Philpott, D.J.; Girardin, S.E. Nod-like proteins in immunity, inflammation and disease. *Nat Immunol* **2006**, *7*, 1250-1257.

77. Inohara, N.; Koseki, T.; del Peso, L.; Hu, Y.; Yee, C.; Chen, S.; Carrio, R.; Merino, J.; Liu, D.; Ni, J.*, et al.* Nod1, an apaf-1-like activator of caspase-9 and nuclear factor-kappab. *J Biol Chem* **1999**, *274*, 14560-14567.

78. Gutierrez, O.; Pipaon, C.; Inohara, N.; Fontalba, A.; Ogura, Y.; Prosper, F.; Nunez, G.; Fernandez-Luna, J.L. Induction of nod2 in myelomonocytic and intestinal

epithelial cells via nuclear factor-kappa b activation. *J Biol Chem* **2002**, *277*, 41701-41705.

79. Girardin, S.E.; Boneca, I.G.; Viala, J.; Chamaillard, M.; Labigne, A.; Thomas, G.; Philpott, D.J.; Sansonetti, P.J. Nod2 is a general sensor of peptidoglycan through muramyl dipeptide (mdp) detection. *J Biol Chem* **2003**, *278*, 8869-8872.

80. Girardin, S.E.; Boneca, I.G.; Carneiro, L.A.; Antignac, A.; Jéhanno, M.; Viala, J.; Tedin, K.; Taha, M.K.; Labigne, A.; Zähringer, U.*, et al.* Nod1 detects a unique muropeptide from gram-negative bacterial peptidoglycan. *Science* **2003**, *300*, 1584-1587.

81. Chen, G.; Shaw, M.H.; Kim, Y.G.; Nuñez, G. Nod-like receptors: Role in innate immunity and inflammatory disease. *Annu Rev Pathol* **2009**, *4*, 365-398.

82. Bryant, C.; Fitzgerald, K.A. Molecular mechanisms involved in inflammasome activation. *Trends Cell Biol* **2009**, *19*, 455-464.

83. Franchi, L.; Warner, N.; Viani, K.; Nuñez, G. Function of nod-like receptors in microbial recognition and host defense. *Immunol Rev* **2009**, *227*, 106-128.

84. Lamkanfi, M.; Kanneganti, T.D.; Franchi, L.; Núñez, G. Caspase-1 inflammasomes in infection and inflammation. *J Leukoc Biol* **2007**, *82*, 220-225.

85. Strober, W.; Murray, P.J.; Kitani, A.; Watanabe, T. Signalling pathways and molecular interactions of nod1 and nod2. *Nat Rev Immunol* **2006**, *6*, 9-20.

86. Zaki, M.H.; Boyd, K.L.; Vogel, P.; Kastan, M.B.; Lamkanfi, M.; Kanneganti, T.D. The nlrp3 inflammasome protects against loss of epithelial integrity and mortality during experimental colitis. *Immunity* **2010**, *32*, 379-391.

87. Inohara, N.; Ogura, Y.; Fontalba, A.; Gutierrez, O.; Pons, F.; Crespo, J.; Fukase, K.; Inamura, S.; Kusumoto, S.; Hashimoto, M.*, et al.* Host recognition of bacterial muramyl dipeptide mediated through nod2. Implications for crohn's disease. *J Biol Chem* **2003**, *278*, 5509-5512.

88. McGovern, D.P.; Hysi, P.; Ahmad, T.; van Heel, D.A.; Moffatt, M.F.; Carey, A.; Cookson, W.O.; Jewell, D.P. Association between a complex insertion/deletion

polymorphism in nod1 (card4) and susceptibility to inflammatory bowel disease. *Hum Mol Genet* **2005**, *14*, 1245-1250.

89. Fox, J.G.; Dewhirst, F.E.; Tully, J.G.; Paster, B.J.; Yan, L.; Taylor, N.S.; Collins, M.J.; Gorelick, P.L.; Ward, J.M. Helicobacter hepaticus sp. Nov., a microaerophilic bacterium isolated from livers and intestinal mucosal scrapings from mice. *J Clin Microbiol* **1994**, *32*, 1238-1245.

90. Fox, J.G.; Li, X.; Yan, L.; Cahill, R.J.; Hurley, R.; Lewis, R.; Murphy, J.C. Chronic proliferative hepatitis in a/jcr mice associated with persistent helicobacter hepaticus infection: A model of helicobacter-induced carcinogenesis. *Infect Immun* **1996**, *64*, 1548-1558.

91. Fox, J.G.; Ge, Z.; Whary, M.T.; Erdman, S.E.; Horwitz, B.H. Helicobacter hepaticus infection in mice: Models for understanding lower bowel inflammation and cancer. *Mucosal Immunol* **2011**, *4*, 22-30.

92. Suerbaum, S.; Josenhans, C.; Sterzenbach, T.; Drescher, B.; Brandt, P.; Bell, M.; Droge, M.; Fartmann, B.; Fischer, H.P.; Ge, Z.*, et al.* The complete genome sequence of the carcinogenic bacterium helicobacter hepaticus. *Proc Natl Acad Sci U S A* **2003**, *100*, 7901-7906.

93. Lara-Tejero, M.; Galán, J.E. Cdta, cdtb, and cdtc form a tripartite complex that is required for cytolethal distending toxin activity. *Infect Immun* **2001**, *69*, 4358-4365.

94. Ge, Z.; Feng, Y.; Whary, M.T.; Nambiar, P.R.; Xu, S.; Ng, V.; Taylor, N.S.; Fox, J.G. Cytolethal distending toxin is essential for helicobacter hepaticus colonization in outbred swiss webster mice. *Infect Immun* **2005**, *73*, 3559-3567.

95. Chow, J.; Mazmanian, S.K. A pathobiont of the microbiota balances host colonization and intestinal inflammation. *Cell Host Microbe* **2010**, *7*, 265-276.

96. Ge, Z.; Sterzenbach, T.; Whary, M.T.; Rickman, B.H.; Rogers, A.B.; Shen, Z.; Taylor, N.S.; Schauer, D.B.; Josenhans, C.; Suerbaum, S.*, et al.* Helicobacter hepaticus hhgi1 is a pathogenicity island associated with typhlocolitis in b6.129-il10 tm1cgn mice. *Microbes Infect* **2008**, *10*, 726-733.

97. Silverman, J.M.; Brunet, Y.R.; Cascales, E.; Mougous, J.D. Structure and regulation of the type vi secretion system. *Annu Rev Microbiol* **2012**, *66*, 453-472.

98. Raskin, D.M.; Seshadri, R.; Pukatzki, S.U.; Mekalanos, J.J. Bacterial genomics and pathogen evolution. *Cell* **2006**, *124*, 703-714.

99. Burne, R.A.; Chen, Y.Y. Bacterial ureases in infectious diseases. *Microbes Infect* **2000**, *2*, 533-542.

100. Tsuda, M.; Karita, M.; Morshed, M.G.; Okita, K.; Nakazawa, T. A urease-negative mutant of helicobacter pylori constructed by allelic exchange mutagenesis lacks the ability to colonize the nude mouse stomach. *Infect Immun* **1994**, *62*, 3586-3589.

101. Ge, Z.; Lee, A.; Whary, M.T.; Rogers, A.B.; Maurer, K.J.; Taylor, N.S.; Schauer, D.B.; Fox, J.G. Helicobacter hepaticus urease is not required for intestinal colonization but promotes hepatic inflammation in male a/jcr mice. *Microb Pathog* **2008**, *45*, 18-24.

102. Alyamani, E.J.; Brandt, P.; Pena, J.A.; Major, A.M.; Fox, J.G.; Suerbaum, S.; Versalovic, J. Helicobacter hepaticus catalase shares surface-predicted epitopes with mammalian catalases. *Microbiology* **2007**, *153*, 1006-1016.

103. Hong, Y.; Wang, G.; Maier, R.J. A helicobacter hepaticus catalase mutant is hypersensitive to oxidative stress and suffers increased dna damage. *J Med Microbiol* **2007**, *56*, 557-562.

104. Mehta, N.S.; Benoit, S.; Mysore, J.V.; Sousa, R.S.; Maier, R.J. Helicobacter hepaticus hydrogenase mutants are deficient in hydrogen-supported amino acid uptake and in causing liver lesions in a/j mice. *Infect Immun* **2005**, *73*, 5311-5318.

105. Sterzenbach, T.; Bartonickova, L.; Behrens, W.; Brenneke, B.; Schulze, J.; Kops, F.; Chin, E.Y.; Katzowitsch, E.; Schauer, D.B.; Fox, J.G., *et al.* Role of the helicobacter hepaticus flagellar sigma factor flia in gene regulation and murine colonization. *J Bacteriol* **2008**, *190*, 6398-6408.

106. Kullberg, M.C.; Jankovic, D.; Gorelick, P.L.; Caspar, P.; Letterio, J.J.; Cheever, A.W.; Sher, A. Bacteria-triggered cd4(+) t regulatory cells suppress helicobacter hepaticus-induced colitis. *J Exp Med* **2002**, *196*, 505-515.

107. Kullberg, M.C.; Ward, J.M.; Gorelick, P.L.; Caspar, P.; Hieny, S.; Cheever, A.; Jankovic, D.; Sher, A. Helicobacter hepaticus triggers colitis in specific-pathogen-free interleukin-10 (il-10)-deficient mice through an il-12- and gamma interferon-dependent mechanism. *Infect Immun* **1998**, *66*, 5157-5166.

108. Kullberg, M.C.; Jankovic, D.; Feng, C.G.; Hue, S.; Gorelick, P.L.; McKenzie, B.S.; Cua, D.J.; Powrie, F.; Cheever, A.W.; Maloy, K.J.*, et al.* Il-23 plays a key role in helicobacter hepaticus-induced t cell-dependent colitis. *J Exp Med* **2006**, *203*, 2485-2494.

109. Read, S.; Malmström, V.; Powrie, F. Cytotoxic t lymphocyte-associated antigen 4 plays an essential role in the function of cd25(+)cd4(+) regulatory cells that control intestinal inflammation. *J Exp Med* **2000**, *192*, 295-302.

110. Cahill, R.J.; Foltz, C.J.; Fox, J.G.; Dangler, C.A.; Powrie, F.; Schauer, D.B. Inflammatory bowel disease: An immunity-mediated condition triggered by bacterial infection with helicobacter hepaticus. *Infect Immun* **1997**, *65*, 3126-3131.

111. Burich, A.; Hershberg, R.; Waggie, K.; Zeng, W.; Brabb, T.; Westrich, G.; Viney, J.L.; Maggio-Price, L. Helicobacter-induced inflammatory bowel disease in il-10- and t cell-deficient mice. *Am J Physiol Gastrointest Liver Physiol* **2001**, *281*, G764-778.

112. von Freeden-Jeffry, U.; Davidson, N.; Wiler, R.; Fort, M.; Burdach, S.; Murray, R. Il-7 deficiency prevents development of a non-t cell non-b cell-mediated colitis. *J Immunol* **1998**, *161*, 5673-5680.

113. Hue, S.; Ahern, P.; Buonocore, S.; Kullberg, M.C.; Cua, D.J.; McKenzie, B.S.; Powrie, F.; Maloy, K.J. Interleukin-23 drives innate and t cell-mediated intestinal inflammation. *J Exp Med* **2006**, *203*, 2473-2483.

114. Maloy, K.J.; Salaun, L.; Cahill, R.; Dougan, G.; Saunders, N.J.; Powrie, F. Cd4+cd25+ t(r) cells suppress innate immune pathology through cytokine-dependent mechanisms. *J Exp Med* **2003**, *197*, 111-119.

115. Buonocore, S.; Ahern, P.P.; Uhlig, H.H.; Ivanov, I.I.; Littman, D.R.; Maloy, K.J.; Powrie, F. Innate lymphoid cells drive interleukin-23-dependent innate intestinal pathology. *Nature* **2010**, *464*, 1371-1375.

116. Erdman, S.E.; Poutahidis, T.; Tomczak, M.; Rogers, A.B.; Cormier, K.; Plank, B.; Horwitz, B.H.; Fox, J.G. Cd4+ cd25+ regulatory t lymphocytes inhibit microbially induced colon cancer in rag2-deficient mice. *Am J Pathol* **2003**, *162*, 691-702.

117. Erdman, S.E.; Rao, V.P.; Poutahidis, T.; Ihrig, M.M.; Ge, Z.; Feng, Y.; Tomczak, M.; Rogers, A.B.; Horwitz, B.H.; Fox, J.G. Cd4(+)cd25(+) regulatory lymphocytes require interleukin 10 to interrupt colon carcinogenesis in mice. *Cancer Res* **2003**, *63*, 6042-6050.

118. Tomczak, M.F.; Erdman, S.E.; Poutahidis, T.; Rogers, A.B.; Holcombe, H.; Plank, B.; Fox, J.G.; Horwitz, B.H. Nf-kappa b is required within the innate immune system to inhibit microflora-induced colitis and expression of il-12 p40. *J Immunol* **2003**, *171*, 1484-1492.

119. Tomczak, M.F.; Gadjeva, M.; Wang, Y.Y.; Brown, K.; Maroulakou, I.; Tsichlis, P.N.; Erdman, S.E.; Fox, J.G.; Horwitz, B.H. Defective activation of erk in macrophages lacking the p50/p105 subunit of nf-kappab is responsible for elevated expression of il-12 p40 observed after challenge with helicobacter hepaticus. *J Immunol* **2006**, *176*, 1244-1251.

120. Wang, Y.; Rickman, B.H.; Poutahidis, T.; Schlieper, K.; Jackson, E.A.; Erdman, S.E.; Fox, J.G.; Horwitz, B.H. C-rel is essential for the development of innate and t cell-induced colitis. *J Immunol* **2008**, *180*, 8118-8125.

121. Tomczak, M.F.; Erdman, S.E.; Davidson, A.; Wang, Y.Y.; Nambiar, P.R.; Rogers, A.B.; Rickman, B.; Luchetti, D.; Fox, J.G.; Horwitz, B.H. Inhibition of helicobacter hepaticus-induced colitis by il-10 requires the p50/p105 subunit of nf-kappa b. *J Immunol* **2006**, *177*, 7332-7339.

122. Eckmann, L.; Nebelsiek, T.; Fingerle, A.A.; Dann, S.M.; Mages, J.; Lang, R.; Robine, S.; Kagnoff, M.F.; Schmid, R.M.; Karin, M.*, et al.* Opposing functions of ikkbeta during acute and chronic intestinal inflammation. *Proc Natl Acad Sci U S A* **2008**, *105*, 15058-15063.

123. Cario, E. Bacterial interactions with cells of the intestinal mucosa: Toll-like receptors and nod2. *Gut* **2005**, *54*, 1182-1193.

124. Asquith, M.J.; Boulard, O.; Powrie, F.; Maloy, K.J. Pathogenic and protective roles of myd88 in leukocytes and epithelial cells in mouse models of inflammatory bowel disease. *Gastroenterology* **2010**, *139*, 519-529, 529.e511-512.

125. Mandell, L.; Moran, A.P.; Cocchiarella, A.; Houghton, J.; Taylor, N.; Fox, J.G.; Wang, T.C.; Kurt-Jones, E.A. Intact gram-negative helicobacter pylori, helicobacter felis, and helicobacter hepaticus bacteria activate innate immunity via toll-like receptor 2 but not toll-like receptor 4. *Infect Immun* **2004**, *72*, 6446-6454.

126. Boulard, O.; Asquith, M.J.; Powrie, F.; Maloy, K.J. Tlr2-independent induction and regulation of chronic intestinal inflammation. *Eur J Immunol* **2010**, *40*, 516-524.

127. Petnicki-Ocwieja, T.; Hrncir, T.; Liu, Y.J.; Biswas, A.; Hudcovic, T.; Tlaskalova-Hogenova, H.; Kobayashi, K.S. Nod2 is required for the regulation of commensal microbiota in the intestine. *Proc Natl Acad Sci U S A* **2009**, *106*, 15813-15818.

128. Chan, V.; Crocetti, G.; Grehan, M.; Zhang, L.; Danon, S.; Lee, A.; Mitchell, H. Visualization of helicobacter species within the murine cecal mucosa using specific fluorescence in situ hybridization. *Helicobacter* **2005**, *10*, 114-124.

129. Sterzenbach, T.; Lee, S.K.; Brenneke, B.; von Goetz, F.; Schauer, D.B.; Fox, J.G.; Suerbaum, S.; Josenhans, C. Inhibitory effect of enterohepatic helicobacter hepaticus on innate immune responses of mouse intestinal epithelial cells. *Infect Immun* **2007**, *75*, 2717-2728.

130. Andersen-Nissen, E.; Smith, K.D.; Strobe, K.L.; Barrett, S.L.; Cookson, B.T.; Logan, S.M.; Aderem, A. Evasion of toll-like receptor 5 by flagellated bacteria. *Proc Natl Acad Sci U S A* **2005**, *102*, 9247-9252.

131. Tian, H.; Biehs, B.; Warming, S.; Leong, K.G.; Rangell, L.; Klein, O.D.; de Sauvage, F.J. A reserve stem cell population in small intestine renders lgr5-positive cells dispensable. *Nature 478*, 255-259.

132. Sangiorgi, E.; Capecchi, M.R. Bmi1 is expressed in vivo in intestinal stem cells. *Nat Genet* **2008**, *40*, 915-920.

133. Crosnier, C.; Stamataki, D.; Lewis, J. Organizing cell renewal in the intestine: Stem cells, signals and combinatorial control. *Nat Rev Genet* **2006**, *7*, 349-359.

134. Rothenberg, M.E.; Nusse, Y.; Kalisky, T.; Lee, J.J.; Dalerba, P.; Scheeren, F.; Lobo, N.; Kulkarni, S.; Sim, S.; Qian, D.*, et al.* Identification of a ckit(+) colonic crypt base secretory cell that supports lgr5(+) stem cells in mice. *Gastroenterology 142*, 1195-1205 e1196.

135. Farin, H.F.; Van Es, J.H.; Clevers, H. Redundant sources of wnt regulate intestinal stem cells and promote formation of paneth cells. *Gastroenterology 143*, 1518-1529 e1517.

136. Krausova, M.; Korinek, V. Wnt signaling in adult intestinal stem cells and cancer. *Cell Signal* **2014**, *26*, 570-579.

137. van Es, J.H.; van Gijn, M.E.; Riccio, O.; van den Born, M.; Vooijs, M.; Begthel, H.; Cozijnsen, M.; Robine, S.; Winton, D.J.; Radtke, F.*, et al.* Notch/gamma-secretase inhibition turns proliferative cells in intestinal crypts and adenomas into goblet cells. *Nature* **2005**, *435*, 959-963.

138. He, X.C.; Zhang, J.; Tong, W.G.; Tawfik, O.; Ross, J.; Scoville, D.H.; Tian, Q.; Zeng, X.; He, X.; Wiedemann, L.M.*, et al.* Bmp signaling inhibits intestinal stem cell self-renewal through suppression of wnt-beta-catenin signaling. *Nat Genet* **2004**, *36*, 1117-1121.

139. Massague, J.; Seoane, J.; Wotton, D. Smad transcription factors. *Genes Dev* **2005**, *19*, 2783-2810.

140. Haramis, A.P.; Begthel, H.; van den Born, M.; van Es, J.; Jonkheer, S.; Offerhaus, G.J.; Clevers, H. De novo crypt formation and juvenile polyposis on bmp inhibition in mouse intestine. *Science* **2004**, *303*, 1684-1686.

141. Bermudez-Brito, M.; Plaza-Diaz, J.; Fontana, L.; Munoz-Quezada, S.; Gil, A. In vitro cell and tissue models for studying host-microbe interactions: A review. *Br J Nutr* **2013**, *109 Suppl 2*, S27-34.

142. Sambuy, Y.; De Angelis, I.; Ranaldi, G.; Scarino, M.L.; Stammati, A.; Zucco, F. The caco-2 cell line as a model of the intestinal barrier: Influence of cell and culture-related factors on caco-2 cell functional characteristics. *Cell Biol Toxicol* **2005**, *21*, 1-26.

143. Rousset, M. The human colon carcinoma cell lines ht-29 and caco-2: Two in vitro models for the study of intestinal differentiation. *Biochimie* **1986**, *68*, 1035-1040.

144. Fogh, J.; Fogh, J.M.; Orfeo, T. One hundred and twenty-seven cultured human tumor cell lines producing tumors in nude mice. *J Natl Cancer Inst* **1977**, *59*, 221-226.

145. Tabuchi, Y.; Ohta, S.; Arai, Y.; Kawahara, M.; Ishibashi, K.; Sugiyama, N.; Horiuchi, T.; Furusawa, M.; Obinata, M.; Fuse, H.*, et al.* Establishment and characterization of a colonic epithelial cell line mce301 from transgenic mice harboring temperature-sensitive simian virus 40 large t-antigen gene. *Cell Struct Funct* **2000**, *25*, 297-307.

146. Inai, T.; Sengoku, A.; Hirose, E.; Iida, H.; Shibata, Y. Comparative characterization of mouse rectum cmt93-i and -ii cells by expression of claudin isoforms and tight junction morphology and function. *Histochem Cell Biol* **2008**, *129*, 223-232.

147. Vidal, K.; Grosjean, I.; evillard, J.P.; Gespach, C.; Kaiserlian, D. Immortalization of mouse intestinal epithelial cells by the sv40-large t gene. Phenotypic and immune characterization of the mode-k cell line. *J Immunol Methods* **1993**, *166*, 63-73.

148. Bens, M.; Bogdanova, A.; Cluzeaud, F.; Miquerol, L.; Kerneis, S.; Kraehenbuhl, J.P.; Kahn, A.; Pringault, E.; Vandewalle, A. Transimmortalized mouse intestinal

cells (m-icc12) that maintain a crypt phenotype. *Am J Physiol* **1996**, *270*, C1666-1674.

149. Cencic, A.; Langerholc, T. Functional cell models of the gut and their applications in food microbiology--a review. *Int J Food Microbiol* **2010**, *141 Suppl 1*, S4-14.

150. Moon, C.; Vandussen, K.L.; Miyoshi, H.; Stappenbeck, T.S. Development of a primary mouse intestinal epithelial cell monolayer culture system to evaluate factors that modulate iga transcytosis. *Mucosal Immunol* **2013**.

151. Watanabe, K.; Ueno, M.; Kamiya, D.; Nishiyama, A.; Matsumura, M.; Wataya, T.; Takahashi, J.B.; Nishikawa, S.; Muguruma, K.; Sasai, Y. A rock inhibitor permits survival of dissociated human embryonic stem cells. *Nat Biotechnol* **2007**, *25*, 681-686.

152. Sato, T.; Stange, D.E.; Ferrante, M.; Vries, R.G.; Van Es, J.H.; Van den Brink, S.; Van Houdt, W.J.; Pronk, A.; Van Gorp, J.; Siersema, P.D.*, et al.* Long-term expansion of epithelial organoids from human colon, adenoma, adenocarcinoma, and barrett's epithelium. *Gastroenterology 141*, 1762-1772.

153. Spence, J.R.; Mayhew, C.N.; Rankin, S.A.; Kuhar, M.F.; Vallance, J.E.; Tolle, K.; Hoskins, E.E.; Kalinichenko, V.V.; Wells, S.I.; Zorn, A.M.*, et al.* Directed differentiation of human pluripotent stem cells into intestinal tissue in vitro. *Nature 470*, 105-109.

154. Jung, P.; Sato, T.; Merlos-Suarez, A.; Barriga, F.M.; Iglesias, M.; Rossell, D.; Auer, H.; Gallardo, M.; Blasco, M.A.; Sancho, E.*, et al.* Isolation and in vitro expansion of human colonic stem cells. *Nat Med 17*, 1225-1227.

155. McCracken, K.W.; Howell, J.C.; Wells, J.M.; Spence, J.R. Generating human intestinal tissue from pluripotent stem cells in vitro. *Nat Protoc 6*, 1920-1928.

156. Ootani, A.; Li, X.; Sangiorgi, E.; Ho, Q.T.; Ueno, H.; Toda, S.; Sugihara, H.; Fujimoto, K.; Weissman, I.L.; Capecchi, M.R.*, et al.* Sustained in vitro intestinal epithelial culture within a wnt-dependent stem cell niche. *Nat Med* **2009**, *15*, 701-706.

157. VanDussen, K.L.; Carulli, A.J.; Keeley, T.M.; Patel, S.R.; Puthoff, B.J.; Magness, S.T.; Tran, I.T.; Maillard, I.; Siebel, C.; Kolterud, Å., *et al.* Notch signaling modulates proliferation and differentiation of intestinal crypt base columnar stem cells. *Development* **2012**, *139*, 488-497.

158. Geis, G.; Suerbaum, S.; Forsthoff, B.; Leying, H.; Opferkuch, W. Ultrastructure and biochemical studies of the flagellar sheath of helicobacter pylori. *J Med Microbiol* **1993**, *38*, 371-377.

159. Koo, B.K.; Stange, D.E.; Sato, T.; Karthaus, W.; Farin, H.F.; Huch, M.; van Es, J.H.; Clevers, H. Controlled gene expression in primary lgr5 organoid cultures. *Nat Methods* **2012**, *9*, 81-83.

160. Schwank, G.; Koo, B.K.; Sasselli, V.; Dekkers, J.F.; Heo, I.; Demircan, T.; Sasaki, N.; Boymans, S.; Cuppen, E.; van der Ent, C.K., *et al.* Functional repair of cftr by crispr/cas9 in intestinal stem cell organoids of cystic fibrosis patients. *Cell Stem Cell 13*, 653-658.

161. Yui, S.; Nakamura, T.; Sato, T.; Nemoto, Y.; Mizutani, T.; Zheng, X.; Ichinose, S.; Nagaishi, T.; Okamoto, R.; Tsuchiya, K., *et al.* Functional engraftment of colon epithelium expanded in vitro from a single adult lgr5(+) stem cell. *Nat Med* **2012**, *18*, 618-623.

162. Howell, J.C.; Wells, J.M. Generating intestinal tissue from stem cells: Potential for research and therapy. *Regen Med* **2011**, *6*, 743-755.

163. Pfaffl, M.W. A new mathematical model for relative quantification in real-time rt-pcr. *Nucleic Acids Res* **2001**, *29*, e45.

164. Korinek, V.; Barker, N.; Moerer, P.; van Donselaar, E.; Huls, G.; Peters, P.J.; Clevers, H. Depletion of epithelial stem-cell compartments in the small intestine of mice lacking tcf-4. *Nat Genet* **1998**, *19*, 379-383.

165. Kuhnert, F.; Davis, C.R.; Wang, H.T.; Chu, P.; Lee, M.; Yuan, J.; Nusse, R.; Kuo, C.J. Essential requirement for wnt signaling in proliferation of adult small intestine and colon revealed by adenoviral expression of dickkopf-1. *Proc Natl Acad Sci U S A* **2004**, *101*, 266-271.

166. Kim, K.A.; Kakitani, M.; Zhao, J.; Oshima, T.; Tang, T.; Binnerts, M.; Liu, Y.; Boyle, B.; Park, E.; Emtage, P.*, et al.* Mitogenic influence of human r-spondin1 on the intestinal epithelium. *Science* **2005**, *309*, 1256-1259.

167. Dignass, A.U.; Sturm, A. Peptide growth factors in the intestine. *Eur J Gastroenterol Hepatol* **2001**, *13*, 763-770.

168. Willert, K.; Brown, J.D.; Danenberg, E.; Duncan, A.W.; Weissman, I.L.; Reya, T.; Yates, J.R.; Nusse, R. Wnt proteins are lipid-modified and can act as stem cell growth factors. *Nature* **2003**, *423*, 448-452.

169. Sasaki, T.; Giltay, R.; Talts, U.; Timpl, R.; Talts, J.F. Expression and distribution of laminin alpha1 and alpha2 chains in embryonic and adult mouse tissues: An immunochemical approach. *Exp Cell Res* **2002**, *275*, 185-199.

170. Lengsfeld, A.M.; Löw, I.; Wieland, T.; Dancker, P.; Hasselbach, W. Interaction of phalloidin with actin. *Proc Natl Acad Sci U S A* **1974**, *71*, 2803-2807.

171. Madara, J.L.; Barenberg, D.; Carlson, S. Effects of cytochalasin d on occluding junctions of intestinal absorptive cells: Further evidence that the cytoskeleton may influence paracellular permeability and junctional charge selectivity. *J Cell Biol* **1986**, *102*, 2125-2136.

172. Cooper, J.A. The role of actin polymerization in cell motility. *Annu Rev Physiol* **1991**, *53*, 585-605.

173. Banan, A.; Smith, G.S.; Kokoska, E.R.; Miller, T.A. Role of actin cytoskeleton in prostaglandin-induced protection against ethanol in an intestinal epithelial cell line. *J Surg Res* **2000**, *88*, 104-113.

174. Bray, D.; Heath, J.; Moss, D. The membrane-associated 'cortex' of animal cells: Its structure and mechanical properties. *J Cell Sci Suppl* **1986**, *4*, 71-88.

175. Stevenson, B.R.; Siliciano, J.D.; Mooseker, M.S.; Goodenough, D.A. Identification of zo-1: A high molecular weight polypeptide associated with the tight junction (zonula occludens) in a variety of epithelia. *J Cell Biol* **1986**, *103*, 755-766.

176. Wright, C.S. Structural comparison of the two distinct sugar binding sites in wheat germ agglutinin isolectin ii. *J Mol Biol* **1984**, *178*, 91-104.

177. Wirth, M.; Kneuer, C.; Lehr, C.M.; Gabor, F. Lectin-mediated drug delivery: Discrimination between cytoadhesion and cytoinvasion and evidence for lysosomal accumulation of wheat germ agglutinin in the caco-2 model. *J Drug Target* **2002**, *10*, 439-448.

178. Maury, J.; Nicoletti, C.; Guzzo-Chambraud, L.; Maroux, S. The filamentous brush border glycocalyx, a mucin-like marker of enterocyte hyper-polarization. *Eur J Biochem* **1995**, *228*, 323-331.

179. Sakarya, S.; Göktürk, C.; Oztürk, T.; Ertugrul, M.B. Sialic acid is required for nonspecific adherence of salmonella enterica ssp. Enterica serovar typhi on caco-2 cells. *FEMS Immunol Med Microbiol* **2010**, *58*, 330-335.

180. Booth, C.; O'Shea, J.A.; Potten, C.S. Maintenance of functional stem cells in isolated and cultured adult intestinal epithelium. *Exp Cell Res* **1999**, *249*, 359-366.

181. Stallmach, A.; Hahn, U.; Merker, H.J.; Hahn, E.G.; Riecken, E.O. Differentiation of rat intestinal epithelial cells is induced by organotypic mesenchymal cells in vitro. *Gut* **1989**, *30*, 959-970.

182. de Lau, W.; Barker, N.; Low, T.Y.; Koo, B.K.; Li, V.S.; Teunissen, H.; Kujala, P.; Haegebarth, A.; Peters, P.J.; van de Wetering, M.*, et al.* Lgr5 homologues associate with wnt receptors and mediate r-spondin signalling. *Nature* **2011**, *476*, 293-297.

183. Mustata, R.C.; Van Loy, T.; Lefort, A.; Libert, F.; Strollo, S.; Vassart, G.; Garcia, M.I. Lgr4 is required for paneth cell differentiation and maintenance of intestinal stem cells ex vivo. *EMBO Rep* **2011**, *12*, 558-564.

184. Ward, J.M.; Fox, J.G.; Anver, M.R.; Haines, D.C.; George, C.V.; Collins, M.J.; Gorelick, P.L.; Nagashima, K.; Gonda, M.A.; Gilden, R.V. Chronic active hepatitis and associated liver tumors in mice caused by a persistent bacterial infection with a novel helicobacter species. *J Natl Cancer Inst* **1994**, *86*, 1222-1227.

185. Sarma-Rupavtarm, R.B.; Ge, Z.; Schauer, D.B.; Fox, J.G.; Polz, M.F. Spatial distribution and stability of the eight microbial species of the altered schaedler flora in the mouse gastrointestinal tract. *Appl Environ Microbiol* **2004**, *70*, 2791-2800.

186. Solnick, J.V.; Schauer, D.B. Emergence of diverse helicobacter species in the pathogenesis of gastric and enterohepatic diseases. *Clin Microbiol Rev* **2001**, *14*, 59-97.

187. Berg, D.J.; Davidson, N.; Kühn, R.; Müller, W.; Menon, S.; Holland, G.; Thompson-Snipes, L.; Leach, M.W.; Rennick, D. Enterocolitis and colon cancer in interleukin-10-deficient mice are associated with aberrant cytokine production and cd4(+) th1-like responses. *J Clin Invest* **1996**, *98*, 1010-1020.

188. Ralph, P.; Nakoinz, I. Antibody-dependent killing of erythrocyte and tumor targets by macrophage-related cell lines: Enhancement by ppd and lps. *J Immunol* **1977**, *119*, 950-954.

189. Abreu, M.T.; Vora, P.; Faure, E.; Thomas, L.S.; Arnold, E.T.; Arditi, M. Decreased expression of toll-like receptor-4 and md-2 correlates with intestinal epithelial cell protection against dysregulated proinflammatory gene expression in response to bacterial lipopolysaccharide. *J Immunol* **2001**, *167*, 1609-1616.

190. Melmed, G.; Thomas, L.S.; Lee, N.; Tesfay, S.Y.; Lukasek, K.; Michelsen, K.S.; Zhou, Y.; Hu, B.; Arditi, M.; Abreu, M.T. Human intestinal epithelial cells are broadly unresponsive to toll-like receptor 2-dependent bacterial ligands: Implications for host-microbial interactions in the gut. *J Immunol* **2003**, *170*, 1406-1415.

191. Lotz, M.; Gütle, D.; Walther, S.; Ménard, S.; Bogdan, C.; Hornef, M.W. Postnatal acquisition of endotoxin tolerance in intestinal epithelial cells. *J Exp Med* **2006**, *203*, 973-984.

192. Bambou, J.C.; Giraud, A.; Menard, S.; Begue, B.; Rakotobe, S.; Heyman, M.; Taddei, F.; Cerf-Bensussan, N.; Gaboriau-Routhiau, V. In vitro and ex vivo activation of the tlr5 signaling pathway in intestinal epithelial cells by a commensal escherichia coli strain. *J Biol Chem* **2004**, *279*, 42984-42992.

193. Nordlander, S.; Pott, J.; Maloy, K.J. Nlrc4 expression in intestinal epithelial cells mediates protection against an enteric pathogen. *Mucosal Immunol* **2014**, *7*, 775-785.

194. Kummer, J.A.; Broekhuizen, R.; Everett, H.; Agostini, L.; Kuijk, L.; Martinon, F.; van Bruggen, R.; Tschopp, J. Inflammasome components nalp 1 and 3 show distinct but separate expression profiles in human tissues suggesting a site-specific role in the inflammatory response. *J Histochem Cytochem* **2007**, *55*, 443-452.

195. Wlodarska, M.; Thaiss, C.A.; Nowarski, R.; Henao-Mejia, J.; Zhang, J.P.; Brown, E.M.; Frankel, G.; Levy, M.; Katz, M.N.; Philbrick, W.M.*, et al.* Nlrp6 inflammasome orchestrates the colonic host-microbial interface by regulating goblet cell mucus secretion. *Cell* **2014**, *156*, 1045-1059.

196. Knodler, L.A.; Crowley, S.M.; Sham, H.P.; Yang, H.; Wrande, M.; Ma, C.; Ernst, R.K.; Steele-Mortimer, O.; Celli, J.; Vallance, B.A. Noncanonical inflammasome activation of caspase-4/caspase-11 mediates epithelial defenses against enteric bacterial pathogens. *Cell Host Microbe* **2014**, *16*, 249-256.

197. Tlaskalová-Hogenová, H.; Stepánková, R.; Hudcovic, T.; Tucková, L.; Cukrowska, B.; Lodinová-Zádníková, R.; Kozáková, H.; Rossmann, P.; Bártová, J.; Sokol, D.*, et al.* Commensal bacteria (normal microflora), mucosal immunity and chronic inflammatory and autoimmune diseases. *Immunol Lett* **2004**, *93*, 97-108.

198. Bohr, U.R.; Glasbrenner, B.; Primus, A.; Zagoura, A.; Wex, T.; Malfertheiner, P. Identification of enterohepatic helicobacter species in patients suffering from inflammatory bowel disease. *J Clin Microbiol* **2004**, *42*, 2766-2768.

199. Wilson, S.S.; Tocchi, A.; Holly, M.K.; Parks, W.C.; Smith, J.G. A small intestinal organoid model of non-invasive enteric pathogen-epithelial cell interactions. *Mucosal Immunol* **2015**, *8*, 352-361.

200. Galán, J.E.; Wolf-Watz, H. Protein delivery into eukaryotic cells by type iii secretion machines. *Nature* **2006**, *444*, 567-573.

201. Brown, N.F.; Vallance, B.A.; Coombes, B.K.; Valdez, Y.; Coburn, B.A.; Finlay, B.B. Salmonella pathogenicity island 2 is expressed prior to penetrating the intestine. *PLoS Pathog* **2005**, *1*, e32.

202. Bhavsar, A.P.; Guttman, J.A.; Finlay, B.B. Manipulation of host-cell pathways by bacterial pathogens. *Nature* **2007**, *449*, 827-834.

203. Neal, M.D.; Leaphart, C.; Levy, R.; Prince, J.; Billiar, T.R.; Watkins, S.; Li, J.; Cetin, S.; Ford, H.; Schreiber, A.*, et al.* Enterocyte tlr4 mediates phagocytosis and translocation of bacteria across the intestinal barrier. *J Immunol* **2006**, *176*, 3070-3079.

204. Kullberg, M.C.; Andersen, J.F.; Gorelick, P.L.; Caspar, P.; Suerbaum, S.; Fox, J.G.; Cheever, A.W.; Jankovic, D.; Sher, A. Induction of colitis by a cd4+ t cell clone specific for a bacterial epitope. *Proc Natl Acad Sci U S A* **2003**, *100*, 15830-15835.

205. Smythies, L.E.; Sellers, M.; Clements, R.H.; Mosteller-Barnum, M.; Meng, G.; Benjamin, W.H.; Orenstein, J.M.; Smith, P.D. Human intestinal macrophages display profound inflammatory anergy despite avid phagocytic and bacteriocidal activity. *J Clin Invest* **2005**, *115*, 66-75.

206. Applequist, S.E.; Wallin, R.P.; Ljunggren, H.G. Variable expression of toll-like receptor in murine innate and adaptive immune cell lines. *Int Immunol* **2002**, *14*, 1065-1074.

207. Schwerk, J.; Köster, M.; Hauser, H.; Rohde, M.; Fulde, M.; Hornef, M.W.; May, T. Generation of mouse small intestinal epithelial cell lines that allow the analysis of specific innate immune functions. *PLoS One* **2013**, *8*, e72700.

208. Nigro, G.; Rossi, R.; Commere, P.H.; Jay, P.; Sansonetti, P.J. The cytosolic bacterial peptidoglycan sensor nod2 affords stem cell protection and links microbes to gut epithelial regeneration. *Cell Host Microbe* **2014**, *15*, 792-798.

209. Coccia, M.; Harrison, O.J.; Schiering, C.; Asquith, M.J.; Becher, B.; Powrie, F.; Maloy, K.J. Il-1β mediates chronic intestinal inflammation by promoting the accumulation of il-17a secreting innate lymphoid cells and cd4(+) th17 cells. *J Exp Med* **2012**, *209*, 1595-1609.